

SPATIOTEMPORAL PATTERNS OF BLUFF EROSION AT GOODNEWS BAY, ALASKA

By

Richard Michael Buzard, B.S.

A Thesis Submitted in Partial Fulfillment of the Requirements

for the Degree of

Master of Science

in

Geology

University of Alaska Fairbanks

August 2017

APPROVED:

Christopher Maio, Committee Chair

David Verbyla, Committee Member

Nicole Kinsman, Committee Member

Paul McCarthy, Chair

*Department of Geosciences*

Paul Layer, Dean

*College of Natural Science and Mathematics*

Michael Castellini, *Dean of the Graduate School*

## Abstract

Coastal erosion is of increasing concern to rural Alaskan communities, yet direct measurements remain absent over much of the coast. In southwestern Alaska, the village of Goodnews Bay has been repeatedly devastated by storms and flooding, events that forced the village to relocate to higher ground in the 1920s. Storm surge continues to damage property and infrastructure that is essential to their subsistence culture. This work assesses shoreline change rates at the new village site based on a 59-year time series of aerial and satellite imagery. Long-term and contemporary shoreline retreat rates were analyzed along nearly 500 meters of the village coastline. The majority of the bluff fronting the village experienced a complex history of erosion and mitigation, exhibiting a maximum erosion rate of  $-0.14$  m/y ( $R^2 = 0.82$ ). Bluff erosion has been mitigated via depositing gravel and large rocks after significant storms. The unmitigated bluff just north of the village eroded at  $-0.10$  m/y rate consistently across its length ( $R^2 = 0.92$ ), suggesting that measurable erosion would have also occurred at the village bluff in the absence of mitigation efforts. Projected future bluff top edge positions indicate that the main road system will be significantly eroded in the coming decades, but no buildings are projected to be directly impacted by 2050.

Storm surge is the primary driver of erosion in Goodnews Bay, thus the reliability of local storm surge modeling is significant to the community. Historical storm surge and marine total water level estimates were quantified using a combination of GPS data, formal reports, anecdotal accounts, and post-storm imagery. These estimates were compared to the modeled height for the 11/11/2011 storm surge in order to assess accuracy of modeling in this area. Storms that caused significant damage had total water levels between 4.3 and 5.3 m above mean sea level. The upper limit of this estimate came from the large 2011 Bering Sea storm. Evidence for the total water level of previous storms was very limited. It is likely that the 1979 storm, which flooded four homes, reached a similar height. Damage from large storms is expected to become more prevalent with shorter land-fast sea ice seasons in Alaska.

A significant portion of this research incorporated community outreach. This included educating youth about coastal science, discussing village history with elders, and installing community-based erosion monitoring sites. Through these efforts, we hope to preserve the traditional knowledge and increase local capacity to adapt to a changing climate.



## Table of Contents

	Page
Title Page .....	i
Abstract .....	iii
Table of Contents .....	v
List of Figures .....	vii
List of Tables .....	ix
List of Appendices .....	ix
List of Abbreviations .....	x
Acknowledgements .....	xi
<b>CHAPTER 1 INTRODUCTION</b> .....	<b>1</b>
<b>1.1. Background</b> .....	<b>1</b>
<b>1.2. Geologic History</b> .....	<b>3</b>
1.2.1. Surface Characteristics .....	4
1.2.2. Bluff Characteristics .....	6
<b>1.3. Coastal Dynamics</b> .....	<b>7</b>
1.3.1. Sea Level Change .....	7
1.3.2. Tidal Data and Local Datums .....	7
1.3.3. Climate and Weather .....	8
1.3.4. Sea Ice .....	9
1.3.5. Storms and Wind-Driven Waves .....	10
<b>1.4. Previous Research</b> .....	<b>12</b>
<b>1.5. Research Question and Objectives</b> .....	<b>14</b>
<b>CHAPTER 2 METHODS</b> .....	<b>15</b>
<b>2.1. Ground Survey Data</b> .....	<b>15</b>
<b>2.2. Beach Profiles</b> .....	<b>16</b>
<b>2.3. Aerial and Satellite Image Correction</b> .....	<b>16</b>
<b>2.4. Shoreline Change Analysis</b> .....	<b>20</b>
2.4.1. Shoreline Proxy .....	20
2.4.2. Digital Shoreline Setup and Uncertainty .....	20

2.4.3.	Digital Shoreline Measurements and Assessment .....	23
<b>2.5.</b>	<b>Projecting Future Shorelines</b> .....	<b>25</b>
<b>2.6.</b>	<b>Estimating Goodnews Tidal Datum</b> .....	<b>25</b>
<b>2.7.</b>	<b>Estimating Total Water Level of Large Storms</b> .....	<b>26</b>
2.7.1.	1979 Storm TWL Estimate .....	26
2.7.2.	1969 and 1989 Storm TWL Estimate .....	27
2.7.3.	2011 Storm TWL Estimate Using Proxy Indicators .....	28
2.7.4.	2011 Storm TWL Estimate Using Ocean and Weather Information .....	28
<b>2.8.</b>	<b>Estimating Wave Impact Hours</b> .....	<b>29</b>
<b>CHAPTER 3 RESULTS</b> .....		<b>31</b>
<b>3.1.</b>	<b>Shoreline Change Analysis (1957 – 2016)</b> .....	<b>31</b>
3.1.1.	Detecting Net Change .....	31
3.1.2.	Detecting Event-Based Change .....	33
<b>3.2.</b>	<b>Bluff Top Edge Projection</b> .....	<b>38</b>
<b>3.3.</b>	<b>Goodnews Bay Tidal Datums</b> .....	<b>40</b>
<b>3.4.</b>	<b>Total Water Level Estimates and Risk Areas</b> .....	<b>40</b>
<b>3.5.</b>	<b>Wave Impact Hours</b> .....	<b>44</b>
<b>CHAPTER 4 DISCUSSION</b> .....		<b>47</b>
<b>4.1.</b>	<b>Erosion Hazards</b> .....	<b>47</b>
4.1.1.	Identifying Areas of Change .....	47
4.1.2.	Determining the Impact of Bluff Armoring .....	51
4.1.3.	Future Shoreline Projections .....	51
<b>4.2.</b>	<b>Storm Surge and Flood Hazards</b> .....	<b>53</b>
<b>4.3.</b>	<b>The Coastal Resiliency of Goodnews Bay in Relation to Other Alaskan Villages</b> ..	<b>56</b>
<b>4.4.</b>	<b>Broader Impacts</b> .....	<b>57</b>
<b>4.5.</b>	<b>Future Work</b> .....	<b>58</b>
<b>CHAPTER 5 CONCLUSION</b> .....		<b>59</b>
<b>LITERATURE CITED</b> .....		<b>61</b>
<b>APPENDICES</b> .....		<b>67</b>

## List of Figures

	Page
Figure 1. The village of Goodnews Bay .....	2
Figure 2. General gradation of beach surface features. ....	5
Figure 3. Aerial and satellite images of large rock quarries opened in Goodnews. ....	6
Figure 4. Historical and projected future temperature and precipitation for Goodnews Bay. ....	9
Figure 5. Annual sea ice concentration 50 km west of Goodnews Bay. ....	10
Figure 6. Cross-shore beach profiles sampled at 100 meters. ....	16
Figure 7. Available imagery of Goodnews Bay with the spatial resolution necessary for shoreline delineation. ....	19
Figure 8. DSAS transects cast for change analysis of the unarmored bluff (left) and armored bluff (right). ....	21
Figure 9. Datasets used for total water level and wave impact hour analyses. ....	30
Figure 10. Net movement and weighted linear change of bluff top edges between 1957 (blue) and 2016 (black). ....	32
Figure 11. Bluff edge change rate (black line) for each time period. ....	35
Figure 12. Total uncertainty footprint of each bluff edge overlaid on a 20x20 meter cell grid. ..	36
Figure 13. Mean distance from the 1957 bluff top edge. ....	37
Figure 14. Net horizontal movement of the bluff edge from 1957 to 1983, and from 1983 to 2016. ....	37
Figure 15. Bluff edge position projected for 2030 (purple) and 2050 (green). ....	39
Figure 16. Plotted tidal datums for Platinum (blue) and Goodnews Bay (green). ....	40
Figure 17. Estimated total water level of 11/11/2011 storm in Goodnews Bay. ....	42
Figure 18. Map of horizontal extent of estimated total water level of strong storms. ....	43
Figure 19. Average monthly wave impact hours contacting and overtopping bluffs from 2009 through 2014. ....	45
Figure 20. Cumulative average monthly wave impact hours contacting and overtopping bluffs from 2009 through 2014. ....	45
Figure 21. Spatial distribution of wave impact hours for the 11/11/2011 storm. ....	46
Figure 22. Armored bluff erosion hot spots, as determined by the shoreline change analysis. ....	49
Figure 23. Estimated number of structures on the armored bluff where the highest erosion rates are observed. ....	50
Figure 24. Pictures of damage from the 11/11/2011 storm. ....	55



## List of Tables

	Page
Table 1. Documented storms that caused damage in Goodnews Bay. ....	11
Table 2. Summary of images used for shoreline delineation. ....	17
Table 3. Bluff top edge position uncertainty values with year and total uncertainty ( $U_t$ ) bolded. ....	23
Table 4. List of DSAS statistics (from Himmelstoss, 2009). ....	24
Table 5. Survey information to estimate 1979 flood elevation. ....	27
Table 6. Water level proxies used to estimate elevation of 2011 storm surge. ....	28
Table 7. Mean weighted linear regression rate-of-change for each bluff. ....	33
Table 8. Tidal datum estimates for Goodnews Bay in meters NAVD88. ....	40
Table 9. Estimated significant total water levels associated with storm surge and flooding events. ....	41

## List of Appendices

	Page
<b>Appendix I. Photos from 11/16/2003 and 11/11/2011 storms in Goodnews Bay</b> .....	67
<b>Appendix II. Flood reports from the Alaska District Corps of Engineers Flood Plain Management.</b> .....	75
<b>Appendix III. Qualitative analysis of sea ice formation trends in Goodnews Bay.</b> .....	85
<b>Appendix IV. Community Profile Maps of Goodnews Bay.</b> .....	86
<b>Appendix V. Coastal Profile Data for Goodnews Bay.</b> .....	88
<b>Appendix VI. Goodnews Bay Airport Master Record</b> .....	96



## List of Abbreviations

ATV	All-terrain vehicle
CI	Confidence interval
CO-OPS	National Oceanic and Atmospheric Administration Center for Operational Oceanographic Products and Services
DGGS	Alaska Division of Geological Surveys (Department of Natural Resources)
DSAS	Digital Shoreline Analysis System (USGS)
DSM	Digital surface model
ECI	EPR confidence interval
EPR	End point rate
GAO	US General Accounting Office (2003), changed name to US Government Accountability (2009)
MHHW	Mean higher high water
MSL	Mean sea level
NAVD88	North American Vertical Datum of 1988
NSM	Net shoreline movement
RMS	Root mean square
RSS	Root sum of squares
RTK-GNSS	Real-time kinematic global navigation satellite system
SD	Standard deviation
TWL	Total water level (tide + surge + wave runup)
USACE	US Army Corps of Engineers
WCI	WLR confidence interval
WIH	Wave impact hours
WLR	Weighted linear regression rate-of-change

## Acknowledgements

The culmination of work put into this thesis is undoubtedly the greatest achievement I have accomplished. I would like to thank my advisor, Dr. Chris Maio, whose vast wisdom and devoted work ethic kept my path clear through even the foggiest of days. Our repeated visits to Goodnews Bay and other communities in Bristol Bay have been unique and exceptional experiences, and I eagerly look forward to the next adventure.

I would also like to thank my committee members, Dr. David Verbyla and Dr. Nicole Kinsman. Since day one, their guidance and feedback has been constructive, extensive, and a healthy challenge to address. For these incredible people to devote their time to me and this thesis, I am truly indebted.

Many talented people assisted me during the years of work that went into this thesis. First, a sincere thank you to Jacquelyn Overbeck, who, with selfless enthusiasm, offered training, direction, and an endless wealth of data that played a major role in the success of this work. I would also like to thank Dr. Franz Meyer and Scott Arko of the Alaska Satellite Facility for assisting in the acquisition and processing of remotely sensed datasets. I also thank George Plumley from the Alaska Department of Commerce, Community, and Economic Development for providing data on previous surveys. A special thanks to Matthew Balazs for an unforgettable aerial mapping training experience.

This project was funded by Alaska Sea Grant, who have also granted me a fellowship for a second project, which has allowed my pursuit of a PhD. For this incredible opportunity, I would like to extend a very special thank you to Paula Cullenberg, Michele Frandsen, Ginny Eckert, and Sue Keller. I would also like to thank the Cooperative Institute for Alaska Research, whom awarded me the 2016 UAF Global Change Student Research Grant, which went toward training, equipment, and travel funds that made this work possible. In addition, I would like to thank the UAF Graduate School for travel funds to present my work at the 2016 AGU Conference.

This project would not have been possible without the support of the residents of Goodnews Bay. I would like to give a very special thank you to Alice and Peter Julius, who shared photographs, stories, and an unforgettable fishing trip. I also thank Willie and Roxanne Ayojiak, The Schouten family, Evan Evan, George and James Bright, Sherri Carmichael, Shannon Hutson, The Tribal Council, and all others who shared their stories with us.

The ability to do this kind of work in the great state of Alaska is due to the incredible opportunity that the University of Alaska Fairbanks provides. I would like to thank Drs. Paul Layer and Paul McCarthy, as well as the professors in the Geoscience Department, who support the work of many aspiring students. I would also like to thank those who taught, advised, and inspired me during my time at the University of Washington Bothell – Drs. Robert Turner, Avery Shinneman, Santiago Lopez, and Karrin Klotz.

To have reached this far on the long road through academia, I can only thank my mother and father, Theresa and Michael Buzard, for believing and investing in my potential, and my sister, Amanda Buzard, for setting the bar so high. I would also like to thank Alexandra Iezzi, my wonderful girlfriend who supported me through countless busy days and nights, and our guinea pig son, Cosmo, who is always a gas. Lastly, and far from least, I extend a heartfelt thank you to Joshua and Laurel Sanford, my best friends and role models who helped me discover my passion for science, stood by my side throughout my entire undergraduate experience, and bravely took in my evil bipolar cat, Weet.

Thank you all.

## CHAPTER 1

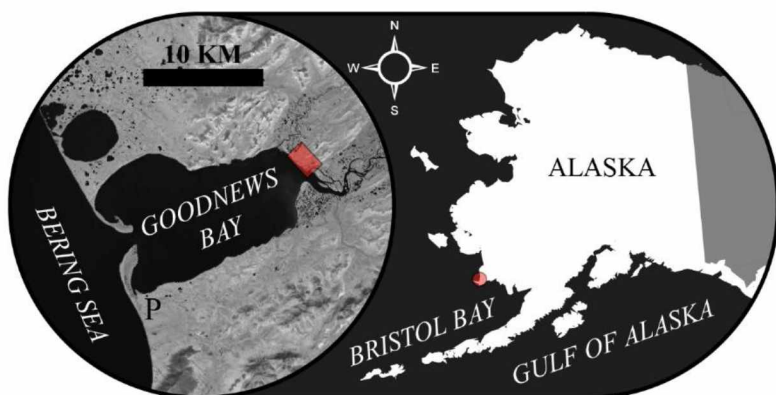
### INTRODUCTION

Coastal communities in Alaska are caught in the throes of dynamic environmental phenomena. Retreating sea ice extents, increasing frequency of storms during open water, and a warming and rising ocean all contribute to historically unprecedented erosion rates along Alaska's coasts, including regions of invaluable economic infrastructure and cultural significance (Chapin et al., 2014; Jones et al., 2009; Walsh and Chapman, 2015). In 2003, the United States General Accounting Office (GAO) reported that 184 out of 213 (86%) of Alaska Native villages are affected by flooding and erosion (GAO, 2003). This list includes Goodnews Bay, for which no formal shoreline erosion study has been conducted.

#### 1.1. Background

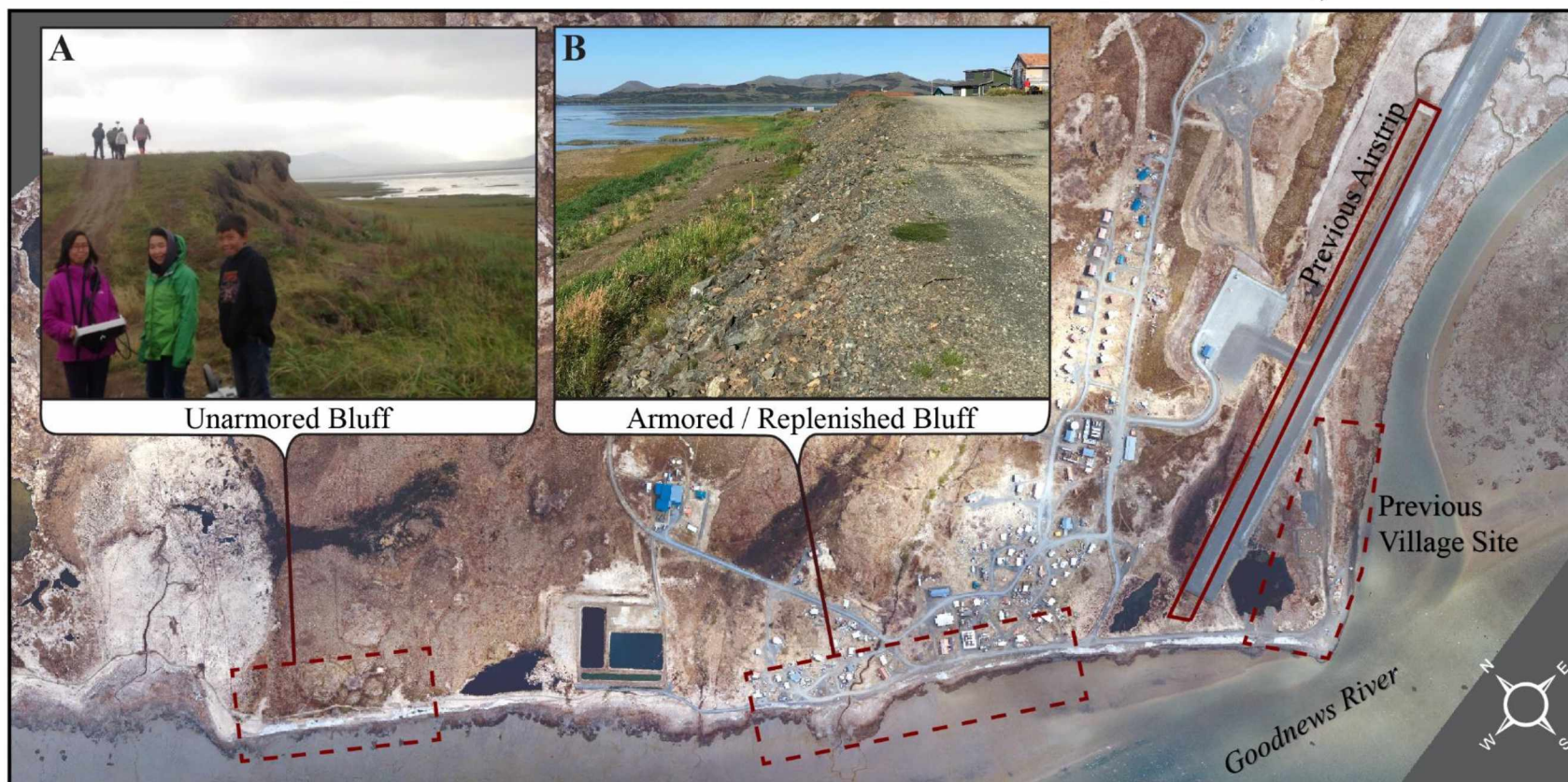
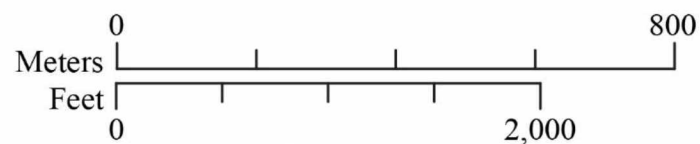
The village of Goodnews Bay (Goodnews) sits at the mouth of the Goodnews River and consists of 9.6 km<sup>2</sup> of land (Figure 1). The village is located 187 km south of Bethel and has a population of approximately 243 residents, of which 36% are under 18 years old (City Data, 2017). The majority of residents are Yup'ik Alaska Natives. The economy is primarily subsistence-based with a per capita income of \$10,085 in 2013 (City Data, 2017). The village received its current name from Russian explorers in 1818, but was originally called Imagpiguak, meaning "Little Ocean" (Calista Corporation, 2016). Goodnews' current Yup'ik name is Mumtraq, sometimes spelled Mumtrak or Mamterat. In 1919, the USGS sent a mapping party to the Goodnews Bay region, although their work focused on the area of Platinum just south of the southern spit where residents of Goodnews had discovered platinum (Calista Corporation, 2016; Mertie, 1940). This focus on economic geology became a recurring theme, and the majority of publications and aerial surveys target Platinum rather than Goodnews (e.g. Harrington, 1921; Mertie, 1939; Oommen et al., 2008).

Figure 1. The village of Goodnews Bay. The bluff fronting the village (B) has been covered with armor rock to protect against erosion. The bluff northwest of the sewage lagoon (A) is not covered. The new airstrip is higher in elevation than the previous, but still experienced partial flooding in the 2011 storm. Inhabitants moved northwest from the previous village site between the 1920s and 1950s due to flooding. New homes are built uphill to the northeast.



## Goodnews Bay, Alaska

Orthomosaic produced by Alaska Division  
of Geological and Geophysical Surveys,  
acquired May 5, 2016  
NAD83 UTM 4N



Goodnews has a long history of flooding due to storm surge, some of which led to erosion of the bluff fronting the village. The village relocated to its current site in the 1920's due to frequent flooding (Calista Corporation, 2016). A federal disaster declaration for western Alaska was filed for the 2011 storm, resulting in \$18,300 for road repairs in Goodnews Bay (FEMA, 2011). Documentation shows that storm-induced flooding has submerged the previous airstrip (1969, 1989) and caused property damage/loss (2003) including boats (2011) and at least one home (1979) (Table 1; Appendix I). While erosion was reported for multiple events, quantitative reports only exist for the 1979 storm, reportedly causing 6 to 10 feet (2 to 3 m) of "bank erosion" (Appendix II). No formal erosion studies have centered on Goodnews to date, but in 1994 the Alaska District Corps of Engineers Flood Plain Management assessed damage reports and concluded that storms and wind-driven waves at high tide are the primary cause of flooding and ice push in Goodnews (Appendix II). Steps were taken by the now-defunct Alaska Coastal Management Program to implement a regional Coastal Management Plan, in which Goodnews was included as part of the Ceñaliurliit Coastal Resource Service Area (DNR, 2008). However, the only significant mitigation effort in place at Goodnews is armoring the bluff fronting the village.

## **1.2. Geologic History**

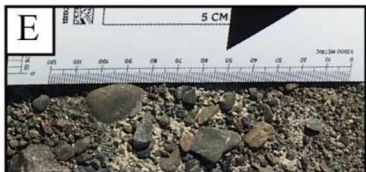
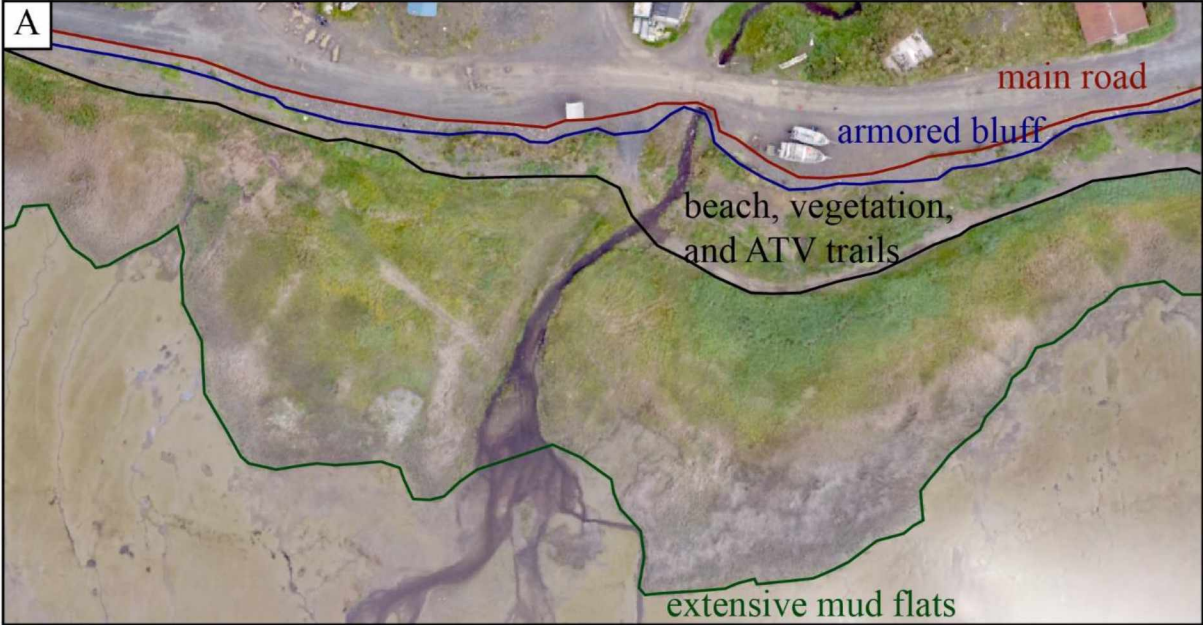
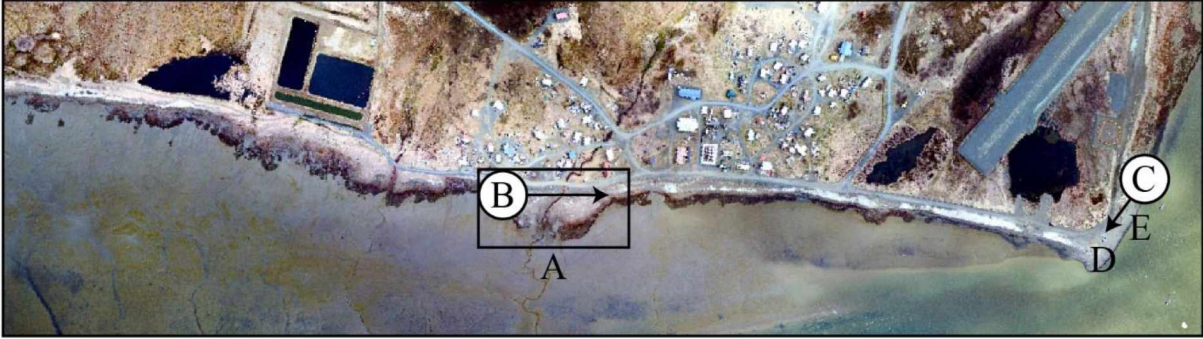
Goodnews Bay is a back-barrier micro tidal (mean range ~ 0.75 m) shallow lagoon (1 to 2 m) located along the eastern Bering Sea coastline of southwestern Alaska (Figure 1). The coastline, which fronts village infrastructure, is approximately 2 km long. The lower Goodnews River valley was estimated to have been most recently glaciated between 40,000 and 70,000 <sup>14</sup>C years before present (Kaufman et al., 2011). The coastal area is composed primarily of unconsolidated quaternary alluvial deposits, and the lithology of the quarried mountain east of the village consists of Permian basalt and serpentinite (Wilson et al., 2013). The location is tectonically stable with potential subsidence of  $1 \pm 2$  mm per year, possibly recovering from a previous forebulge from the last glacial maximum in the Ahklun Mountains between 11.0 to 12.4 years before present (Briner et al., 2002; Degrandpre, 2015).

### *1.2.1. Surface Characteristics*

Surface features change gradually from the mountains to the bay. The village infrastructure is built on the surrounding low-shrub tundra, which is mixed with tussock-sedge, dwarf-shrub, and moss (CAVM Team, 2003). The road gravel is sourced from three local serpentinite quarries (see Section 1.2.2), and is typically broken down to 0.5 – 3 cm angular grains. Grain size increases to as much as 10 cm at The Point, the southernmost section of beach where boats are stored and launched. Grain size gradually decreases seaward, also becoming more rounded, before terminating at the mud (clay) line. From this observation, it seems likely that the angular gravel and rock is brought from the quarry in order to allow vehicle access to The Point, although no record of beach replenishment has been found. Beach sediments also vary alongshore, gradually shifting from the large angular gravel on The Point in the south into sand, and ultimately mud northwest of Quirkik Hill. Vegetation cover increases from southeast to northwest, opening up into extensive low-lying reed grass beyond the unarmored bluff. In general, the beach transitions from gravel-topped road to gravel- and rock-topped bluff, into the mixed beach with varying degrees of vegetation, before gradually decreasing slope into extensive mud flats out to the Goodnews River and Bay (Figure 2).



Figure 2. General gradation of beach surface features. White circles with arrows denote the direction a picture was taken. A) The main road runs adjacent to the armored bluff, and beach, ATV tracks separate vegetation, and vegetation gradually gives way to extensive mud flats. Image acquired August, 2016. B) Creek culvert allowing water through the armored bluff. C) Gravel beach at The Point (boat launch). D) Coarse gravel (3-10 cm) at The Point. E) Finer gravel (1-3 cm) east of The Point.



### 1.2.2. Bluff Characteristics

The two bluffs in the Goodnews area identified in Figure 1 are composed of unconsolidated, primarily fine-grained sediments. The unarmored bluff northwest of the village is examined as a control variable. There is no evidence of attempted erosion mitigation or replenishment for the unarmored bluff. The bluff fronting the village is designated as the “armored bluff” because residents have placed large (10 - 50 cm) angular serpentinite and basalt rocks sourced from the local quarries. The date when armoring began is not known, but evidence from aerial imagery suggests that the first two large quarries were excavated between 1957 and 1983 (Figure 3). This corresponds with the construction of the previous airstrip, which is a probable cause for quarrying (as well as for roads and infrastructure foundation). The area of the current armored bluff appears to be vegetated in aerial imagery from 1983, suggesting either it has not been armored or it was overgrown. The third large quarry was excavated between 1983 and 2005, before the current runway was built. The 2005 image shows that the bluff is armored with exposed rock. The frequency of armoring is also unknown; whether armoring is a direct response to large events, is gradually replenished, or a combination, is still being investigated. The discussion of armoring history and impact is continued in Section 4.1.

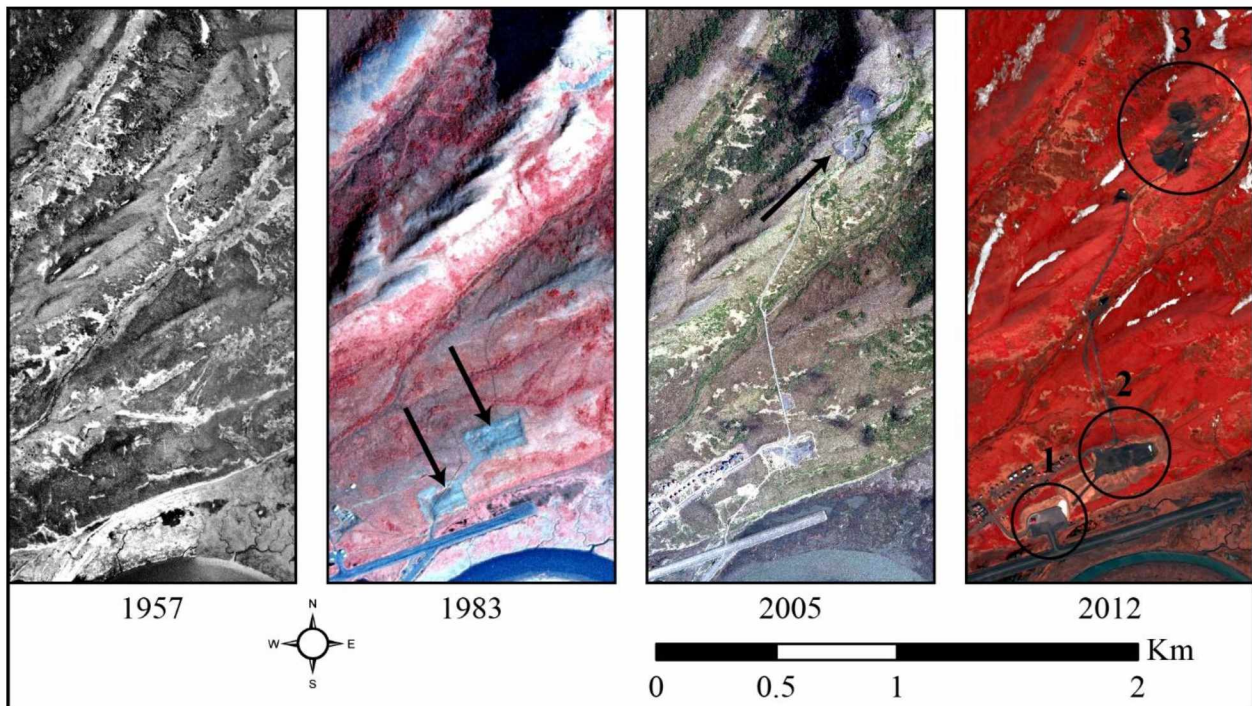


Figure 3. Aerial and satellite images of large rock quarries opened in Goodnews. Two quarries opened between 1957 and 1983, and a third was opened by 2005.

Both bluffs are important to the village. An all-terrain vehicle (ATV) trail runs on top of the unarmored bluff, providing access to berry-picking and hunting areas. The main road system for the village runs on top of the armored bluff, and the bluff edge is generally the road edge, too. Important infrastructure including homes and the diesel station are located near the armored bluff edge. No homes or large structures have been lost to bluff erosion, although smokehouses may have been lost due to a combination of flooding and erosion (Table 1).

### **1.3. Coastal Dynamics**

#### *1.3.1. Sea Level Change*

Long-term changes in sea level directly impact nearshore processes, which can lead to significant changes in erosion rates (Nicholls and Cazenave, 2010). Satellite altimetry data suggests that offshore mean sea level (MSL) is dropping near Goodnews Bay by 0.25 mm/year (SD = 0.08), but GPS and glacial isostatic adjustment models show tectonic vertical velocity is -1.71 mm/year (SD = 0.61) and -0.997 mm/year, respectively (Degrandpre, 2015). Thus, this analysis finds relative sea level is changing at a rate that could not be distinguished from 0 mm/year. A rise in relative sea level is found across western Alaska from Bristol Bay to the Chuckchi Sea, but, due to lower rates of eustatic sea level rise in Arctic regions, this rise is much lower than the estimated global average rate of sea level rise, 3.2 mm/year (Ablain et al., 2009; Church and White, 2011). For this study of Goodnews, it is simply important to note that relative sea level is likely rising, but this rise is slow and unlikely to be a significant factor in the observed coastal erosion. Additional work in the area, especially in regards to measuring sea level change with high precision, is required to better understand the influence of sea level rise on erosion.

#### *1.3.2. Tidal Data and Local Datums*

Goodnews experiences mixed semi-diurnal tides. The nearest accepted tidal datum was established at station 9465396 in Platinum, 16 km west at the head of the bay. The referenced dataset runs from May 25 to October 1, 2007, but the tidal datums are based on a first reduction of the July data, with no control tide station. While this datum is likely similar to Goodnews' it is not acceptable for this study; local hydrographic conditions associated with the Goodnews River are likely to cause significant variations in local water levels and timing, an error that amplifies

considerably for shoreline studies on low-profile beaches (e.g. Ruggerio et al., 2013). No permanent infrastructure has been installed to monitor and record water level in or around the bay. In late August 2015, the Department of Natural Resources Alaska Division of Geological and Geophysical Surveys (DGGs) installed a temporary water level sensor in Platinum. However, the sensor began experiencing errors on November 17, 2015, and ceased operation in January 2016. The nearest active water level sensor is in Port Moller, AK, about 350 kilometers south. Without an appropriate tidal datum or an active water level sensor in the region, the ability for coastal hazard assessments to provide robust results becomes limited. This study addresses that data gap by tying a 4-day water pressure gauge to the tidal datum of Platinum station 9465396. While this estimated tidal datum proves effective for this study, its high uncertainty prevents it from being a suitable replacement for a formal tidal analysis.

### *1.3.3. Climate and Weather*

Goodnews is in the western transitional climate zone, influenced both by the Bering Sea and air masses moving over the interior. Average temperatures are below freezing for half of the year in Goodnews, with monthly means ranging from about -10 to 10°C (Figure 4). This climate leads to isolated (> 0 to 10%) permafrost, thus permafrost thaw is not thought to play a major role in this study (Jorgenson et al., 2008). Mean monthly temperature and precipitation are projected to increase for the remaining century, based on mid-range emission climate models from the International Panel on Climate Change (SNAP, 2017). Peak precipitation occurs in late summer and slowly diminishes through fall, when the typical storm season begins (Terenzi, Jorgenson, and Ely, 2014). Heavy rainfall coinciding with a storm surge can lead to substantial flooding.

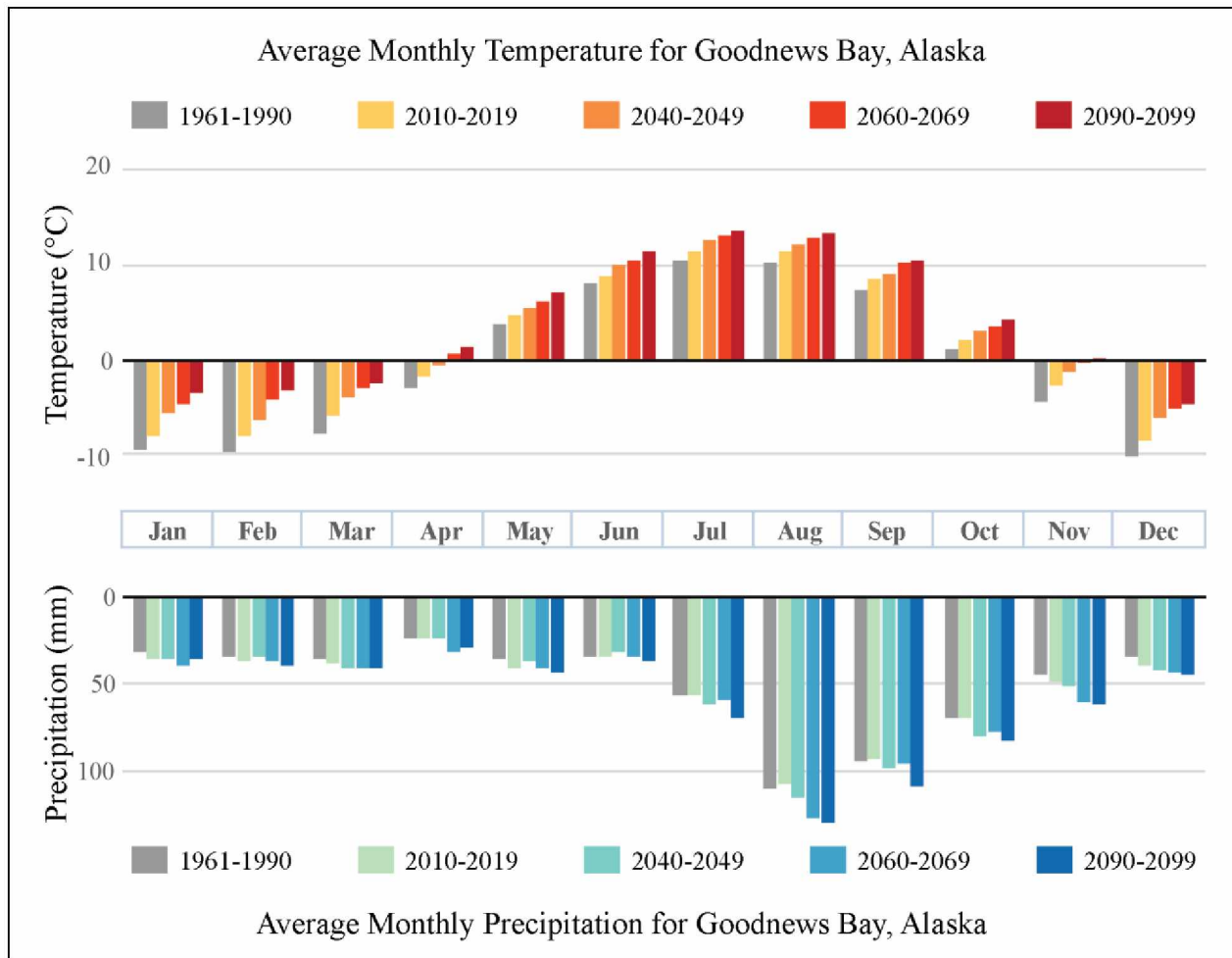


Figure 4. Historical and projected future temperature and precipitation for Goodnews Bay. Data provided by Scenarios Network for Alaska + Arctic Planning (SNAP). The 5-model projected average values are determined on a 2 km resolution grid, based on mid-range emissions (RCP 6.0) from the International Panel on Climate Change’s fifth Assessment Report published in 2014. Error in these projections, especially precipitation, is significantly high (SNAP, 2017).

#### 1.3.4. Sea Ice

The Goodnews River and Bay tend to freeze over from late fall until spring. Residents travel on the ice for subsistence hunting and to connect with Platinum, the nearest city (Wildlife Service, 1986). Residents reported that the bay ice was repeatedly broken up by strong winds in recent years, and they could not travel on it. No assessment of sea ice concentration in the bay has been quantified, but these anecdotal accounts are consistent with the qualitative observations of the bay using Landsat imagery (Appendix III). Sea ice concentration data from approximately 50 km west of the bay suggests annual maximum sea ice concentration decreasing in recent years, with formation occurring later and breakup occurring earlier (Figure 5). Some climate

models project an ice-free November for the entire Bering Sea by 2050 (Douglas, 2010; Perovich and Richter-Menge, 2009).

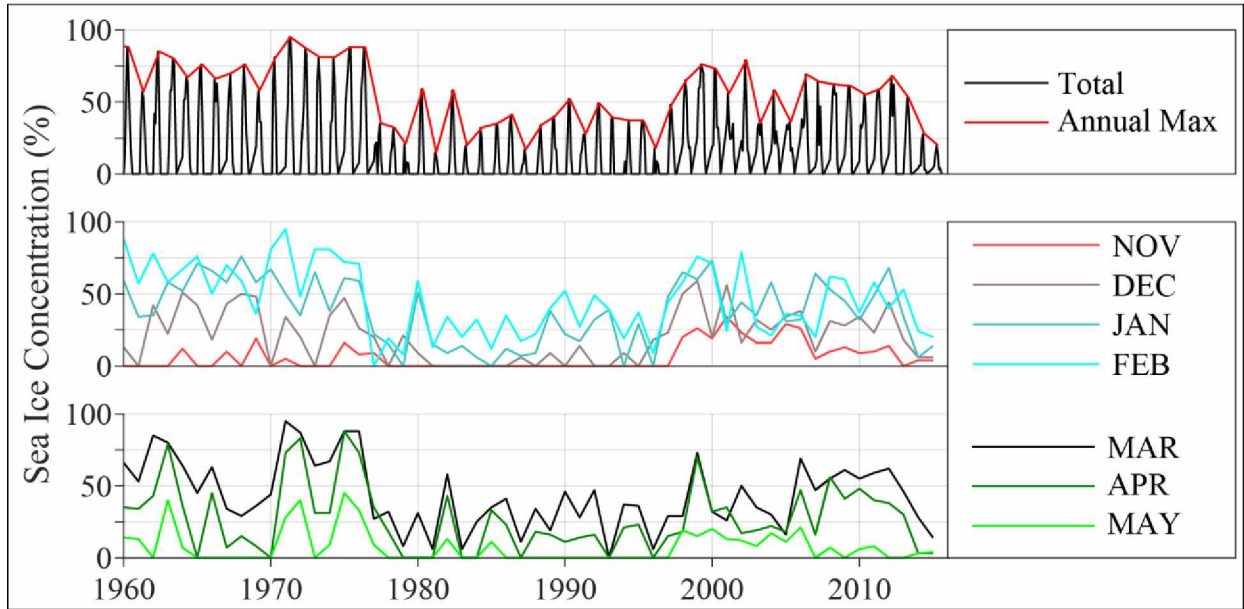


Figure 5. Annual sea ice concentration 50 km west of Goodnews Bay. Offshore sea ice began steeply declining in 2012, such that total concentrations dropped below 25% in 2015. Calculated from data produced by the Historical Sea Ice Atlas (2017).

### 1.3.5. Storms and Wind-Driven Waves

Goodnews has weathered several large storms in the contemporary record, the most recent being on November 11, 2011 (Table 1). This storm caused damage and flooding in at least 37 coastal villages (Parnell, 2011). The automated weather observing system operated by the Federal Aviation Administration, which measures temperature, pressure, wind speed and wind direction in Platinum, failed on October 19, 2011, less than one month before the most recent large storm. All instruments were restored on February 16, 2012 and continued to function, although some small lapses exist. The Goodnews village public safety officer George Bright was monitoring the wind during the storm, “The highest it hit was 114 [mph]. I don’t know how much higher it got because my wind vane blew off” (Denning-Barnes, 2011). The damage and storm surge flooding rivaled reports of the 1979 storm (Table 1).

Table 1. Documented storms that caused damage in Goodnews Bay.

Storm Date	Description
1920s	Village relocates due to flooding and storms. <sup>2</sup>
1969	Storm causes flooding of airstrip up to 6 to 12 inches. <sup>3</sup>
1974	Large storm impacts the village, causes flooding. <sup>7,8</sup>
1979 Nov 8-9	Large storm causes flooding from storm surge. Three houses flooded and unbalanced, one is destroyed. Estimated 6 to 10 feet of bank erosion, and “flood depth” of 8 to 9 feet. Previous airstrip narrowed (noted that flood water commonly floods previous airstrip). Residents claimed worst storm-driven waves in 20 years. 36 meters/sec (80 mph) winds reported in the region, 26.2 m/s (59 mph) winds measured in Bethel. <sup>1,3</sup>
1982	Flood occurs. <sup>3</sup>
1984 FEB	Erosion of gravel bank fronting village due to heavy rains. The creek bridge washed away, and the creek froze. <sup>3</sup>
1989 AUG 17	Strong winds from the south cause storm surge and flooding, high water goes over airstrip (noted that flooding occurs annually). <sup>3</sup>
2003 NOV 16	Storm surge causes damage to boats. <sup>4</sup>
2011 NOV 11-12	Large storm causes flooding from storm surge. Surge erodes bluff, damages airstrip, airport fence, property and homes, and displaces one family. Six to twelve boats are damaged or missing. Several Conex shipping containers with construction supplies washed out to mud flats. 100 mph winds reported. <sup>4,5,6</sup>

<sup>1</sup> Terenzi, Jorgenson, and Ely, 2014

<sup>2</sup> Calista Corporation, 2016

<sup>3</sup> Flood Plain Management, Appendix II

<sup>4</sup> Alice Julius, personal communication, Appendix I (photos of 2003 damage)

<sup>5</sup> Denning-Barnes, 2011

<sup>6</sup> Appendix I (photos of 2011 damage)

<sup>7</sup> Anna, Goodnews resident, personal communication

<sup>8</sup> Evan Evan, Goodnews resident, personal communication

The amount of damage from a storm and subsequent flooding in Goodnews may be closely linked to the tidal stage and sea ice cover. A storm surge occurring at high tide amplifies the total water level (TWL) well above mean higher high water (MHHW). Bering Sea storms tend to occur in Autumn, when offshore sea ice is only beginning to reach the region (Douglas, 2010; Terenzi, Jorgenson, and Ely, 2014). Large concentrations of sea ice over a wide area can reduce wind drag significantly, nullifying the potential for a surge to build (Macklin, 1983). The absence of offshore sea ice over a fetch as little as 50 km is enough for high-power storms to



build a significant surge, although more typical storms require several hundred kilometers of fetch to generate surge greater than 1 meter (Barnhart, Overeem, and Anderson, 2014; Erikson et al., 2015; Jones et al., 2009; Macklin, 1983; Pease, Salo, and Overland, 1983). Unconsolidated bay ice can still allow surge to reach the village, contributing ice blocks as a battering component of wave attack (e.g. Appendix I). It is important to note that future assessments of storm surge impact in Goodnews would require quantifying trends in bay ice timing and conditions in addition to offshore fetch.

#### **1.4. Previous Research**

Alaska's western and northern coastlines are experiencing rapid changes in response to longer sea ice-free seasons, increasing frequency of storms during open water, and a changing Arctic climate (Barnhart, Overeem, and Anderson, 2014; Gibbs, Nolan, and Richmond, 2015; Serreze and Stroeve, 2015; Walsh and Chapman, 2015). As scientists, journalists, and policymakers turn a new focus on this region, it is of great importance to identify where high erosion rates are occurring (e.g. Mason et al., 2012). However, methods vary and there exists no widely accepted standard for how to measure, analyze, and report shoreline change (Gibbs and Richmond, 2015).

Several methods exist to document erosion and coastal changes (e.g. Boak and Turner, 2005; Vieira da Silva et al., 2016; Moore, 2000; Thieler and Danforth, 1994). Repeat beach profiles are a simple and proven way to directly measure erosion and volumetric change (e.g. Emery, 1961; Kinsman and Gould, 2014; Theuerkauf and Rodriguez, 2012). Recent advances in remote sensing applications allow researchers to effectively quantify multi-meter changes across broad landscapes using historic aerial photographs coupled with satellite imagery (e.g. Gibbs, Nolan, and Richmond, 2015; Manley et al., 2006; Mars and Houseknecht, 2007; Mason et al., 2012). Limitations include resolution of imagery, availability of data with high spatial and temporal resolution, and cloud-free coastlines with clear shoreline position proxies such as a visible high water line, rack line, wet/dry line, bluffs, or vegetative indicators (Boak and Turner, 2005; Moore, 2000; Thieler and Danforth, 1994). Geometric errors can be reduced using orthorectified imagery and ground-truth measurements, but this approach can be challenging given the limited availability of high-resolution (< 1 m) imagery of the remote Alaskan coastline. The USGS Digital Shoreline Analysis System tool (DSAS) is commonly implemented to

quantify change rates and project future shoreline positions (Ford, 2013; Gibbs and Richmond, 2015; Jones et al., 2008; Mars and Houseknecht, 2007). This geographical information software extension casts virtual transects along temporal vector shorelines and uses distances between shorelines intersecting the transect to calculate rates of change (Maio et al., 2012; Thieler et al., 2009). Regardless of the method of quantifying erosion, measurements are typically reported in meters per year. This practice is useful to standardize erosion for comparison to other areas. However, erosion in many places is non-linear, and is often linked to seasonal variations, storms, and even decadal geomorphic changes (e.g. Kinsman and Gould, 2014). Thus when measuring, interpreting, and reporting erosion it is important to consider the meaning of the units and their relationship to the driver(s) of change.

As mentioned previously, no formal erosion study has focused on Goodnews Bay. Following the 2003 GAO report, the US Army Corps of Engineers (USACE) conducted an erosion assessment of 178 of the listed villages. Goodnews and Platinum were not assessed because they are listed under flooding on the GAO report, not erosion (USACE, 2009b). Although this assessment opportunity was missed, community profile maps were generated for both villages in 2005 by Global Positioning Services, Inc., with funding from the Coastal Village Regions Fund (Appendix IV). The data products include two scanned raw aerial images during high water: one of the village (bluff not in image frame) at 1:1200 scale, 1-foot (0.3 m) pixel resolution, and the other with the village and coastline at 1:2400 scale, 2-foot (0.61 m) pixel resolution (Appendix IV).

In 2009, the USACE Alaska District published a barge landing report, which assessed the current conditions of landing barges in several Alaskan cities. Goodnews was recommended for priority funding; according to the report the bay is shallow (2-21 m), the currents are strong, and the beach at The Point is growing (USACE, 2009a). The report recommends dredging the bay for easier barge access, but also notes that an environmental impact assessment must first be accomplished to allow such activities in the highly productive salmon habitat. The report also recommends moving the fuel header closer to the landing site. Inquiries into erosion and flood damage due to storm surge were beyond the scope of the barge landing report, but are recommended to be included in an environmental impact assessment (DOE, 2010).

Planimetric imagery of sufficient resolution for coastal erosion assessments is limited in Goodnews. In 2016, the DGGS funded the creation of an orthorectified aerial image and

corresponding photogrammetrically derived digital surface model of Goodnews with 0.2 m ground sampling distance. This dataset will also be used by the DGGs to create a color-index map of quantitative elevations of village features, in order to visualize their relationships to specific tidal datums and coastal hazards (e.g. Tschetter, Kinsman, and Fish, 2014). However, tying elevation to tidal data requires both datasets to be in the same vertical datum, which is only possible with reliable local tidal records. This data gap is addressed in Section 2.6.

### **1.5. Research Question and Objectives**

The main objective of this thesis is to analyze shoreline change in Goodnews Bay based on the full record of available planimetric orthoimagery, which ranges from 1957 to 2016. Because direct observations of shoreline movement on the timescales in which it occurs at this location is neither practical nor feasible, secondary indicators, or proxies, are measured and analyzed to infer the shoreline activity.

This study uses measurements of long-term bluff movement to identify bluff response to large storms and project future bluff positions. These projections will aid the residents of Goodnews in decision-making and future planning to avoid significant damage and loss from storms. This analysis will also provide insight into the effectiveness of bluff armoring at preventing erosion.

Overarching Research Question: At what rate is the Goodnews Bay village coastline changing, and how has this rate changed historically?

#### Objectives:

- (1) Conduct shoreline change analysis to determine contemporary and historical change rates.
- (2) Project future shoreline positions.
- (3) Identify areas at risk of erosion and flooding.

## CHAPTER 2

### METHODS

This study was conducted to analyze the extent and severity of shoreline change in Goodnews, as well as to build a baseline dataset for future studies. This was accomplished through a ground-based survey and the processing and analysis of remotely sensed products within a geographic information system. The image processing software used are ESRI ArcGIS and Agisoft Photoscan. GPS data was processed in Trimble Business Center, and all other data were processed in MATLAB R2015b and Microsoft Excel. The following subsections describe the data acquired and processed, the shoreline indicator identified, and how analyses were accomplished. Project objectives were achieved using a combination of these methods.

#### **2.1. Ground Survey Data**

A real-time kinematic global navigation satellite system (RTK-GNSS) survey was conducted in August 2016 with a Trimble R8s base receiver and Trimble R8-4 rover receiving GPS and GLONASS signals. Features were surveyed in the North American Datum of 1983, Universal Transverse Mercator global coordinate system, with orthometric heights calculated using Geoid12B. Occupations were typically 3-epochs over 3-seconds. Occupation times and epochs were increased in areas of poor reception. Due to range limitations, three base station positions were used throughout the survey: one on a temporary benchmark set up north of the airport runway; one on a temporary benchmark on the bluff fronting the village; and the third on a permanent benchmark “DOWL GNB-1 1999 6714-S” on Quirkik Hill. Base station coordinates were logged at 4- to 5-hour intervals, corrected using the Online Positioning User Service tool, then averaged into one point per base station location using the merge function in the Trimble Business Center software. All corrected base coordinates were within 0.02 m horizontal and vertical agreement. Mean precisions for roved coordinates were 0.0149 m horizontal and 0.0195

vertical (95% confidence). The rover coordinate precisions incorporated root mean square (RMS) error from the averaged corrected base points (i.e. the rover precision includes the base precision).

## 2.2. Beach Profiles

A cross-shore beach profile survey was conducted from August 25 to 27, 2016, in order to create a baseline dataset for the village. Beach profiles were placed every 100 m running parallel to the shore from southeast of the airport runway to the northwest end of Quirkik Hill (Figure 6). Recorded features included the current water line, vegetation line, high water line (wet/dry or rack line), beach berms, bluff toe and top, and infrastructure features such as road edges, fences, and buildings. See Appendix V for data table.

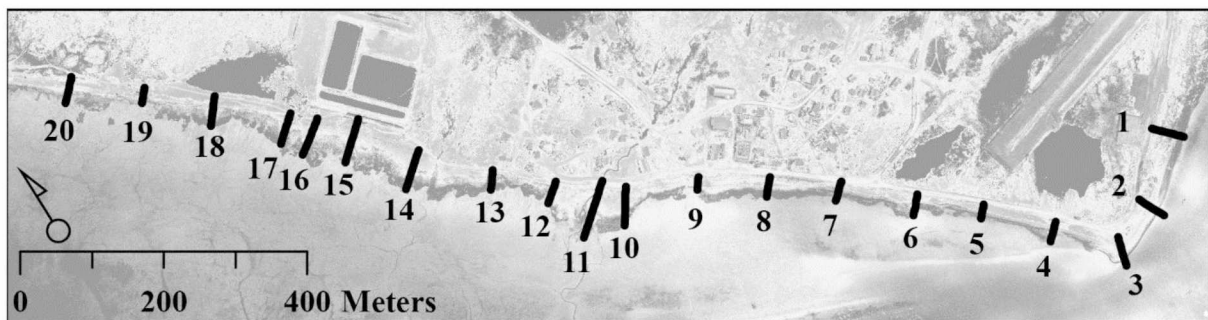


Figure 6. Cross-shore beach profiles sampled at 100 meters. Sub-sampled profiles occur in areas of higher variability.

## 2.3. Aerial and Satellite Image Correction

From repeat imagery, it is possible to extract clear, unambiguous evidence of change (e.g. Anders and Byrnes, 1991; Ford, 2013). However, the utility of making measurements in imagery is limited by a number of factors that are described here. For topographic measurements, uncertainties commonly arise from orthographic distortion (i.e. projecting three-dimensional topography on a two-dimensional plane) due to camera properties, position, and perspective (Moore, 2000; Thieler and Danforth, 1994). Comparing orthometrically-corrected (orthorectified) imagery requires that the images are co-registered on a relative horizontal metric, most commonly a projected coordinate system (e.g. Gibbs and Richmond, 2015; Hapke and Reid, 2007; Ruggiero et al., 2013). In order to identify change in image comparisons, these initial corrections are critical for reducing uncertainty.

This study used aerial photos originally collected for photogrammetric applications in 1957 by the United States Air Force, and in 1983 by NASA’s Alaska High Altitude Aerial Photography Program (Table 2; Figure 7). These images were processed in Agisoft Photoscan to correct for lens distortion, resolve camera positions in a geographic coordinate system, generate a dense point cloud, and ultimately create an orthomosaic. Ground control was not placed during this step, but reported camera position and height estimates were used with a 1000 m error. The orthomosaics were imported into ESRI ArcMap and georectified using permanent features within the most recent 2016 orthoimage. Given the age and resolution of imagery, it was not always possible to find an adequate number of ground control features, resulting in a qualitative best-fit model with a georectification residual error. However, geometric distortions were minimal because the images are orthometrically corrected.

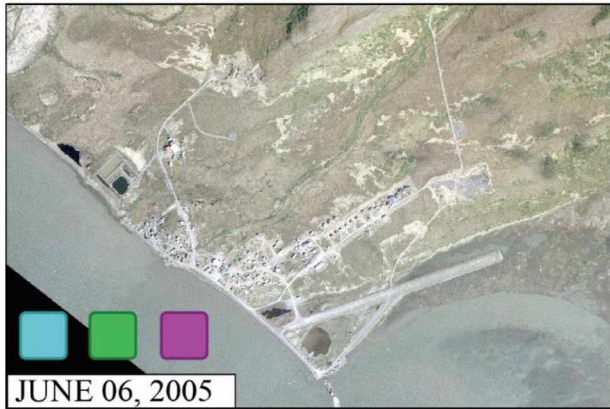
Table 2. Summary of images used for shoreline delineation.

Date	Type	Source	Scale / resolution	Post-processing pixel size (m)
1957/06/04	Aerial	US Air Force	1:42,800	1.10
1983/08/19	Aerial	NASA AHAP	1:65,500	1.26
2005/06/06	Aerial	Global Positioning Services, Inc.	1:2,400	0.61
2012/06/28	Satellite	Worldview-2, Digital Globe	0.61 m	0.61
2016/05/05	Aerial	Fairbanks Fodar	1:1,200	0.20

The 2005 aerial image was intended to be orthometrically corrected using 2004 RTK-GNSS survey data from Global Positional Services Incorporated. Contour lines were calculated for the village using photogrammetric and ground-based techniques, but no orthorectified image was created (Appendix IV). Of the two images produced, only the 1:2400 scale image displayed pertinent information for this study. This image was georeferenced using 35 ground control points and a first order polynomial solution on mostly near-bluff features that represented the bluff top plane. The image could not be orthorectified, so the uncertainty of obliquity to the bluff top plane is estimated. Using off-nadir roof displacement, upper-limit horizontal offsets were estimated to be 5.15 m at the farthest section of the studied bluffs. Because this estimate was based on loosely verifiable measurements, a conservative rounding to 8 m was used.

The 2012 Worldview-2 satellite multispectral (2.09 m) and panchromatic (0.61 m) images were received as a level one product with rational polynomial coefficient metadata, thus needing orthorectification. The ArcticDEM initiative used stereo auto-correlation techniques to produce digital surface models (DSM), which can be used to orthorectify Worldview imagery (Noh and Howat, 2015; DEM(s) were created from DigitalGlobe, Inc., imagery and funded under National Science Foundation awards 1043681, 1559691, and 1542736). The two strip files considered were computed from Worldview-2 image pairs, one set acquired on 10/10/2012, and the other on 11/22/2014. Mosaic files were not used because they contained significant artifacts disrupting the coastal areas of interest. The 2014 DSM (2.78 m) was used for orthorectification because it had sufficient overlap with the 2012 image. To address concern over landscape changes occurring between the image and DSM acquisitions, the 2012 DSM was subtracted from the 2014 DSM to determine differences in elevation. Within the study area, the largest variations occur because slight building offsets existed, significantly changing pixel values. Frequent variation also existed in water, mud flats, and the airport runway due to the inherent noisiness of these regions during auto-correlation (Noh and Howat, 2015). Differences in the DSMs were typically much lower along the beaches and bluff tops that this study focuses on. Thus, the 95% confidence interval (CI) provided a conservative estimate for DSM accuracy. This translated to an orthorectification error of 1.32 m for the 2012 images. The resulting raster datasets required minimal georeferencing to the 2016 dataset (RMS error = 0.00).

The 2016 imagery and DSM were produced through GNSS-tied structure-from-motion techniques by Fairbanks Fodar Incorporated, funded by the DGGS. No ground control were placed or surveyed for the acquisition, but the onboard dual- or multi-frequency GPS or GNSS was used to georeference the DSM (e.g. Nolan, Larsen, and Sturm, 2015). The DSM was compared to the 2016 RTK-GNSS survey for accuracy, controlling for bare-earth positions (NDEP, 2004). The mean difference in the DSM and the survey elevations found was  $-0.11 \text{ m} \pm 0.22 \text{ m}$  (95% CI;  $n = 64$ ). Incorporating GPS precision in horizontal (0.0156 m) and vertical (0.0196 m) for this set of points, the total error of the 2016 SFM image in the study area was 0.22 m.



Dataset Attributes





 High Water	 Elevation Model
 Near Flood Year	 Infrared

Figure 7. Available imagery of Goodnews Bay with the spatial resolution necessary for shoreline delineation.



## **2.4. Shoreline Change Analysis**

### *2.4.1. Shoreline Proxy*

Choosing a proxy indicator for shoreline change is an integral decision that influences every aspect of the study (Boak and Turner, 2005). Traditional shoreline erosion studies often compare the position of high water, or indicators of high water, over time to determine how quickly and in what direction the shoreline or beach is changing (e.g. Anders and Byrnes, 1991; Crowell, Leatherman, and Buckley, 1991; Ruggiero et al., 2013; Vieira da Silva et al., 2016). However, the relationship between the high water position and erosion is not always linear, especially when considering erosion of bluffs that are not submerged or contacted by waves at high tide (Boak and Turner, 2005). Goodnews erosion reports indicate that the bluff is eroded by large storms and flooding, but do not indicate beach erosion or sea level change is occurring at a significant rate (Table 1). Changes in beach morphology and extent cannot be detected if they are smaller in horizontal extent than the uncertainty of the images used for comparison. Beach-based shoreline proxies, such as the wrack line or high/instantaneous water line, were not observed in most images, do not directly relate to the problems the village is reporting, and induce heightened uncertainty because they cannot be tied to a tidal datum with reasonable accuracy without a long-term tide gauge (e.g. Gibbs and Richmond, 2015). For these report-based and data limitation-based reasons, the bluff top was the most suitable proxy indicator for erosion in the village (e.g. Gibbs and Richmond, 2015; Hapke and Reid, 2007). Of the entire coastline, two segments are backed by a bluff: the armored bluff fronting the village, and the unarmored bluff north of the sewage lagoon (Figure 1; Figure 8). The unarmored bluff has not been modified after erosion, so it served as a control variable for the area, representing natural (unmitigated) erosion rates. The efficacy of this control variable is discussed in Section 4.1.

### *2.4.2. Digital Shoreline Setup and Uncertainty*

Acknowledging, addressing, and reducing uncertainty is crucial for making precise, reliable measurements (Moore, 2000; Thieler and Danforth, 1994). Several variables are introduced between acquiring two raw images and making measurements between them, and each variable has the potential to offset the dataset or mislead the interpreter. For these reasons, uncertainty is conservatively accounted for.

Shoreline change was quantified by examining various statistics on the distance and time between shoreline positions. Bluff tops were delineated manually in ArcMap and statistics were calculated using DSAS: a baseline was drawn to run approximately parallel to the shoreline, and transects were cast perpendicular at 5-meter spacing with 100-meter smoothing (Figure 8). Along each transect, the horizontal distance between each shoreline was calculated.

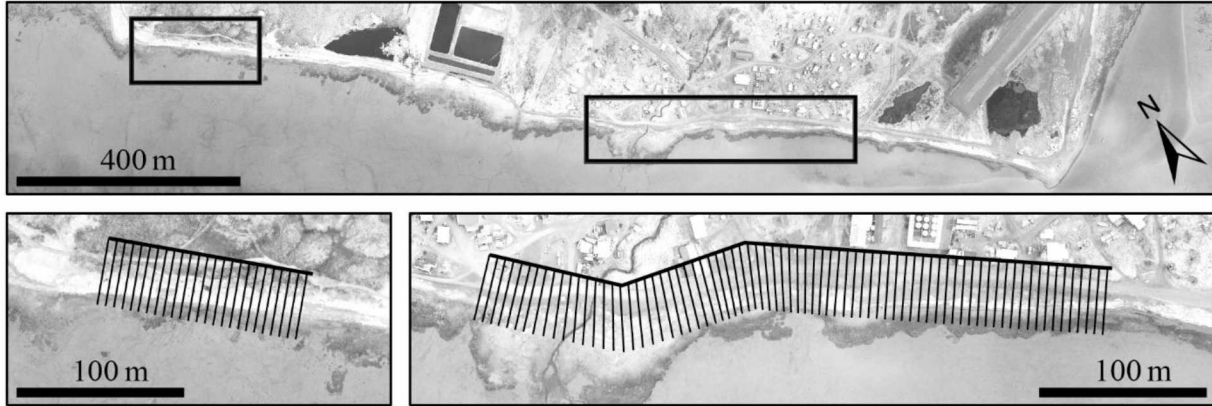


Figure 8. DSAS transects cast for change analysis of the unarmored bluff (left) and armored bluff (right).

Total horizontal position uncertainty ( $U_t$ ) for each shoreline was calculated by the root sum of squares (RSS) of the digitizing uncertainty ( $U_d$ ), orthorectification uncertainty ( $U_o$ ), georectification error ( $U_g$ ), and base image ground control uncertainty ( $U_c$ ) (Eq. 1; Table 3). This is the most common method for summarizing uncertainty in shoreline delineation (e.g. Gibbs and Richmond, 2015; Kinsman and Gould, 2014; Ruggiero et al., 2013). Using the bluff top, instead of a highly variable or seasonally influenced feature such as the high water line, eliminated other commonly factored uncertainties related to changes in the tidal regime (Boak and Turner, 2005).

$U_t$  – position unc.

$U_d$  – digitizing unc.

$U_o$  – orthorectification unc.

$U_g$  – georectification err.

$U_c$  – ground control unc.

$$U_t = \sqrt{U_d^2 + U_o^2 + U_g^2 + U_c^2} \quad [1]$$

No standard is set to fully quantify digitizing uncertainty, but shoreline studies generally assume the ability of the user to interpret features accurately is directly related to pixel size or image scale (e.g. Crowell, Leatherman, and Buckley, 1993; Gibbs and Richmond, 2015; Ruggiero et al., 2013). When interpreting features in imagery, user bias is an important

consideration. This is commonly quantified as a horizontal uncertainty value calculated by comparing the results of different operators digitizing the imagery (e.g. Kinsman and Gould, 2014; Romine et al., 2009). However, user bias describes the level of consistency between operators and the sole digitizer, which may vary considerably with each individual's familiarity of the area of interest and the information contained in different types of imagery. On the other hand, user precision describes the consistency of the sole digitizer (e.g. Ford, 2013). Working under the assumption that the user is adequately familiar with the image information and contents, it is inferred in this study that the user precision statistic would prove more suitable than user bias as a digitizing uncertainty value, thus precision was used.

Factors not often accounted for in manual digitization uncertainty are parameters and techniques that enhance features of interest, such as spectral resolution, wavelengths used, and image augmentation. These can be as simple as contrast stretching and histogram thresholding, to more sophisticated methods using near infrared bands to distinguish vegetation types and bare earth. The availability and practicality of these parameters is highly variable from 1950s imagery to modern satellites and aerial surveys, but overall their application can increase qualitative certainty in accurate feature interpretation. With the help of these remote sensing parameters and techniques, the bluff top was manually delineated three times in each image of Goodnews. Digitizing precision ( $U_p$ ) was calculated for each image by taking the mean of the maximum distance between the three lines ( $L_1, L_2, L_3$ ) on each transect, *i.e.* the average difference between digitizing attempts (Eq. 2). The total digitizing uncertainty ( $U_d$ ) was then considered to be the sum of the digitizing ability (pixel size =  $U_a$ ) and digitizing precision for each image (Eq. 3). For actual analysis, either the shoreline was digitized again, or a qualitative best-fit shoreline was chosen from the three lines.

$L_n$ – distance to baseline $U_a$ – pixel size $U_d$ – digitizing unc. $U_p$ – digitizing precision	$U_p = \sum_{i=1}^n \max( L_{1i} - L_{2i} ,  L_{1i} - L_{3i} ,  L_{2i} - L_{3i} )$	[2]
	$U_d = U_a + U_p$	[3]

Table 3. Bluff top edge position uncertainty values with year and total uncertainty ( $U_t$ ) bolded.

Year	Digitizing Errors						$U_t$
	$U_p$	$U_a$	$U_d$	$U_o$	$U_g$	$U_c$	
<b>1957</b>	1.41	1.10	2.51	0.16	0.04	0.22	<b>2.53</b>
<b>1983</b>	1.44	1.26	2.70	0.12	0.05	0.22	<b>2.71</b>
<b>2005</b>	1.27	0.61	1.88	8.00	0.01	0.22	<b>8.22</b>
<b>2012</b>	1.39	0.61	2.00	1.32	0.00	0.22	<b>2.41</b>
<b>2016</b>	0.49	0.20	0.61	0.00	0.00	0.22	<b>0.72</b>

#### 2.4.3. Digital Shoreline Measurements and Assessment

Analyzing changes in the position of the bluff top edge requires predetermining the parameters and statistics used for comparison. Positions were compared sequentially, and were divided into the armored and unarmored zones. Comparisons were always made on the same set of virtual transects (Figure 8). Erosion rates were normalized into meters per year (m/y) in order to make consistent comparisons, as temporal resolution was too low to perform an event-to-event or pre- and post-event analysis. However, the use of this metric did not intend to assert that erosion happens at an annual rate, as it has been reported that erosion occurs in individual, stochastic events rather than gradually (Table 1). The following statistics, summarized in Table 4, were calculated using DSAS and described in more detail in the DSAS user guide (Himmelstoss, 2009).

To evaluate at what rate the Goodnews coastline is changing over time, multiple change statistics were taken into account. Average change of the area over the entire study period was quantified using the weighted linear regression rate-of-change statistic (WLR) computed on each transect using all available shorelines. Unlike the linear regression approach, this method uses  $U_t$  to give more control to shoreline positions with higher certainty (Genz, 2007). The WLR is supported with a 90% confidence interval (WCI) and R-squared value (WR2). Total change of the area was calculated using the net shoreline movement (NSM), which describes the distance between the oldest and most recent shoreline along each transect. The NSM is reported as a negative distance in meters for landward movement (erosion), and positive for seaward movement (progradation). The WLR and NSM for all shorelines were used to describe the magnitude and linearity of erosion over the entire study period.

Table 4. List of DSAS statistics (from Himmelstoss, 2009).

EPR	End point rate (m/y)	Distance between oldest and youngest shorelines divided by the time elapsed between them
ECI	EPR confidence interval (m/y)	Root mean sum of squares of the EPR shorelines' total uncertainties divided by the time elapsed between them
NSM	Net shoreline movement (m)	Distance between oldest and youngest shorelines
WLR	Weighted linear regression rate-of-change (m/y)	Linear regression rate of change weighted by the inverse of the squared variance in the uncertainty
WCI	WLR 90% confidence interval (m/y)	90% confidence interval for the standard error of the WLR slope
WR2	WLR R <sup>2</sup> value (unitless)	Percentage (0.0 – 1.0) of variance in the data that is explained by a regression

Calculating the NSM of each sequential image pair (e.g. from 1953 to 1983, then 1983 to 2005, etc.) describes the horizontal position change on the smallest temporal scale achievable by this dataset, but is less useful when comparing time periods of different lengths (e.g. 1953 to 1983 vs. 2012 to 2016). Thus, movement per period was standardized by the end point rate (EPR) statistic. The EPR is calculated by dividing the NSM by the number of decimal years between the two images, resulting in the m/y rate of change. This value is supplemented by the end point rate confidence interval (ECI), which is the RSS of the total uncertainty of each image ( $A_U, B_U$ ) divided by the years ( $A_y, B_y$ ) between them (Eq. 4).

$A_U$  – image A unc.  
 $A_y$  – image A year  
 $B_U$  – image B unc.  
 $B_y$  – image B year

$$ECI = \frac{\sqrt{A_U^2 + B_U^2}}{A_y - B_y} \quad [4]$$

Variability between the armored and unarmored bluff was addressed in order to determine the effect of mitigation. This assessment was made by testing the significance of the mean WLR, EPR, and NSM of each site to the 95% CI, per time period and over the entire study as appropriate.

## 2.5. Projecting Future Shorelines

This study projected future positions using the dataset and corresponding statistics described in Section 2.4. For each transect, the WLR ( $T_{WLR}$ ) in m/y was multiplied by the number of years between the last recorded shoreline ( $C_y$ ) and the future projection ( $F_y$ ). The resulting number ( $T_f$ ) represented the along-transect distance that the new shoreline is positioned, relative to the most recent shoreline. This distance was converted into a coordinate, and each coordinate was linked sequentially into a line to define a future shoreline in a geospatial context. The WCI of each transect ( $T_{WCI}$ ) in m/y was incorporated exactly as WLR was used in Eq. 5, and converted into a line of linked coordinates in order to determine a spatial footprint of confidence in the estimate ( $T_U$ ) (Eq. 6). This calculation was accomplished using a custom ArcGIS tool described by Gould, Kinsman, and Hendricks (2015).

$$\begin{array}{ll} T_f & \text{– distance of change} \\ T_{WLR} & \text{– WLR of the transect} \\ C_y & \text{– most recent shoreline year} \\ F_y & \text{– future projection year} \end{array} \quad \begin{array}{l} T_f = T_{WLR} \times (F_y - C_y) \\ T_U = T_{WCI} \times (F_y - C_y) \end{array} \quad \begin{array}{l} [5] \\ [6] \end{array}$$

## 2.6. Estimating Goodnews Tidal Datum

As mentioned previously, no tidal datum has been established for the city of Goodnews Bay, but a datum does exist for Platinum, 16 km west at the head of the bay. In order to estimate the tidal datum at Goodnews, a HOBO pressure gauge was deployed from August 25-29<sup>th</sup>, 2015 in the Goodnews River terminus approximately 100 m southwest of The Point. This gauge measured water level above the sensor in meters at 30-second intervals. Unfortunately, GPS equipment failure prevented the data series from being tied to an absolute vertical datum. Instead, the NAVD88 elevation of the gauge was estimated using the approximate ( $\pm 3$  m) horizontal position and a quadratic fit of the slope of the mud flats, based on the 2016 DSM elevation values. This 5-day water level series was used in conjunction with the Platinum station's NOAA Center for Operational Oceanographic Products and Services (CO-OPS) tide prediction and tidal datums to calculate the tidal datums at Goodnews. A tide-by-tide analysis was performed using the modified range ratio method for semidiurnal tides (USDC, 2003).

## **2.7. Estimating Total Water Level of Large Storms**

Nearly every storm damage report from Goodnews involved flooding, but corresponding total water level estimates have yet to be referenced to a common vertical datum. This included the most recent storm in 2011. Available data on storm surge elevations was compiled in this thesis to fill this data gap. Primary indicators of storm surge and wave run-up were scarcely documented, so state reports and local anecdotal accounts were used to best estimate water level during large storms. The estimates were made in the North American Vertical Datum of 1988 (NAVD88), and later referenced to the approximate local tidal datum, as established in this study. Storm surge and tidal datum estimates will be included in the color-index elevation map described in Section 1.4, which is meant to serve as a tool to visualize where previous storm surge has reached (Tschetter, Kinsman, and Fish, 2014).

### *2.7.1. 1979 Storm TWL Estimate*

Accounts about the destructive 1979 storm and subsequent flooding in Goodnews come from community interviews and reports directed by the Alaska District Corps of Engineers Flood Plain Management (Appendix II). In 1994, a survey was conducted in order to estimate the 1979 flood elevation relative to a temporary benchmark (Table 5; Appendix II). They found that water went under resident James Bright's house, but did not flood the first floor. The house still stands to this date, but is unoccupied.

Two of the 1994 survey targets were re-measured during this study's 2016 survey, manhole #4 and the seaward-most ground point of James Bright's house. Using these as reference points, the 1979 water level was estimated to have reached 4.80 m NAVD88. The elevations between the two surveys varied by 0.20 m.

Table 5. Survey information to estimate 1979 flood elevation. Survey information was recorded verbatim from the survey conducted by the Alaska District Corps of Engineers Flood Plain Management (Appendix II).

Survey Information	Elevation (ft)	Elevation (m)	Elevation (m NAVD88)
TBM [temporary benchmark], door sill of city hall main entrance	100.00	30.48	--
Rim of manhole cover #1, the first manhole north of city hall	98.16	29.92	--
Rim of manhole cover #2, the second manhole north	91.11	27.77	--
Rim of manhole cover #3, the third manhole north of city hall, and the first south of the creek	87.36	26.63	--
Rim of manhole cover #4, first manhole north of the creek	83.98	25.60	4.97
Ground level at James Bright's House	83.11	25.33	4.66
Tide level of Goodnews bay at 9:45 am, 9/15/94 tide estimated to be about mid-range	71.35	21.75	--
Estimated 1979 flood elevation	83.50	25.45	4.80
Recommended minimum building elevation	85.50	26.06	5.39

### 2.7.2. 1969 and 1989 Storm TWL Estimate

The Flood Plain Management report stated that the 1969 storm flooded the airport runway with 6-12 inches (0.15 – 0.30 m) of water, and the 1989 storm also flooded the airstrip (to what degree was not stated). Thus, these two storms were treated as having the same surge elevation. The footprint of the previous runway is still visible in the 2016 dataset, with elevations ranging between 2.5 - 4.0 m. However, the magnitude of its demolition during the construction of the new runway is not known. The only surveyed elevation information found for the previous airstrip came from the 2004 map prepared by Global Positioning Services, Inc. They surveyed several points in the village in order to tie GCPs for a photogrammetric survey, which produced contour elevations of the runway. These contours depicted the runway surface between 12 to 14 feet (3.7 to 4.3 m) relative to the published ellipsoid height of the referenced benchmark “BLM EC 10757 1980”. The benchmark could not be recovered in 2016, so the survey points were compared to the 2016 DSM for elevation offsets in order to place them in the NAVD88 vertical datum. Points were first filtered to remove areas with vegetation, high-angle features, and



significant changes such as road grading. Then their relative elevation in meters was subtracted by the elevation of the DSM cell they represent. On average, the 2004 points lay 0.80 meters below the 2016 elevation (SD = 0.20 m; n = 15). This offset estimate placed the previous runway surface between 4.5 and 5.0 m NAVD88.

### 2.7.3. 2011 Storm TWL Estimate Using Proxy Indicators

Data for this storm surge came from images taken the day after the storm, anecdotal accounts, and physical evidence of water levels (Table 6). Features either were surveyed with RTK-GNSS (0.02 m accuracy), or estimated using the 2016 DSM (0.22 m accuracy). Several photographs of wave-carried ice and debris, taken directly following the storm, were compared to the 2016 DSM to determine their elevation. Estimates of the peak water level ranged from 5.0 to 5.5 m, with one report stating wave-tips reached 5.57 m.

Table 6. Water level proxies used to estimate elevation of 2011 storm surge. Numbers in parenthesis correspond to the photo number in Appendix I.

	Water Level Proxy	2016 GNSS Elev. (m NAVD88)	2016 DSM Elev. (m NAVD88)
Upper Limit	Evan Evan’s porch step (095)	5.57	
	Debris around pump station (075, 090)		5.3-5.5
	Current airport runway surface (069, 071, 072, 111)		4.6-5.5
	Debris up to road behind Bright house (079, 087)		5
Lower Limit	James Bright Jr.’s former house (086)	4.66	
	Airport fence (downed) (072)		4.6
	Surge-carried muddy debris	4.34	
	Surge-carried muddy debris	4.02	

### 2.7.4. 2011 Storm TWL Estimate Using Ocean and Weather Information

As explained in Section 1.3, no active tide gauge exists in Goodnews Bay or the surrounding area. In the absence of direct water level measurements, TWL can be estimated using tide, surge, and wave runup models. A tidal datum was established at Platinum, 16 km west on the bay side of the inlet between the Bering Sea and Goodnews Bay (station 9465396)

(Figure 9). Astronomical tide predictions, made by NOAA CO-OPS, are computed relative to Platinum datums, although the data are not quality controlled by National Ocean Service procedures. The NWS operationally models storm surge using the Sea Lake and Overland Surge from Hurricanes model for Alaska. The NWS model incorporates storm pressure, extent, forward speed, and track in order to estimate surge height from a simulated wind field (Jelesnianski, Chen, and Shaffer, 1992). Surge heights are reported as a height above predicted astronomical tide levels (storm tide = tide + surge). In order to estimate marine TWL (TWL = tide + surge + wave runup), wave runup is calculated using a parametrized model (Stockdon et al., 2006). Offshore deep-water (20 m) peak wave period and significant wave height measured by the USACE Wave Information Studies station 82234 are combined with the average beach slope from 20 beach profiles in Goodnews Bay to estimate maximum setup (Eq. 7) and maximum 2% runup (Eq. 8).

$$\begin{array}{ll}
 R_2 & \text{-- 2\% runup exceedance} \\
 \beta_f & \text{-- beach slope} \\
 H_0 & \text{-- significant wave height} \\
 L_0 & \text{-- peak wave period} \\
 \langle \eta \rangle & \text{-- maximum setup height}
 \end{array}
 \quad
 \begin{array}{l}
 \langle \eta \rangle = 0.35\beta_f(H_0L_0)^{\frac{1}{2}} \quad [7] \\
 R_2 = 1.1 \left( \langle \eta \rangle + 0.5[H_0L_0(0.563\beta_f^2 + 0.004)]^{\frac{1}{2}} \right) \quad [8]
 \end{array}$$

For this study, CO-OPS water level predictions, NWS storm surge estimates, and wave runup and setup estimates were combined at 6-minute intervals from November 11 to 14, 2011 AKST (GMT – 09:00). The sum of the datasets were used to estimate marine TWL. Vertical error in the NWS model is estimated to be 20% of the surge height (Jelesnianski, Chen, and Shaffer, 1992; Taylor and Glahn, 2008).

## 2.8. Estimating Wave Impact Hours

Wave Impact Hours (WIH) are used to describe erosion susceptibility based on temporal exposure to wave energy (Hapke and Plant, 2010; Ruggiero et al., 2001). WIH are estimated by calculating the amount of time TWLs exceed the elevation of specific coastal features. To model WIH in Goodnews, hourly TWL estimates from 2009 to 2014 are compared to elevations of MHHW, bluff toe, and bluff top (elevations are extracted from the beach profile survey and Goodnews tidal datums) (Figure 9).

Three categories of wave impact are used:

1. Beach erosion  $MHHW \leq TWL_t < \text{bluff toe}$
2. Bluff collision  $\text{bluff toe} \leq TWL_t < \text{bluff top}$
3. Bluff overtopping  $\text{bluff top} \leq TWL_t$

WIH are computed for the 11/11/2011 storm, as well as annual monthly means to determine if the event was an anomaly.

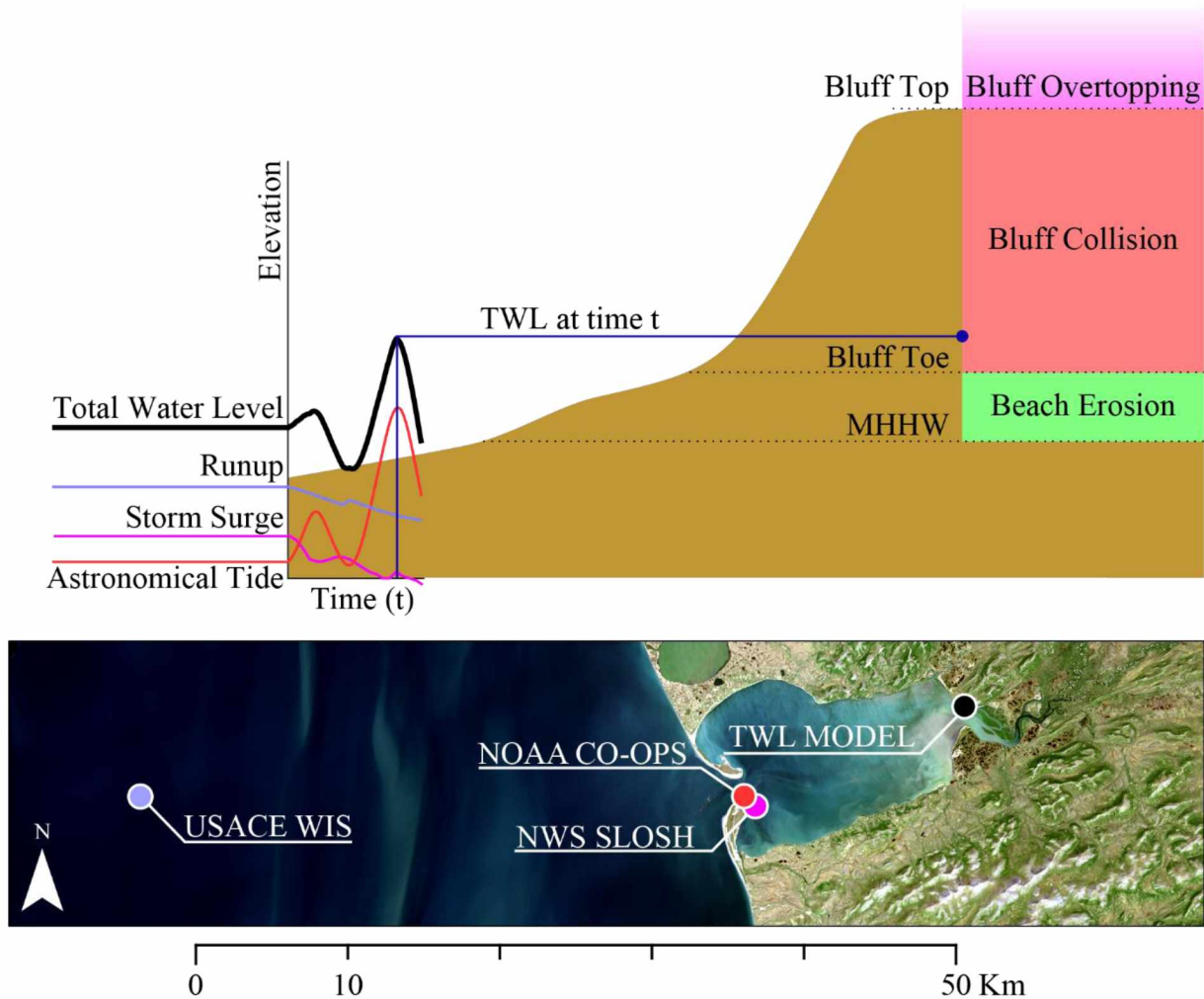


Figure 9. Datasets used for total water level and wave impact hour analyses. Total water level at Goodnews is computed as the summation of NOAA tide estimates (red), NWS storm surge estimates (purple), and USACE offshore data with the Stockdon et al. (2006) runup equation (periwinkle). In a given time period, the number of hours that total water level exceeds MHHW, the bluff toe, and the bluff top is calculated and categorized into beach erosion, bluff collision, and bluff overtopping. In this schematic, the total water level at selected time  $t$  exceeds the bluff toe, but not the bluff top, resulting in bluff collision.

## CHAPTER 3

### RESULTS

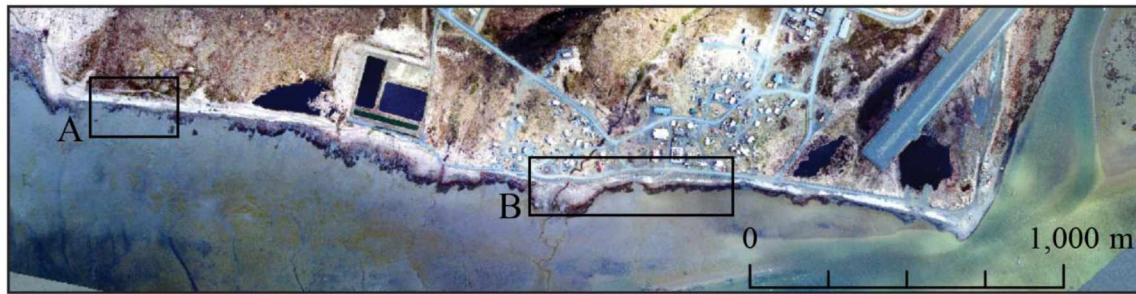
The following subsections describe and illustrate the results found through the shoreline change analysis, future shoreline projections, and modeling storm surge extent based on the estimated TWL. Changes are analyzed across the entire study period and for image-to-image periods in an effort to identify trends that may relate to specific storms. Some statistics are reported in meters per year in an effort to compare periods of different lengths of time, but the use of this unit does not intend to assert that change occurs at a constant rate through time. Estimated storm surge elevations are mapped in a single-value model, as well as the local MHHW estimate. A sample of the single beach profile survey is provided, and the dataset can be found in Appendix V.

#### **3.1. Shoreline Change Analysis (1957 – 2016)**

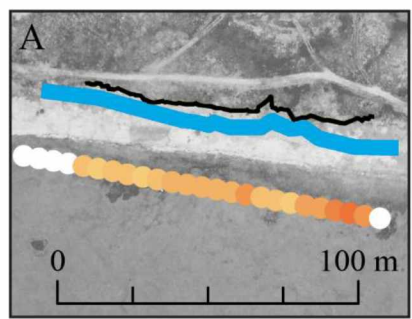
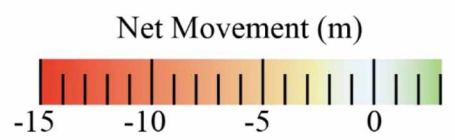
##### *3.1.1. Detecting Net Change*

From 1957 to 2016, significant erosion is detected at both bluffs (Figure 10). The highest net movement (NSM) of the bluff edge is 13 m, which occurred at both promontories directly north and south of the creek running through the village. The unarmored bluff north of the village exhibited between 3.4 to 9.8 m of net erosion, with a general increase toward the southeast. All NSMs of the unarmored bluff are statistically significant from zero, but the armored bluff experienced considerable spatial variability. On average, the unarmored bluff edge eroded  $5.9 \pm 1.1$  m, and the armored bluff eroded  $3.2 \pm 2.8$  m (95% CI). Measurements could not be made directly on the creek bridge, but net movement remains statistically significant on either side of the creek (Figure 10). The majority of the bluff edge south of the headlands exhibits no significant movement, so this region of the bluff may be considered moderately stable over the period of analysis.

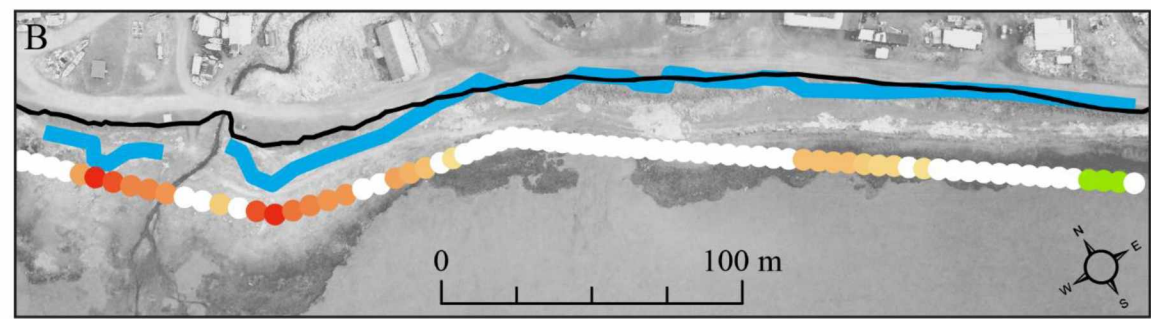
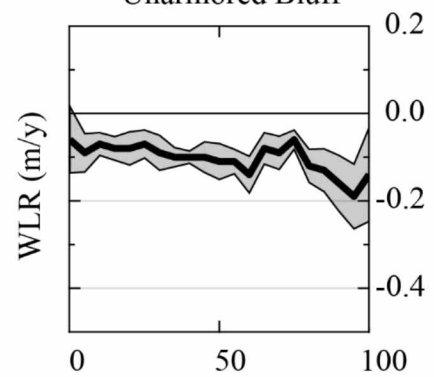
Figure 10. Net movement and weighted linear change of bluff top edges between 1957 (blue) and 2016 (black). The footprint of each line represents total uncertainty. Net movement is shown by the color of the circles following each bluff: red circles are high landward movement and green circles are seaward movement. White circles are plotted where the bluff is considered stable, based on when the WLR is less than the 90% CI. The unarmored bluff (A) exhibits fairly consistent erosion, whereas the spatially variable armored bluff (B) has the highest net movement in both directions, as well as the greatest area of stable shoreline. For averaging change of the armored bluff, the region is divided by the dotted line into *North* and *South* to account for this transition.



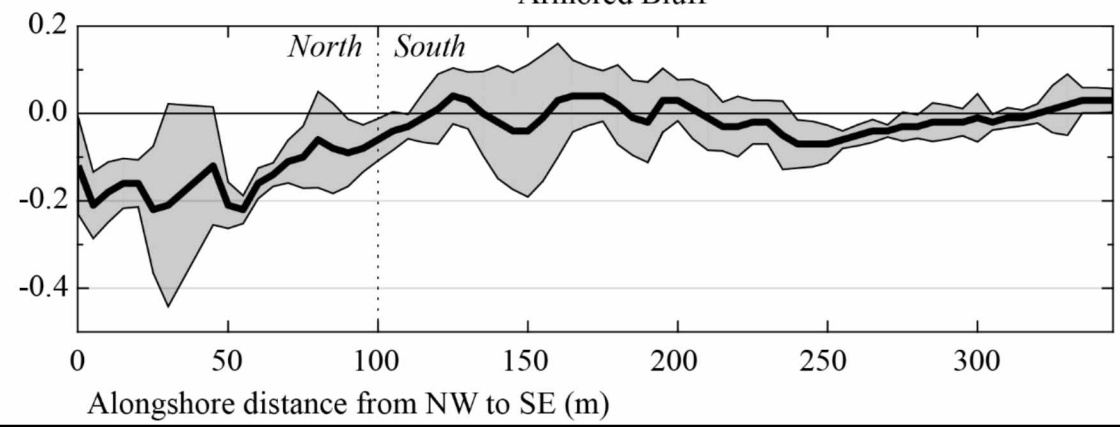
Bluff Position Change 1957 - 2016  
Goodnews Bay, AK



Unarmored Bluff



Armored Bluff



The weighted linear rate of change statistic (WLR) incorporates all available shorelines and their uncertainties to calculate the rate of movement per year. Based on these calculations, the unarmored bluff eroded at an average rate of  $0.10 \pm 0.07$  m/y (95% CI;  $R^2 = 0.92$ ; Table 7). The armored bluff exhibited spatially variable erosion rates, and was thus sub-divided into northern and southern regions (Figure 10). The northern 100-meter section of the armored bluff eroded  $0.14 \pm 0.11$  m/y on average (95% confidence;  $R^2 = 0.82$ ). Meanwhile, mean change of the 245-meter southern armored bluff remained insignificant from 0 m/y (Table 7). Thus, the northern armored bluff and the unarmored bluff are shown to erode at similar rates, while the southern armored bluff appeared fairly stable overall.

Table 7. Mean weighted linear regression rate-of-change for each bluff. Sub-sectioning the armored bluff highlights that the northern area exhibits significant erosion, whereas the southern area is stable.

Bluff	WLR (m/y)		$R^2$	
	Mean	2SD	Mean	2SD
Unarmored	-0.10	0.07	0.91	0.13
Armored <sub>total</sub>	-0.05	0.14	0.50	0.69
Armored <sub>north</sub>	-0.14	0.11	0.82	0.34
Armored <sub>south</sub>	-0.01	0.06	0.37	0.61

### 3.1.2. Detecting Event-Based Change

To determine the impact of specific storms on the bluffs, measurements need to be taken on the smallest timeline possible. End point rates (EPRs) are measured for each chronological image pair, and their annualized unit allows each time period to be compared (Figure 11). However, for the majority of sequential image pairs, the change detected is often less than the EPR confidence interval (ECI). This approach results in no significant regional change over each time period, but this is largely due to the high uncertainty of the 2005 shoreline. By removing 2005 from the analysis, clear localized changes are found (Figure 12).

After removing the 2005 image, the data are resorted into two categories: pre- and post-1983 shorelines. For these comparisons, the net shoreline movement (NSM) is used to determine the extent of movement over the time period, since both time periods are nearly the same. From

1957 to 1983, two major storms occurred which reportedly flooded the airstrip (Figure 13; Table 1). During this period, the armored bluff eroded up to 9 m at certain points around the creek area (Figure 14). In contrast, the unarmored bluff did not exhibit any change that could be detected. From 1983 to 2016, two major storms occurred which reportedly caused flooding and erosion of the airstrip (Figure 13; Table 1). The unarmored bluff eroded uniformly along its extent, with an average along-shore retreat of 4.4 m. The armored bluff eroded up to 9 m near the creek, but seaward change was also detected in the southern region, which had eroded significantly before 1983. This apparent progradation of the bluff face is likely from re-armoring the bluff (see Section 4.1). It is important to note that the net movement in parts of the southern region is identified as stable in Figure 10, but this evidence suggests that that the bluff has undergone intense modification.



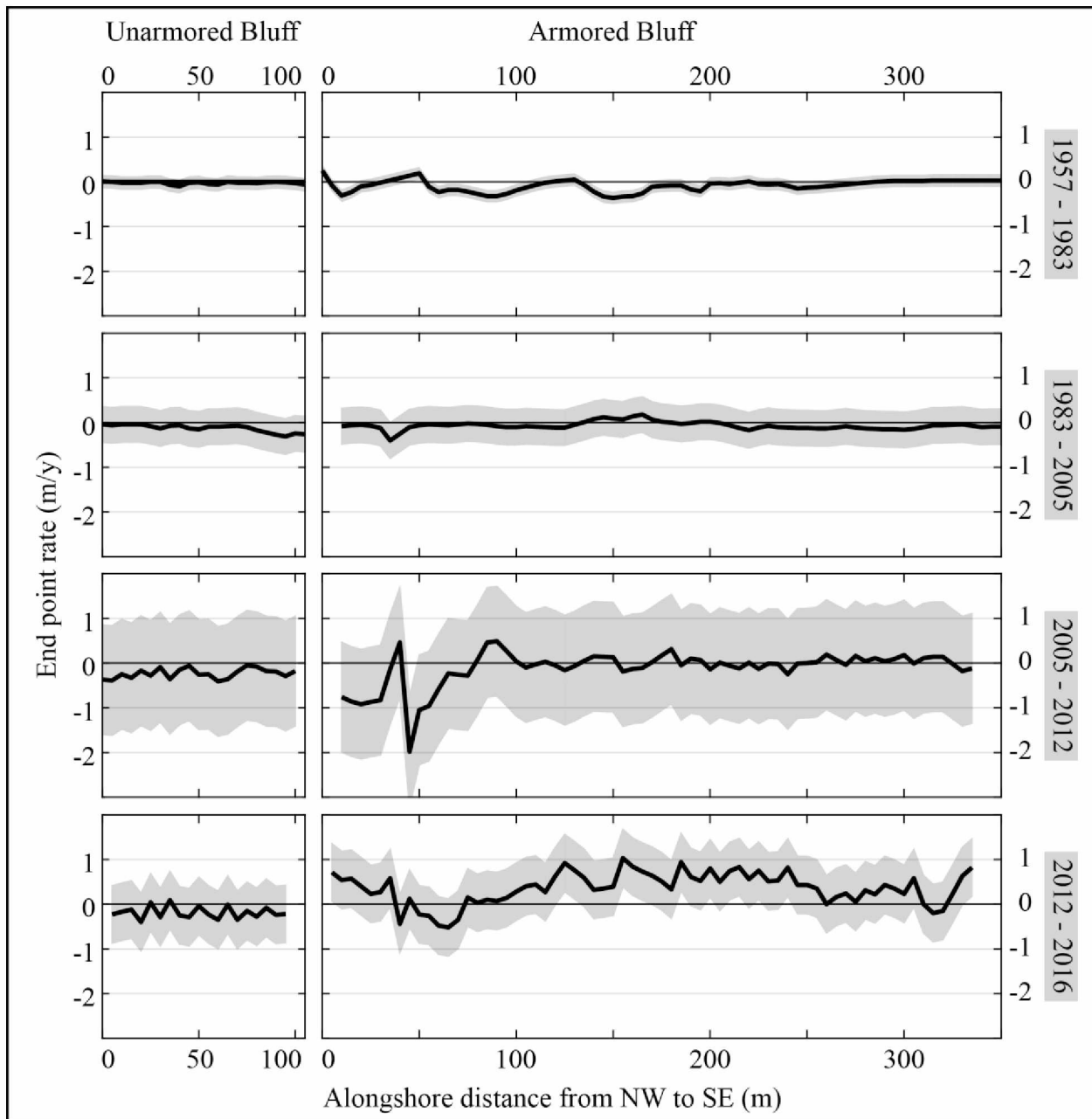


Figure 11. Bluff edge change rate (black line) for each time period. The gray region represents the 95% confidence interval. When the gray region is not crossing 0, a significant change was detected. Change in the unarmored bluff (left) is not detected for any period, and for most periods the armored bluff (right) exhibits no detectable change.

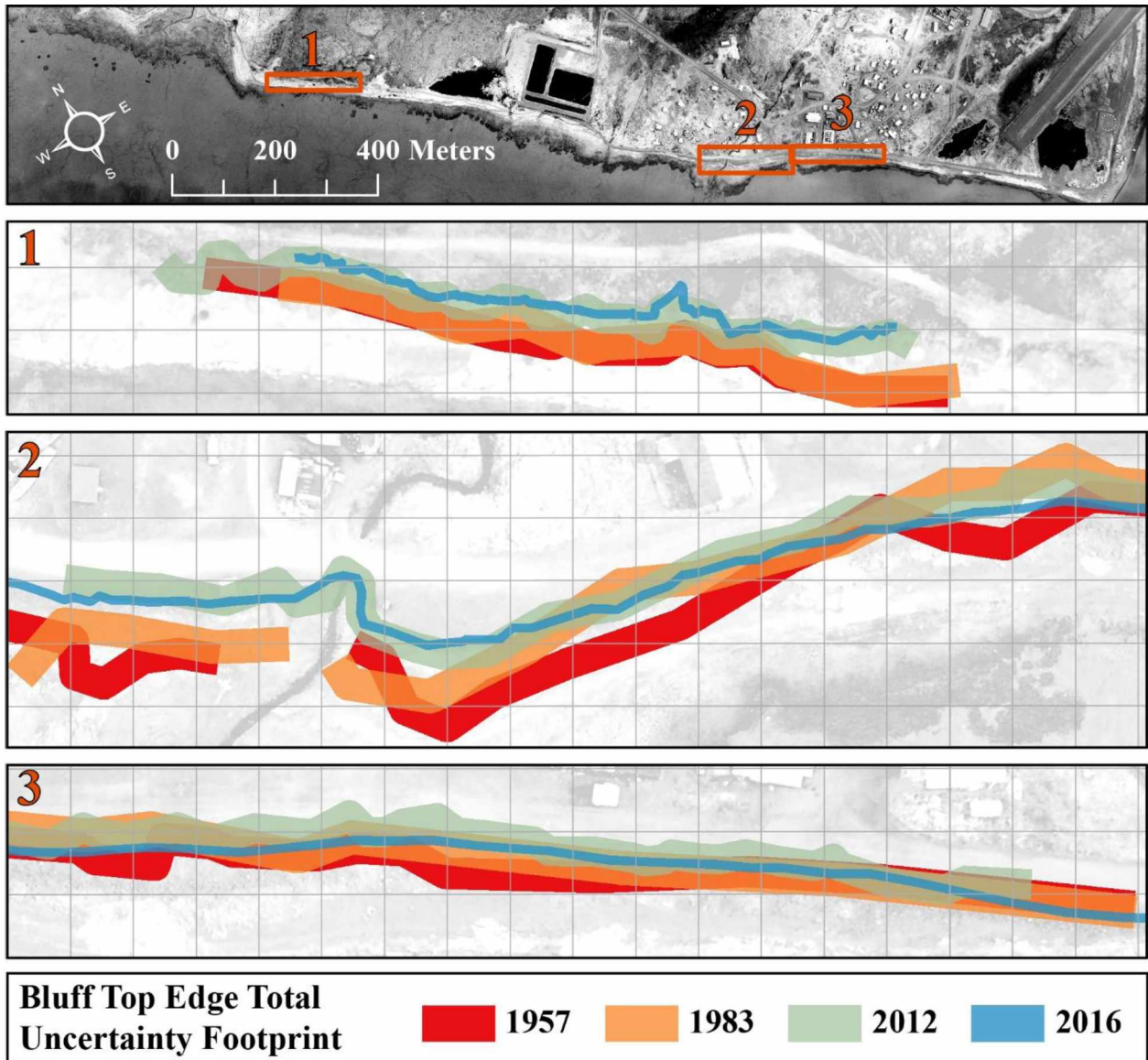


Figure 12. Total uncertainty footprint of each bluff edge overlaid on a 20x20 meter cell grid. Overlapping footprints indicate insignificant change measured in that location. The majority of the unarmored bluff (zone 1) is indistinguishable on an image-to-image basis, but exhibits detectable change over longer periods. The armored bluff displays distinct movement between the 1983 and 2012 in zone 2, but essentially no change between any periods in zone 3. The 2005 footprint intersects all other bluff edges (due to very high uncertainty), and thus was left out of this graphic for simplicity.

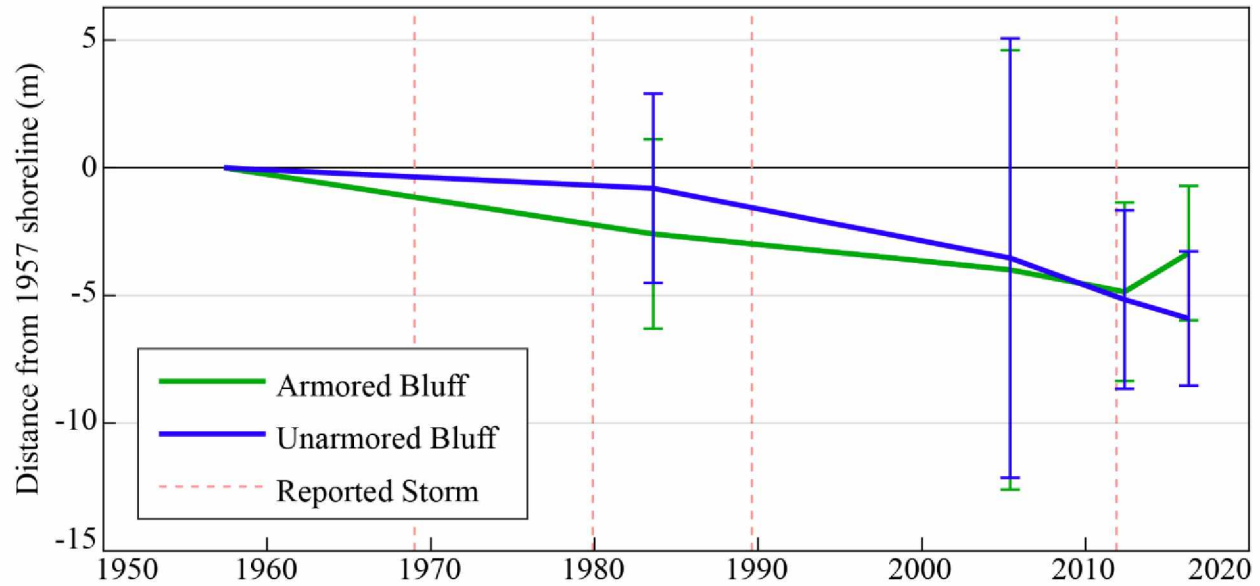


Figure 13. Mean distance from the 1957 bluff top edge. Error bars reflect the RSS of the uncertainties of 1957 and the respective year. Dashed red lines represent strong storms that reportedly flooded the airstrip. Only since 2012 do mean distances become statistically significant from 1957 positions.

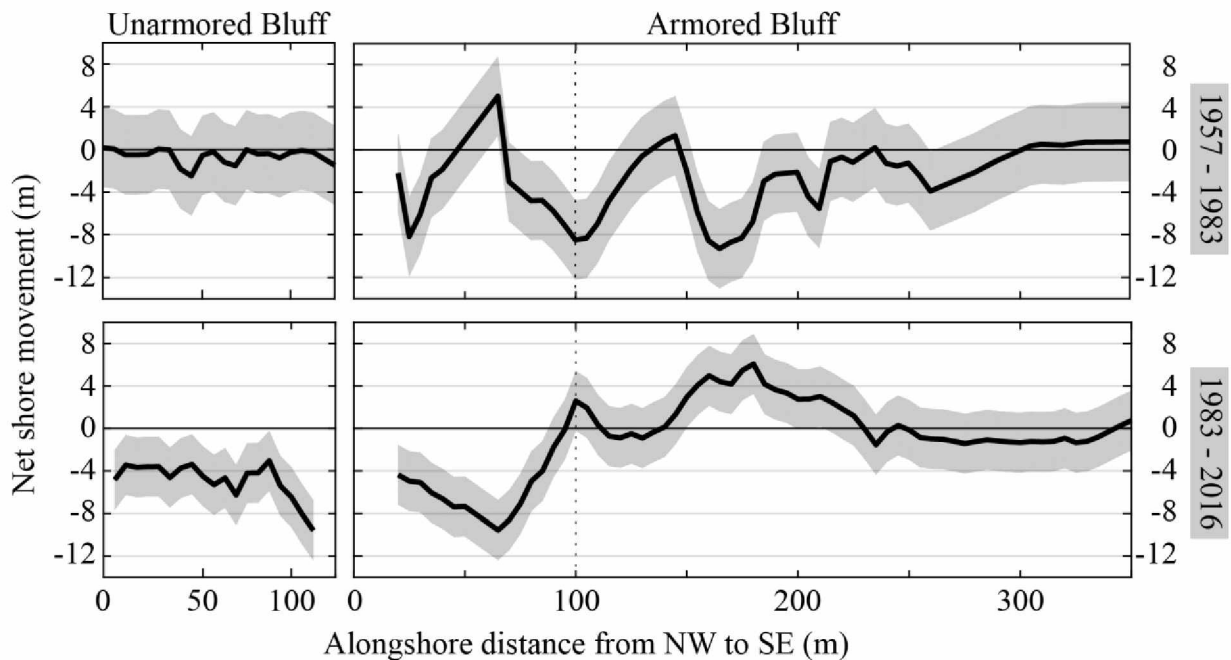


Figure 14. Net horizontal movement of the bluff edge from 1957 to 1983, and from 1983 to 2016. The gray area represents the RSS of the respective uncertainties. The unarmored bluff eroded consistently across its face in the recent period. The armored bluff experienced significant erosion near the creek in both periods, but erosion and replenishment in the southern section.

### 3.2. Bluff Top Edge Projection

Projecting the bluff top edge, while quantitative and statistical in method, is also reliant on assumption and interpretation. For example, contemporary rates show net seaward change for parts of the armored bluff, so a projection from this period would show this section of bluff building outward into the bay. However, it is assumed that the community does not intend to expand the bluff beyond its current extent. Instead, the contemporary seaward change is interpreted as the anthropogenic response (bluff armoring) to the significant erosion that occurred in the historic period. For these reasons, only the combination of all available datasets sufficiently captures the net movement of this bluff edge, however uncertain or non-linear these changes may be. Future bluff top edge positions are projected for 2030 and 2050 using the WLR for all datasets over the study period (Figure 15). Uncertainty of the projected position is an important part of the result; uncertainty increases with the complexity of the bluff history.

The unarmored bluff is projected to erode 1 to 2 m back by 2030, and 2 to 4 meters by 2050. The northern section of the armored bluff is projected to erode between 3 to 5 meters by 2030, and up to 9 meters by 2050. In contrast, the southern section remains stable, although the high end of the uncertainty of this projection suggests some erosion of the highest point on the bluff near the fuel tank farm. The region around the creek is projected to be the most vulnerable to erosion based on this analysis. This is consistent with local accounts citing erosion and damage around the creek (Table 1). It is important to note that these projections are based on net movement between image dates. This includes repair efforts such as the addition of armor rock on the bluff. For example, the area with higher uncertainty northeast of the fuel tanks in Figure 15 experienced considerable erosion from 1957 to 1983, as well as deposition from 1983 to 2016 (Figure 14). The projection results in a net-stable shoreline because it is based on a trend in total movement. Therefore, these projections do not represent the actual erosion over time, but rather the relationship between erosion and mitigation. Unmitigated erosion of the unarmored bluff is much more likely to represent the natural erosion that occurs in the area, which occurs at a steady, albeit slightly slower rate in comparison to the creek region (Table 7).

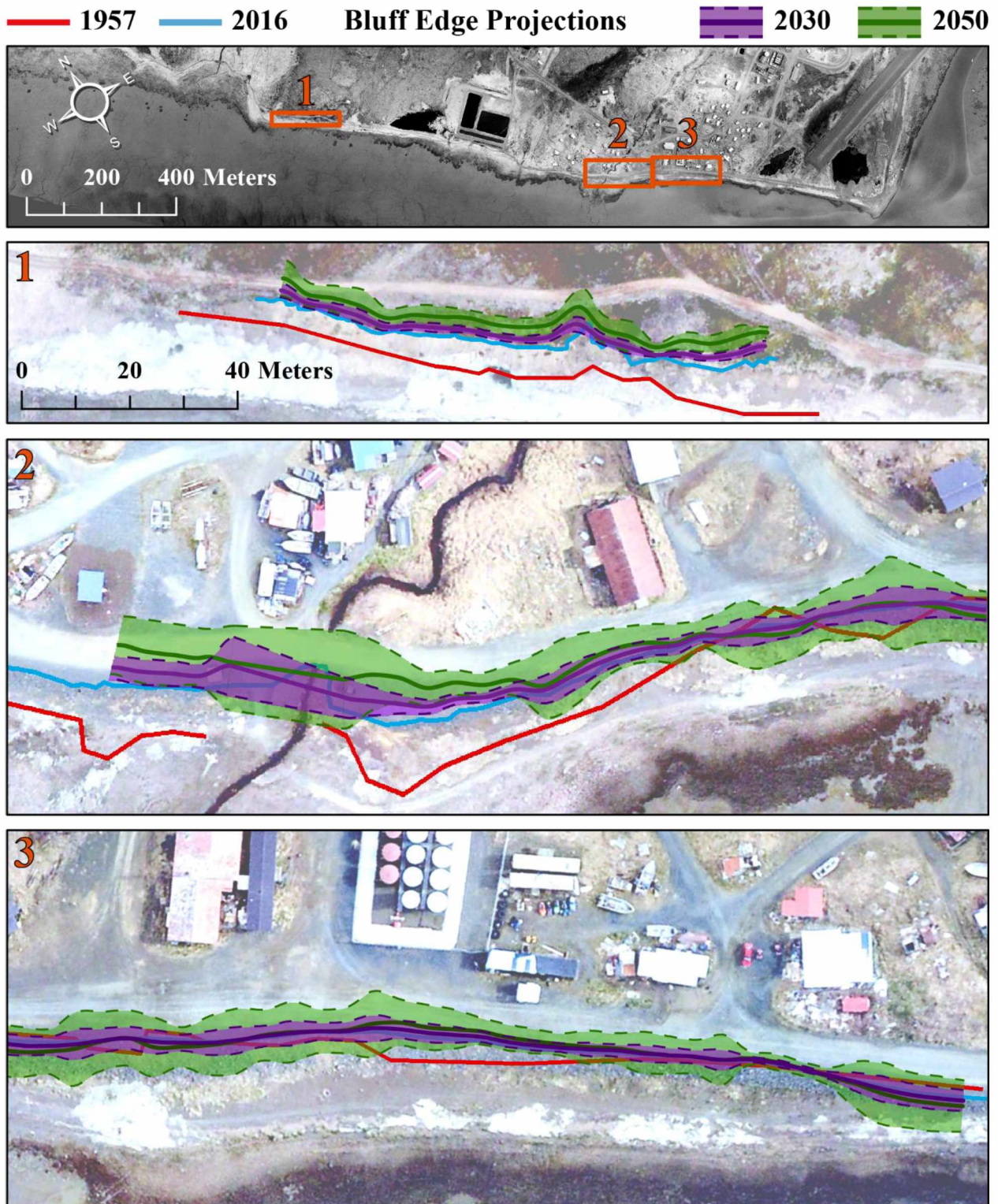


Figure 15. Bluff edge position projected for 2030 (purple) and 2050 (green). The 1957 (red) and 2016 (blue) bluff edges are overlaid for reference. All zones have equal scale. The unarmored bluff edge consistently retreats inland, while the armored bluff is variable. Greatest erosion is projected in the creek area in zone 2. Projections are interpolated across the creek bridge.

### 3.3. Goodnews Bay Tidal Datums

The tidal datum estimates for Goodnews are based on 4 days of tide data measured in the Goodnews River terminus, a CO-OPS tidal prediction for the Platinum station, a beach slope reconstruction model, and a DSM of high accuracy (Table 8; Figure 16). The estimated RSS error for all of these factors is 0.44 m. The temporary gauge coordinates were 59.1144 N, 161.5849 W (World Geodetic System 1984).

Table 8. Tidal datum estimates for Goodnews Bay in meters NAVD88. The Platinum values are published by NOAA CO-OPS for station 9465396.

Local Tidal Datum	Platinum, AK	Goodnews Bay, AK
MHHW	2.648	2.095
MHW	1.827	1.182
MTL	0.895	0.060
MSL	0.945	0.235
DTL	1.210	0.410
MLW	-0.037	-1.061
MLLW	-0.228	-1.275
GT	2.876	3.370
MN	1.864	2.243
DHQ	0.821	0.920
DLQ	0.191	0.197

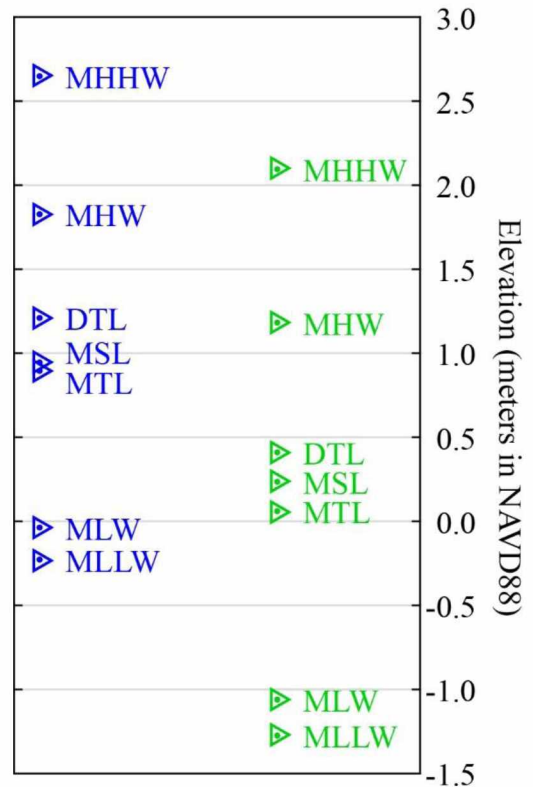


Figure 16. Plotted tidal datums for Platinum (blue) and Goodnews Bay (green).

### 3.4. Total Water Level Estimates and Risk Areas

Total water level (TWL) estimates are made for specific storms from the data sources described in Section 2.7 (Table 9). These estimates suggest that the 2011 storm surge reached the highest elevation of any recorded flood event, 5.3 m MSL. The 1979 storm surge reached up to 4.6 m MSL, enough to flood the previous runway, but not high enough to impact any currently occupied homes. This elevation is the lowest recommended for new construction by flood plain

management (Appendix II). The 1969 and 1989 storms range from 4.3 to 4.9 m MSL based on the previous runway elevation, but these estimates are less certain.

Table 9. Estimated significant total water levels associated with storm surge and flooding events.

Storm Date	Elev. (m MSL)	Elev. (m NAVD88)
2011	5.3	5.5
1979	4.6	4.8
1969, 1989	4.3 to 4.9	4.5 to 5.0

The summation of model results from NWS and the Stockdon et al. (2006) models were overestimated compared to observed TWL. The Stockdon et al. (2006) modeled wave setup was most similar to observed TWL, and therefore used as a proxy for TWL. TWL using wave runup may have been overestimated due to the difference in coastal setting between locations used to create the parameterized model compared to that of Goodnews Bay. It is possible that the offshore wave conditions are not representative of the fetch-limited embayment wave conditions, due to wave dampening during translation through the inlet and bay. The maximum modeled TWL of the 2011 storm was 5.5 m MSL (Figure 17). The 1.6 m of wave runup in Goodnews is consistent with empirical data for other locations in western Alaska impacted by the storm (2 to 4 m; Kinsman and DeRaps, 2012). In addition, the modeled timing of the event is consistent with local reports (Denning-Barnes, 2011). These findings suggest that the model can be used for other time periods in Goodnews. The model could be improved by accounting for and addressing sources of uncertainty, including situational variables such as storm/wave bearing, and temporal variables like beach slope variability (Doran, Long, and Overbeck, 2015).

Approximate historical flooding levels for 1969, 1979, 1989, and 2011 are projected onto the 2016 DSM using a simple single-value (bathtub model) visualization (Figure 18). In this model, every storm estimate reaches the lowest-lying residential building in the village, and the 2011 storm is shown to reach up to five residential buildings. Most residences and some public and private infrastructure such as the diesel station and school are located at least 4 m (13 ft) above historic flooding levels. This simplistic graphical representation of peak TWLs confirms observed reports that the sewage lagoon was effectively surrounded by the 2011 storm water, but was not breached and did not sustain significant damage. The previous airport runways were

lower in elevation than the current runway, thus, while all storms flooded their respective runway, none but the 2011 storm would have flooded the current runway. Regardless, all of these storms would cut off access to the runway during their peak.

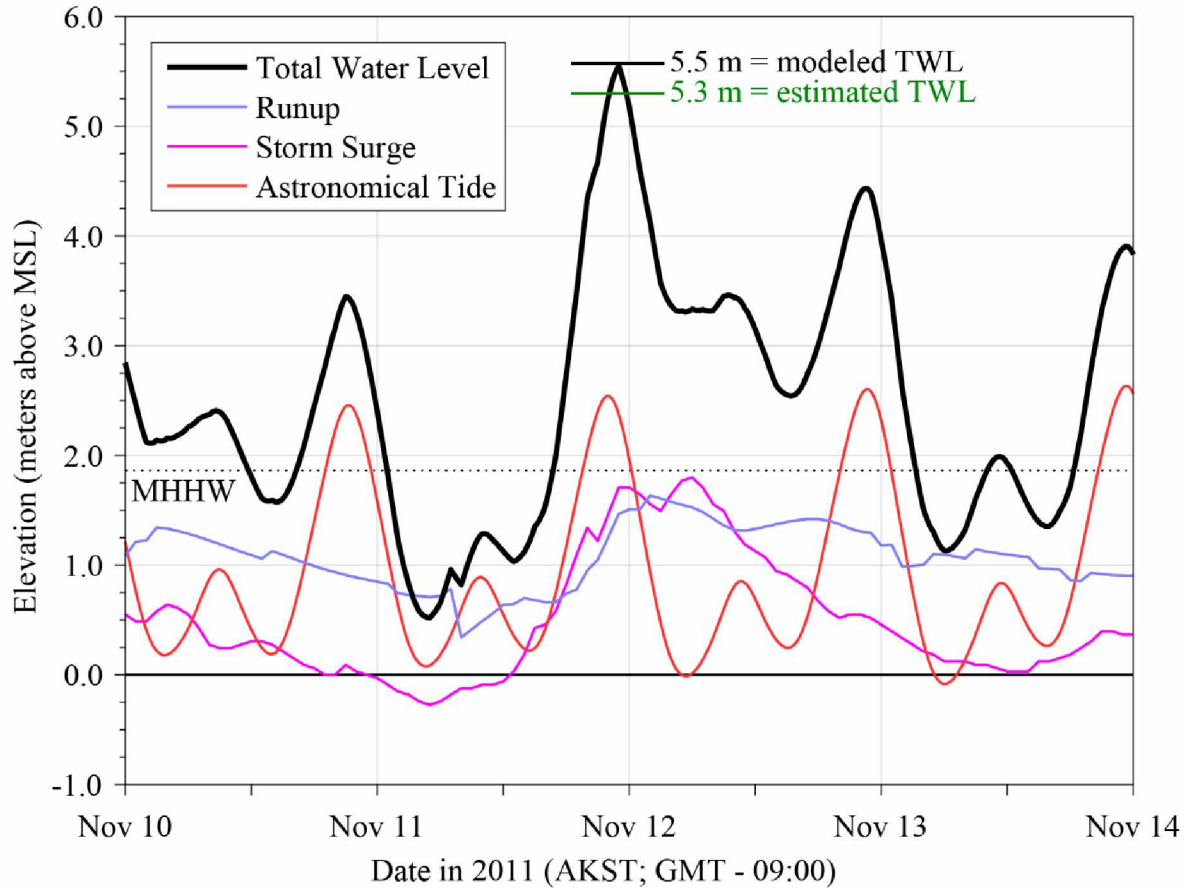
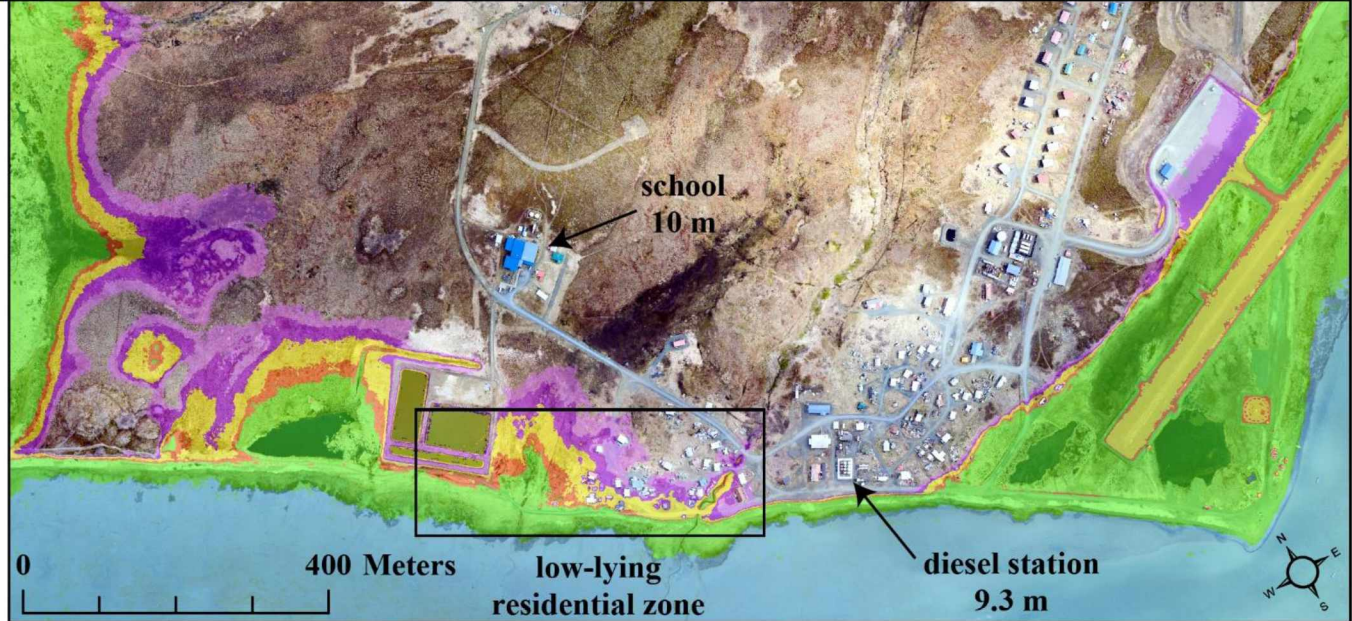
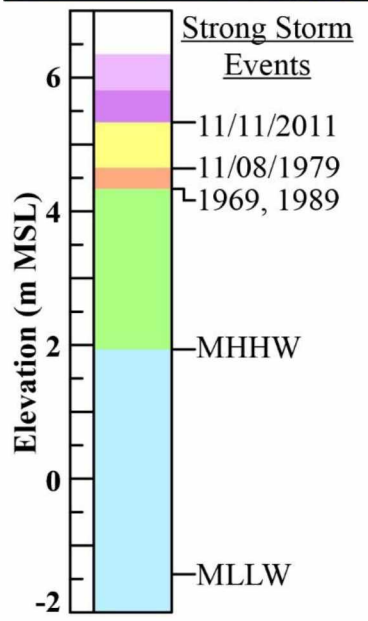
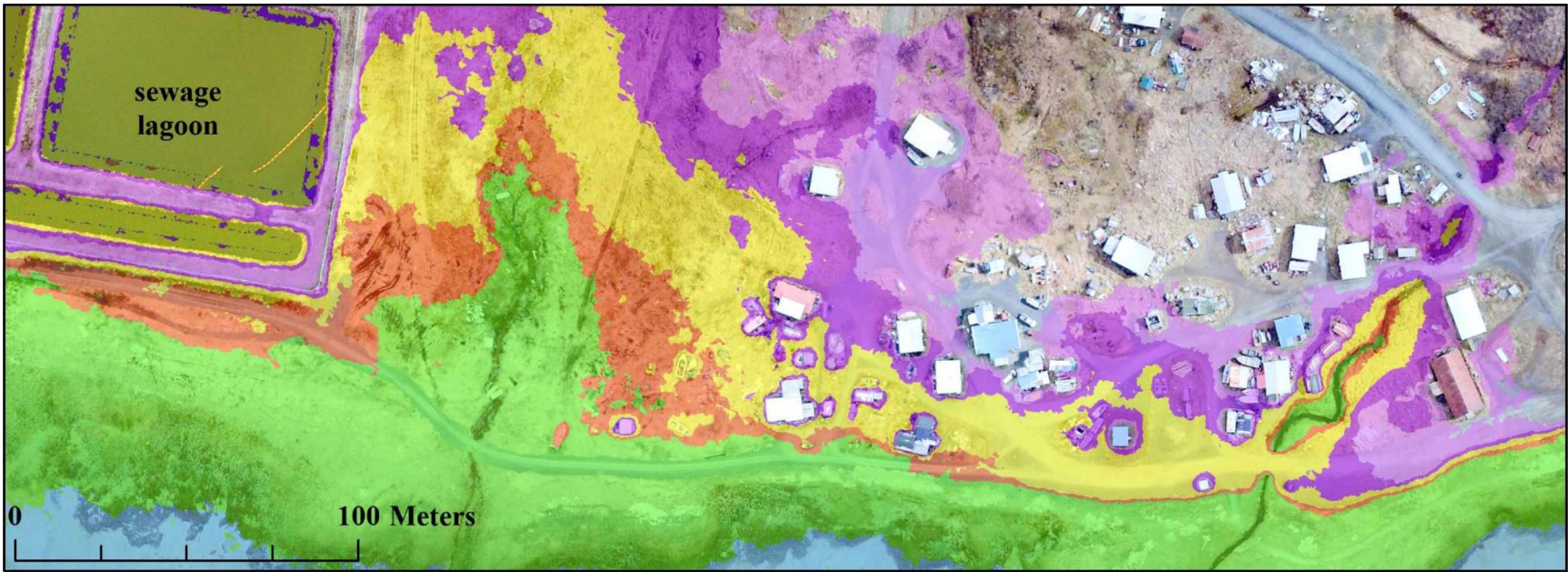


Figure 17. Estimated total water level of 11/11/2011 storm in Goodnews Bay. NOAA CO-OPS-predicted astronomical tide for the bay entrance (red), historical extra-tropical storm surge (ETSS) predictions by the NWS Meteorological Development Laboratory (purple), and empirically adjusted runup values from the Stockdon et al. (2006) equation (periwinkle) are combined to model total water level (black). The maximum modeled height during the storm is within 0.2 m of the maximum estimated height (based on imagery and RTK-GNSS survey data).



Figure 18. Map of horizontal extent of estimated total water level of strong storms. All structures in the yellow zone were flooded during the 2011 storm. All but one were abandoned homes, the last being abandoned after the storm. The 1969, 1979, and 1989 storms were not projected to cover the current runway. Purple zones do not represent any known flooding events, but are displayed to visualize extent of a hypothetical storm reaching up to 1 meter above the 2011 storm.



### **3.5. Wave Impact Hours**

Wave impact hours (WIH) were calculated by determining the amount of time specific coastal features were exceeded by the modeled TWL. The average monthly WIH show that bluffs tended to be impacted most by waves from October through December, which is consistent with the fall storm season (Figure 19) (Terenzi, Jorgenson, and Ely, 2014). The 2011 ice-free season exhibited 110 WIH on the bluffs, only to be exceeded in the year of 2013 when mean monthly sea and bay ice concentrations never reached above 50% (Figure 20). This finding suggests that the later formation of sea ice or significant degradation of sea ice cover can result in annual WIH that rival significant storm years.

The spatial variability of WIH was also examined during the Nov 2011 storm (Figure 21). Throughout the storm, profiles to the northwest experienced the greatest wave impact on the bluff, whereas the tallest part of the armored bluff (profiles 8 and 9) received the least. When the storm peaked, every bluff was impacted and the majority of profiles were overtopped. TWL was modeled to exceed the roadway at The Point (profiles 1-6) for at least 10 hours.

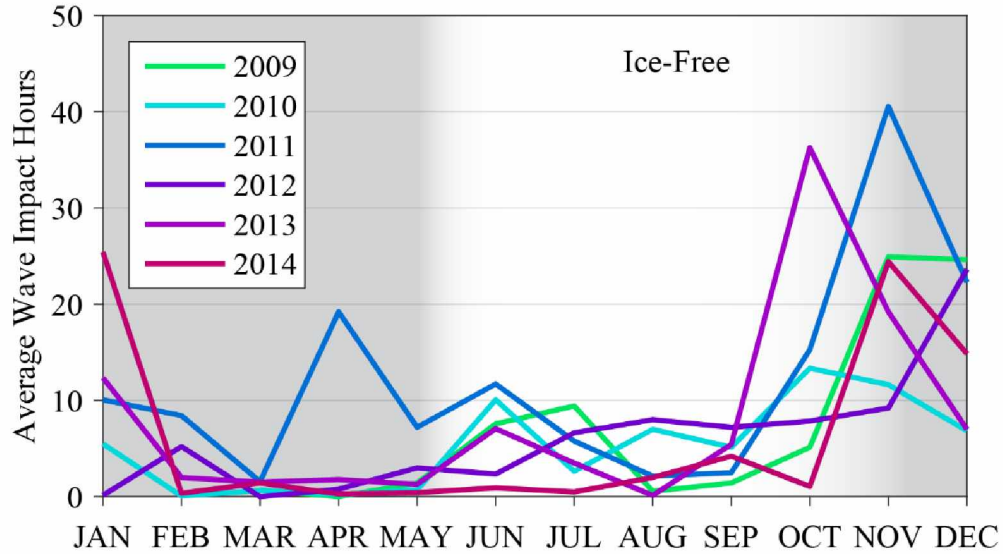


Figure 19. Average monthly wave impact hours contacting and overtopping bluffs from 2009 through 2014. Offshore and bay ice concentration, not accounted for in this model, is typically highest between January and May, denoted by the gray area. The total WIH are calculated during the ice-free season.

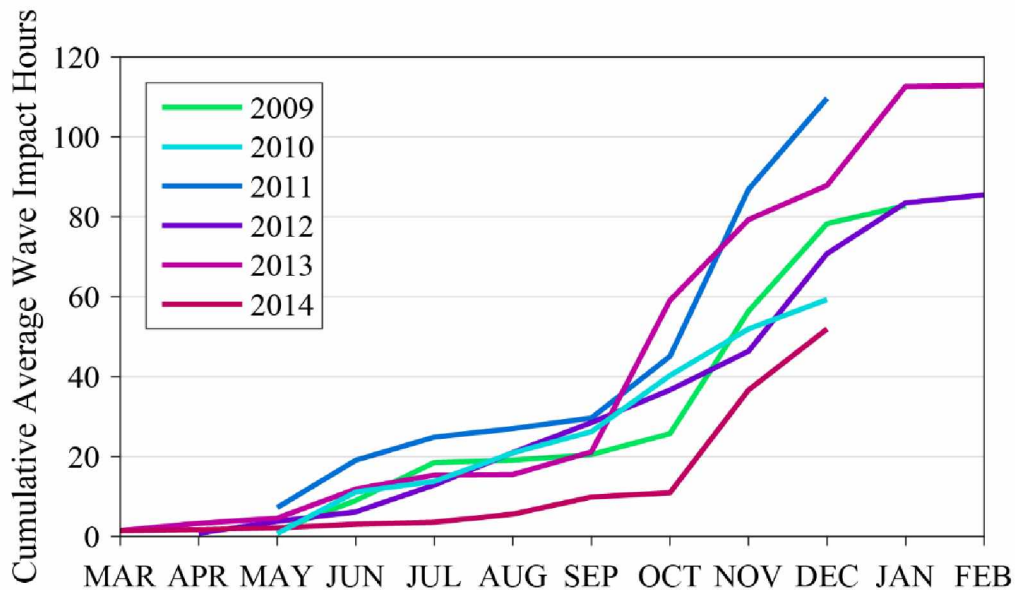


Figure 20. Cumulative average monthly wave impact hours contacting and overtopping bluffs from 2009 through 2014. Data are modeled from March to February to show one year of related open water and ice cover. Data are constrained by ice timing: open-water is determined as when sea or bay ice concentration is less than 50%. This demonstrates how significant ice cover can dampen annual wave energy.

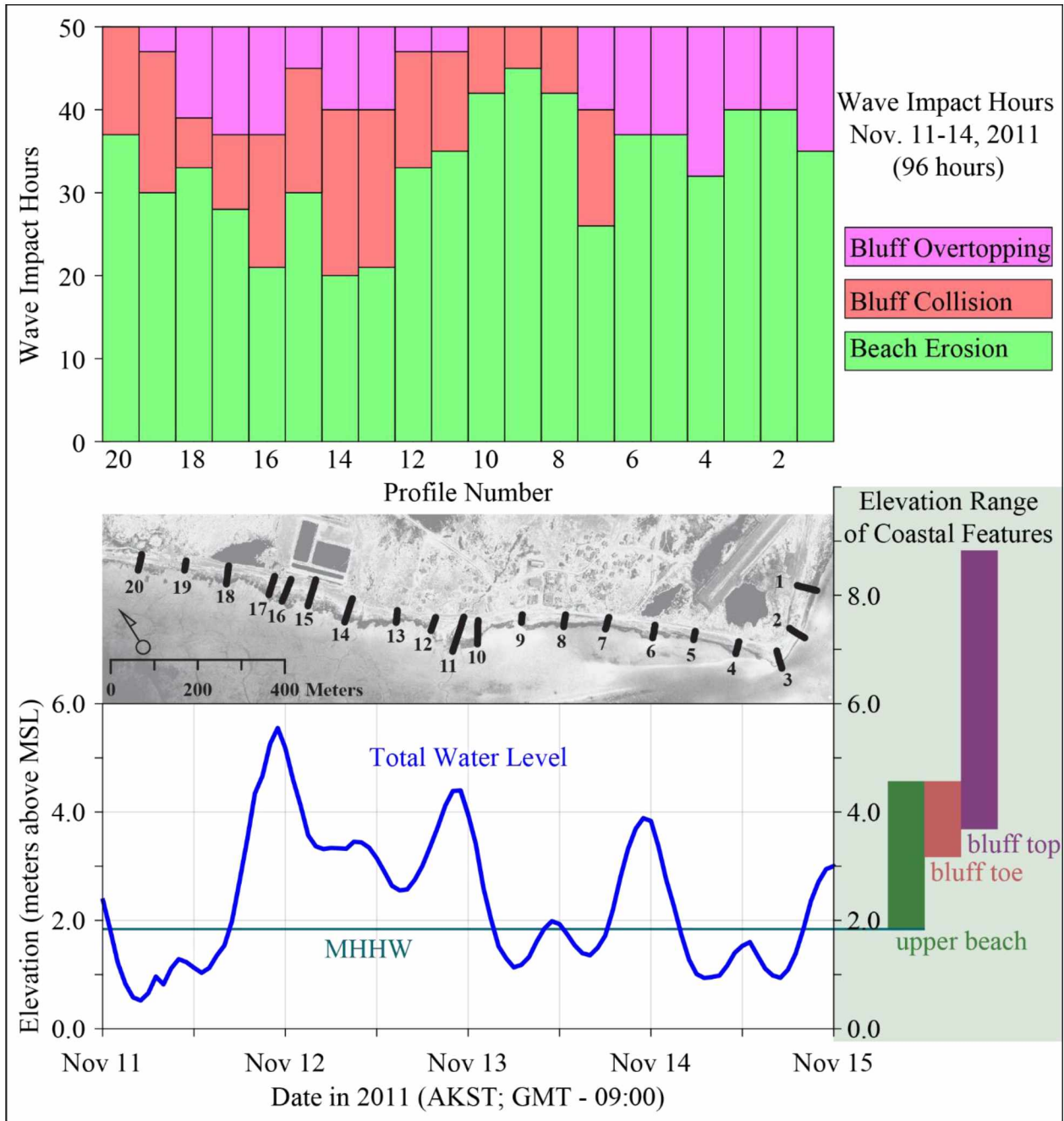


Figure 21. Spatial distribution of wave impact hours for the 11/11/2011 storm. Where bluffs are not present (profiles 1 - 6), overtopping was measured where water reached the road. Because MHHW is the same elevation for all profiles, each experienced the same total number of wave impact hours (i.e. the modeled surge spent 50 hours above MHHW).

## CHAPTER 4

### DISCUSSION

#### 4.1. Erosion Hazards

Based on the results of the shoreline change analysis and projections, the bluffs in Goodnews Bay have eroded several meters and will likely continue to do so in the future. The extent and degree of erosion varies considerably over the study area, and an interplay between erosion and mitigation may be inferred.

##### *4.1.1. Identifying Areas of Change*

Mean erosion rates derived from the shoreline change analysis are found to be statistically significant over the entire study period, and areas of substantial change are visualized in Figure 10, Figure 12, and Figure 22. The unarmored bluff eroded at a relatively consistent rate of  $0.10 \pm 0.07$  m/y, whereas the highly variable armored bluff exhibited mean erosion of  $0.05 \pm 0.15$  m/y (Table 7). Even though portions of the southern section experienced significant erosion during the 1957-1983 period, the bluff averaged near-zero net change due to mitigation (Figure 10; Figure 14). In contrast, the northern section eroded  $0.14 \pm 0.11$  m/y on average, exhibiting the largest and fastest movement recorded. The majority of erosion at both sites occurred after the 1983 image acquisition (Figure 14).

Erosion detection through measurements of aerial and satellite imagery is often accompanied by high positional uncertainty (e.g. Crowel, Leatherman, and Buckley, 1993; Romine et al., 2009; Vieira da Silva et al., 2016). Even with statistically significant erosion detected, it is difficult to confidently ascribe the numbers to actual change without ground-based evidence. Verification via more precise methods such as in-situ measurements is not possible, but several qualitative indicators exist that may assist in confirming that erosion has truly been detected. For example, erosion of the armored bluff by the creek is consistent with local reports

that detail the bridge washing out, and with images taken after the 2011 storm (Table 1; Figure 22; Appendix I). In addition, there are fewer structures on the bluff after the 2011 storm (Figure 23). These observations help to validate that the event caused a significant amount of damage in the creek area.

Through this analysis, two main regions of the armored bluff are found to experience erosion which, without mitigation, poses a threat to village infrastructure (Figure 22). The most significant site impacted is the aforementioned creek region, which is a transition zone between the high bluff and the low-lying graded road. This area exhibited clear and chronic erosion, despite experiencing similar wave impact hours as the stable section of the armored bluff (Figure 14). Heightened erosion may be attributed to the creek itself, which allows water and wave energy to flow through the bluff culvert instead of reflecting and dissipating. One household on the edge of the creek behind the road reported water reaching the house in 2011 via the culvert (Table 6). The other vulnerable area identified is the region of the bluff fronting the diesel station (Figure 22). This site has experienced net erosion despite significant mitigation efforts done after 2012 (Figure 10; Figure 12). Based on the overall rate, the shoreline change analysis projects that the road seaward of the diesel station will experience several meters of erosion by 2050 (Figure 15). The likelihood of the projections here and for the rest of the bluff depends on how mitigation played a role in the measured erosion, as well as the success of mitigation for future events.

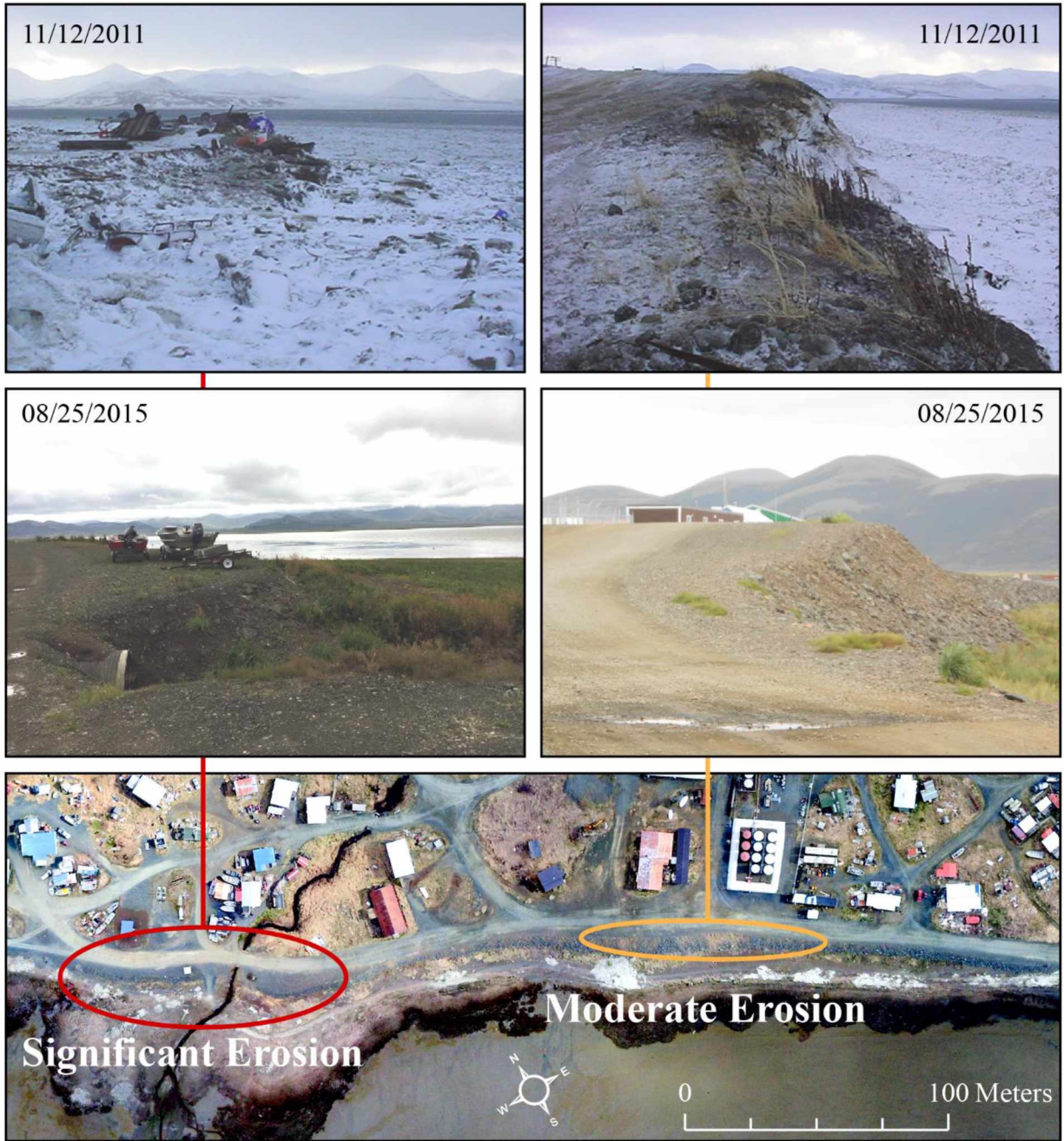


Figure 22. Armored bluff erosion hot spots, as determined by the shoreline change analysis. The creek area (left) has steadily eroded over the study period, and is projected to continue eroding. Previous bridges have washed out in past storms, but the graded culvert remained after the 2011 storm. The highest region of the bluff only experiences moderate net erosion, due to mitigation. Note that the 2011 storm left the bluff at an uncharacteristically steep angle compared to the angle of repose when it is re-armored bluff. The weighted linear regression analysis identified this bluff as stable because, while it suffered significant erosion from 1957-1983, armor material was deposited to near the same extent by 2016.



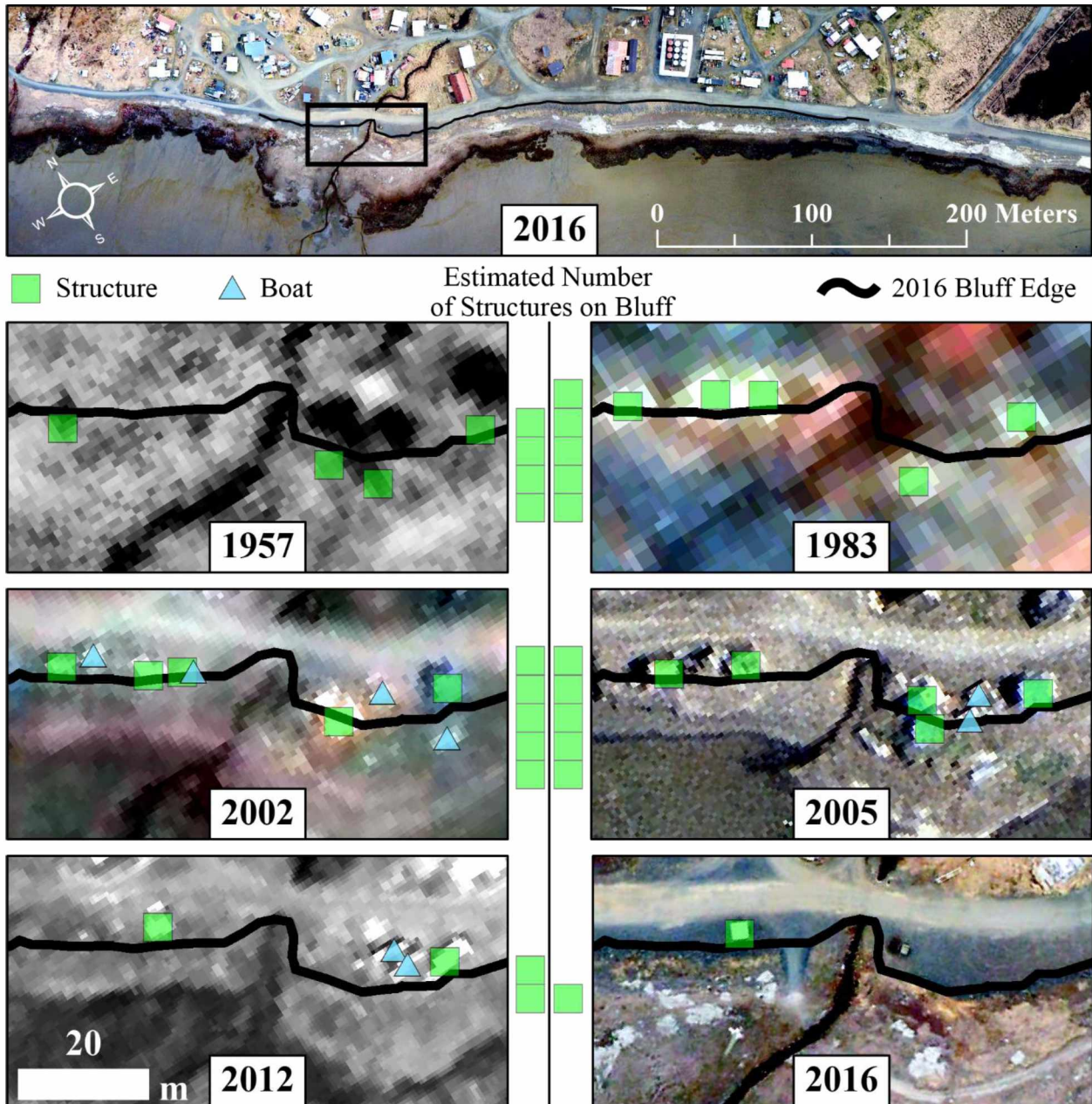


Figure 23. Estimated number of structures on the armored bluff where the highest erosion rates are observed. These structures, reported to be smokehouses in Denning-Barnes (2011), are all absent in the 11/12/2011 photographs, but one smokehouse was rebuilt. This type of qualitative verification supports the results of the shoreline change study, especially in conjunction with Figure 11, which depicts a significant erosion pulse in this region from the 2011 storm. Given the relative stability of the structures from 1983-2005, this also suggests that storms in this period were not as severe at this location.

#### 4.1.2. *Determining the Impact of Bluff Armoring*

Across the United States, armoring is a common response to erosion, although in some cases it can be ineffective, have significant upkeep costs, or redirect erosion elsewhere (Griggs, 2005; Mason et al., 2012; Pilkey and Wright III, 1988). In Goodnews' case, the armoring and repair appears to be working effectively, given that the majority of the bluff remains near the same place as in 1957. If the unarmored bluff represents the natural erosion regime of the coastline, then a lack of armoring and upkeep of the village bluff would have allowed several meters of erosion to occur across its entire extent. However, only the creek area appears to have undergone significant net retreat, so the overall stability of the bluff is likely attributed to mitigation and upkeep. Many villages on Alaska's western coast have to ship in gravel and rock, but Goodnews fortunately has a source near town, as does Platinum. Overall, it appears through this analysis that the bluff armoring and upkeep in Goodnews has a positive impact on the village. The creek area continues to erode despite armoring, demonstrating the limitation of this mitigation approach. Regardless, no residences or critical infrastructure appear to be threatened by erosion in the coming decades.

#### 4.1.3. *Future Shoreline Projections*

The history of bluff armoring is not known, limiting confidence in projecting future bluff positions. Projections are based simply on the linear movement of the shoreline over the time period, weighted by the uncertainty of each shoreline. Areas with consistent linear motion through time exhibit a higher mean  $R^2$  value than those with non-linear motion, meaning that those with a complicated history of erosion and mitigation may exhibit a lower  $R^2$  value. A low  $R^2$  value could also signify a stable shoreline, but distinguishing stability from mitigation is difficult with low temporal sampling and no bluff armoring history.

When interpreting uncertainty of projections, it is important to keep in mind that the uncertainty is closely related to the statistical correlation of the linear regression. Across the entire study period, the mean  $R^2$  value of the unarmored bluff is 0.92 (SD = 0.05), the northern section of the armored bluff is 0.80 (SD = 0.18), and the southern section is 0.16 (SD = 0.16) (Table 7). The  $R^2$  values for the unarmored bluff are high and consistent, which may be due in part to the lack of mitigation. This results in projected erosion with low uncertainty (Figure 15). In contrast, the southern section of the armored bluff is mostly stable, but the uncertainty

footprint is very large because the linear estimate is poorly correlated. This observation should not be interpreted as the uncertainty in whether the shoreline will move several meters in either direction, but more as an artifact due to the inability to precisely calculate a change rate. On the other hand, the armored bluff near the creek exhibits significant net erosion, even though several transects have poorly correlated linear trends (possibly due to the complicated history of erosion and deposition). Because of the greater overall movement, this area's projection uncertainty is more likely to reflect a minimum-maximum type estimate driven by the magnitude of future erosion and mitigation. Keeping these linear correlations in mind will help to interpret these projections and the extent of their uncertainty.

The overarching question in this study asks how the shoreline is changing, but the question in regards to the resiliency and livelihood of the village asks how the shoreline will change in the future. The calculated rates predict that the bluff adjacent to the creek will steadily erode into the road system (Figure 15). The areas proximal to the culvert could not be projected with high confidence, but the bridge (graded road on culvert) has been reportedly washed out at least once in 1984, and likely will face significant damage in tandem with the adjacent areas of projected erosion (Table 1). The calculated rates also predict that the bluff edge fronting the diesel farm will erode to some degree, but, as discussed previously, this depends on the effectiveness of future mitigation. Other than smokehouses on the bluff edge, no permanent structures are projected to be impacted directly by erosion by 2050. However, erosion is very likely to affect the road system adjacent to the armored bluff by 2030, and the road on the unarmored bluff by 2050. While uncertainty in these projections is on the order of several meters, they are statistically significant from the current shoreline in numerous locations.

Considering that these projections took into account all mitigation efforts applied over the study period and a linear landward trend was still observed in the creek region, the estimated future erosion here is likely. The projections could be over-predicting if more effective mitigation strategies are used in the future. However, the only known armoring technique practiced here is depositing gravel and rock onto the bluff face, which was the response after the most recent storm in 2011. So long as this practice continues, the projections are not considered to be over-predicting.

Limitations to future shoreline projections cannot be overstated, especially considering that these are the first in this area, and inaccurate interpretations of this type of information could

preclude effective policy (e.g. Mason et al., 2012). The study is already limited by applying a linear fit to a small sample size without in-situ verification. In addition, several natural signals further reduce confidence in projecting future shorelines. One basic assumption made through this process is that the geology and terrain remain consistent with that which produced the current dataset. Even if this were accurate or insignificant, geomorphic modifications may occur as a result of storm surge, erosion, and deposition which reshape and redirect future movement. Adding to this, the bluffs may have permafrost, which can thaw and degrade as annual temperatures rise, weakening resistance to eroding forces. The variables from coastal dynamics discussed in Section 1.3 (sea level, sea ice, storms, climate) may undergo enough change in the future to significantly change the rate of erosion, especially with the projected longer sea ice-free seasons (Douglas, 2010; Perovich and Richter-Menge, 2009; Walsh and Chapman, 2015). Incorporating these parameters in rate calculations to project future shorelines is beyond the scope of this study, but they should be considered when interpreting these results.

#### **4.2. Storm Surge and Flood Hazards**

Flooding due to storm surge has cost Goodnews land, property, and homes (Table 1). This element of the study ties past storm surge and flooding events into a vertical datum and identifies areas that are vulnerable to storm surge flooding. Before discussing vulnerable zones, this section must be prefaced by the important distinction between a formal risk analysis and the information being presented here. Firstly, flooding is simply an environmental phenomenon; environmental phenomena are considered a risk when it threatens to damage something of value. Therefore, risk analysis involves assigning a value to assets and their vulnerability, the latter manifesting as the probability that the asset will be impacted (e.g. Culver et al., 2012). Because the single-value (bathtub) model does not incorporate probability like a formal flood or inundation model, no measurement of risk is made. Several studies attempt to link lidar-based single-value models to vulnerability maps for sea-level rise, but these techniques are beyond the scope of this work (e.g. Chapman, Kim, and Mark, 2009; Gesch, 2009; Leon, Heuvelink, and Phinn, 2014; Schmid, Hadley, and Waters, 2014). Instead, potential risks are discussed based on past evidence of similar events occurring.

Given the landward extent of strong storms and the damage they caused, any features in the green, orange, and yellow zones of Figure 18 can be confidently presumed vulnerable. The

largest of these features is the airport runway, which is historically flooded by particularly strong storm surges. The current runway, constructed in 2009 with a surveyed height of 5.3 m MSL, is higher than the previous by about 0.5 m (Appendix VI). The 2011 storm surge estimate is also 5.3 m MSL, suggesting that the runway flooded during this event. No observations of the runway during the 2011 storm peak are known to exist, which may be because the storm surge peaked around midnight. However, given the evidence of large sea ice debris left on the runway, it is likely that the storm surge covered a significant portion of the current runway (Figure 24 b). The other significant storms identified in this study come within 0.40 m of the 2011 storm, and would pose a significant threat to the current runway.

Even the lowest storm surge estimate of 4.3 m MSL exceeds the elevation at The Point, where boats and shipping containers are stored. However, no damage to boats is mentioned for storms prior to 2011. Many boats, a vital resource for this subsistence-based community, were also badly damaged or destroyed in the most recent storm, being carried as far as 6.5 km upriver. Homes, smokehouses, and other property near the shore were badly damaged or destroyed during the 2011 storm, and similar accounts are made for the 1979 storm. Based on the events of the 1979 storm and other reports, buildings are recommended to be higher than 5.2 m MSL (Appendix II). At least one current household sits at this elevation, and is inland of the creek area where the highest erosion rates were observed. This home and other lower-lying structures in the area are considered at risk of storm surge.

The storm surge bathtub model depicts the sewage lagoon being surrounded on three sides during the 2011 storm, but no reports were found citing damage to the lagoon. The lagoon is surrounded by an uncovered rock berm with thick vegetation in places, which may have played a role in its stability throughout the flood. Like the berm, the sewage lagoon fence was not damaged (Figure 24 a). In contrast, the airport fence was destroyed, displaying the destructive potential of the 2011 storm surge and possible ice battering (Figure 24 c, d).

It has been shown here that these storm surge estimates consistently correlate to proxy indicators of surge elevations, and there are no known reports of damage that are not covered by the estimates. Thus, these estimates are considered reliable in predicting the general extent of storm surge in the area, at least to a degree of accuracy that should be cause for alarm if such a surge is projected to reach Goodnews. Improving the total water level model will support enhanced mechanism-based analysis of bluff retreat in the future.

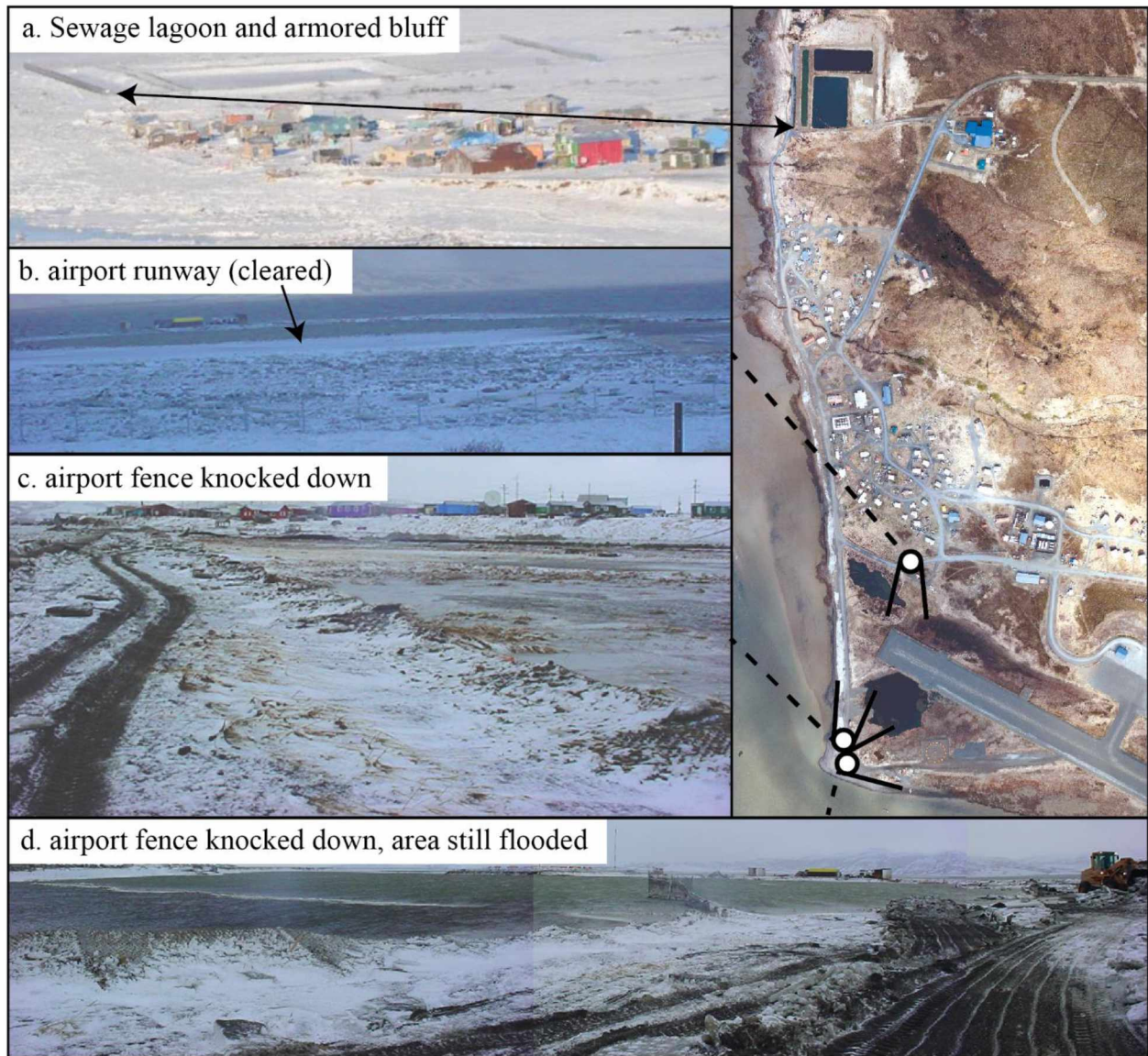


Figure 24. Pictures of damage from the 11/11/2011 storm. Each photo is connected by a dashed line to map symbols that represent the estimated camera position and field of view. (a) The sewage lagoon and lowest-lying region of the village, taken from a plane ten days after the storm. (b) The airport runway's northwestern terminus seen the day following the storm. The runway has been bulldozed, and the cleared debris is piled up around the edges. (c) The airport fence was completely knocked down on the road to The Point. (d) Photomosaic of the knocked down fence and floodwater remaining between the fence and the runway. Photo credit: Alice Julius.

#### **4.3. The Coastal Resiliency of Goodnews Bay in Relation to Other Alaskan Villages**

Erosion and flooding are widespread concerns among coastal and riverine communities in Alaska, including others near Goodnews Bay (GAO, 2003; USACE, 2009b). Platinum, the nearest city to Goodnews, has a landfill only 24 meters from a small bluff eroding at an unknown rate into Kuskokwim Bay (Huntman and Timmons, 2014). Quinhagak, 72 km north of Goodnews, experiences annual flooding, rapid erosion, and permafrost degradation (City of Quinhagak, 2012). They developed a comprehensive hazard mitigation plan that received grant funding through the Federal Emergency Management Agency. In Togiak, 141 km east of Goodnews, the African ironwood seawall, installed in 1984, has recently begun uplifting and splitting for currently unresolved reasons. Storm surge also breaches the wall via boat ramps, scouring the bulkhead sediment behind the wall (USACE, 2009b). Erosion, and projections of erosion, are so extensive in some villages that total relocation is being considered, an action Goodnews took in the 1920s in response to frequent flooding (Calista Corporation, 2016; Chapin et al., 2014). The native village of Port Heiden (formerly Meshik), 300 km south of Goodnews, began relocating in 1981 due to rapid erosion of coastal bluffs, which have since retreated through most of the old village site (Kinsman and Gould, 2014; USACE, 2007). Some villages are investing in relocation reconnaissance due to frequent flooding and erosion (GAO, 2009; Mason et al., 2012). In light of these communities, Goodnews' erosion is not so severe in both extent and risk to infrastructure. Major reasons why Goodnews is relatively resilient against coastal erosion include:

1. Environment:
  - a. sea-level change is minimal
  - b. no significant permafrost
  - c. low annual wave impact hours
2. Resources:
  - a. presence of rock quarry for gravel and armor rock
  - b. developable uplands
3. Community:
  - a. relocated themselves in 1920s
  - b. new construction high above flood levels
  - c. active engagement in mitigation and erosion monitoring

Flooding and storm surge are still significant concerns for Goodnews. Sufficient data to do formal storm surge analyses is lacking for much of Alaska (Tschetter, Kinsman, and Fish, 2014). The color-index maps being prepared by DGGGS provide a low-cost, interim solution for villages, resulting in graphics similar to, but more robust than the one produced here. As demonstrated here, these models can present practical results for which communities can plan.

#### **4.4. Broader Impacts**

This work has generated datasets for scientists, visual aids for decision makers, and personal connections with community members. The results from this work will increase the capacity of Goodnews Bay to respond to an ever-changing environment.

Sharing data through publication and freely available downloads is an important aspect of this work. All available information about storms which have impacted Goodnews are archived into one source, coupled with storm surge estimates using survey-grade GNSS data, a high-resolution contemporary DSM, and a local tidal datum. The bluff top edge shapefiles will be added to the DGGGS Coastal Hazard Program's Shoreline Change Tool (<http://maps.dggs.alaska.gov/shoreline>), and the beach profiles added to the Alaska Coastal Profile Tool (<http://maps.dggs.alaska.gov/acpt>). These datasets feed into the growing archive of freely available coastal data. The orthomosaics from 1957 and 1983 will be made publicly available for download, as well as photographs from fieldwork and provided by the community. In addition to datasets, this work also provides a thorough explanation of a method to obtain statistically significant results with limited imagery and relatively small-scale changes within the imagery. The methods used are a composite of published techniques for turning raw images into shoreline measurements, and their descriptions are written to be at least as informative as the sources from which they are gleaned. Through these networks, scientists and decision makers are able to access the data to help answer their own questions.

The most important aspect of this work is disseminating the results to the community in Goodnews Bay. Each fieldwork visit includes a classroom visit with coastal science lectures and outdoor activities. One distance delivery session was performed to share preliminary results with the students who had helped gather data themselves. Through funding from the Cooperative Institute for Arctic Research, Goodnews was included in the Alaska Sea Grant-funded Stakes for Stakeholders project (<https://seagrant.uaf.edu/research/projects/summary.php?id=1041>). This



involved training local leaders and students how to precisely measure changes in their bluff and beach. The project also includes the installation of two time-lapse cameras at the village that can precisely measure erosion during a storm. Through these efforts, a connection has been made between Goodnews and UAF, and Goodnews is now on a growing network of erosion monitoring sites.

Another important aspect of this work, and one too often overlooked, is publishing the invaluable information given by the residents of Goodnews. The bulk of this study, from beginning reconnaissance to validating results, was accomplished using the knowledge of elders, tribal council members, and all others willing to share their experiences and memories. Data about rural Alaska is sparse and often scattered throughout many sources. This document pieces together several facets of the history of the village that will serve as a useful tool for future work in the area, but more importantly, it will be a resource for the people of the Goodnews Bay. Future researchers and engineers would do well to reach out to the community, explain and share their work, ask questions, and, most importantly, listen.

#### **4.5. Future Work**

Continued work is being done to improve this study. In August 2017, another field campaign will include repeat beach profiles and an unmanned aerial systems survey, along with continued correspondence with members of the community. Comparing these beach profiles to the 2016 profiles will illuminate annual erosion and changes in beach sediment during a non-storm year. A high resolution (~ 0.10 m GSD) DSM will be generated from the aerial survey, which can be subtracted from the 2016 DSM to detect major changes.

## CHAPTER 5

### CONCLUSION

Bluff erosion in Goodnews Bay has damaged property and caused concern for existing infrastructure. Armoring the bluffs with large rocks appears to have slowed erosion, but some areas continue to erode regardless of mitigation efforts. Future bluff positions are projected based on the measured interplay of erosion and mitigation. The most vulnerable section of bluff in the village, exhibiting the highest net erosion, is the low-lying area adjacent to the creek. The remainder of the bluff is also vulnerable to episodic erosion, but mitigation has historically stabilized this area. Despite the relative stability of this area, continued armor rock campaigns likely will not halt erosion of the creek area.

Relative to the dozens of Alaskan communities caught between the throes of climate change, Goodnews Bay is successful at mitigating erosion and recovering from storm surge. However, their journey is not without struggle. Frequent flooding forced them to relocate in the 1920s, and almost one hundred years later the village continues to lose homes to large storms. The airport runway, which provides the only access for emergency evacuation, is also threatened by storms and flooding. Each storm brings destruction to the protective bluff that the village must re-armor, or else risk the loss of vital buildings and homes. While inspecting the ruins of her former beachfront property, one resident solemnly explained, “We didn’t want to move, but the ice and tide made us.” In respect to the experience of those who suffer through these events, one must keep in mind that no subset of images will tell the whole story. Measuring the distance from this line to that line; picking this elevation but not that one; these actions are simple, and yet they can have sweeping impacts for the people who live near those lines and pixels, people who may weather future disasters. Goodnews Bay appears successful through the lens of five cameras in the sky, but the whole story is told by those who live on the water’s edge.



## LITERATURE CITED

- Ablain, M.; Cazenave, A.; Valladeau, G., and Guinehut, S., 2009. A new assessment of the error budget of global mean sea level rate estimated by satellite altimetry over 1993-2008. *Ocean Science*, 5(2), 193–201.
- Anders, F.J. and Byrnes, M.R., 1991. Accuracy of shoreline change rates as determined from maps and aerial photographs. *Shore and Beach*, 59(1), 17–26.
- Barnhart, K.R.; Overeem, I., and Anderson, R.S., 2014. The effect of changing sea ice on the physical vulnerability of Arctic coasts. *Cryosphere*, 8(5), 1777–1799.
- Boak, E.H. and Turner, I.L., 2005. Shoreline definition and detection: a review. *Journal of Coastal Research*, 21(4), 688–703.
- Briner, J.P.; Kaufman, D.S.; Werner, A.; Caffee, M.; Levy, L.; Manley, W. F.; Kaplan, M.R., and Finkel, R.C., 2002. Glacier readvance during the late glacial (Younger Dryas?) in the Ahklun Mountains, southwestern Alaska. *Geology*, 30(8), 679–682.
- Calista Corporation, 2016. *Goodnews Bay*.  
<http://www.calistacorp.com/shareholders/village/goodnews-bay>.
- CAVM Team., 2003. *Circumpolar Arctic Vegetation Map*. Anchorage, Alaska: U.S. Fish and Wildlife Service, Conservation of Arctic Flora and Fauna (CAFF) Map No. 1, scale 1:7,500,000, 1 sheet.
- Chapin, F.S., III; Trainor, S.F.; Cochran, P.; Huntington, H.; Markon, C.; McCammon, M.; McGuire, A.D., and Serreze, M., 2014. Ch. 22: Alaska. In: Melillo, J.M.; Richmond, Terese (T.C.), and Yohe, G.W., (eds.), *Climate Change Impacts in the United States: The Third National Climate Assessment*. U.S. Global Change Research Program, pp. 514–536.
- Chapman, R.S.; Kim, S.-C., and Mark, D.J., 2009. Storm-induced water level prediction study for the western coast of Alaska. *U.S. Army Engineer Research and Development Center - Coastal and Hydraulics Laboratory*, 92p.
- Church, J.A. and White, N.J., 2011. Sea-level rise from the late 19th to the early 21st century. *Surveys in Geophysics*, 32(4–5), 585–602.
- City Data, 2017. *Goodnews Bay, Alaska (AK 99589) profile*. <http://www.city-data.com/city/Goodnews-Bay-Alaska.html>.
- City of Quinhagak Mitigation Planning Team, 2012. *City of Quinhagak Hazard Mitigation Plan*, 172p.
- Crowell, M.; Leatherman, S.P., and Buckley, M.K., 1991. Historical shoreline change: error analysis and mapping accuracy. *Journal of Coastal Research*, 7(3), 839–852.

- Crowell, M.; Leatherman, S.P., and Buckley, M.K., 1993. Shoreline change rate analysis: long term versus short term data. *Shore and Beach*, 61(2), 13–20.
- Culver, M.; Bierwagen, B.; Burkett, V.; Cantral, R.; Davidson, M.A., and Stockdon, H., 2012. Introduction and context. In: Burkett, V. and Davidson, M. (eds.), *Coastal Impacts, Adaptation, and Vulnerabilities. NCA Regional Input Reports*. Washington, D.C.: Island Press, pp. 1–9.
- Degrandpre, K.G., 2015. Relative sea level change in western Alaska estimated from satellite altimetry and repeat GPS measurements. Fairbanks, AK: University of Alaska Fairbanks, Master's thesis, 169p.
- Denning-Barnes, A., 2011. *Goodnews Bay and Platinum suffer weekend storm damage*. <http://archive.kyuk.org/goodnews-bay-and-platinum-suffer-weekend-storm-damage>.
- Department of Natural Resources (DNR), 2008. Ceñaliulriit coastal resource service area coastal management plan: final plan amendment. *Ceñaliulriit Coastal Management District, Bethel, Alaska*, 189p.
- Doran, K.S.; Long, J.W., and Overbeck, J.R., 2015. A method for determining average beach slope and beach slope variability for U.S. sandy coastlines. *U.S. Geological Survey Open-File Report 2015-1053*, 5p.
- Douglas, D.C., 2010. Arctic sea ice decline: Projected changes in timing and extent of sea ice in the Bering and Chukchi Seas. *U.S. Geological Survey Open-File Report 2010-1176*, 32p.
- Emery, K.O., 1961. A simple method of measuring beach profiles. *Limnology and Oceanography*, 6(1), 90–93.
- Erikson, L.H.; McCall, R.T.; van Rooijen, A., and Norris, B., 2015. Hindcast storm events in the Bering Sea for the St. Lawrence Island and Unalakleet regions, Alaska. *U.S. Geological Survey Open-File Report 2015-1193*, 47p.
- Federal Emergency Management Agency (FEMA), 2011. *President declares a major disaster for Alaska*. <https://www.fema.gov/news-release/2011/12/22/president-declares-major-disaster-alaska>.
- Ford, M., 2013. Shoreline changes on an urban atoll in the central Pacific Ocean: Majuro atoll, Marshall Islands. *Journal of Coastal Research*, 28(1), 11–22.
- Genz, A.S.; Fletcher, C.H.; Dunn, R.A.; Frazer, L.N., and Rooney, J.J., 2007. The predictive accuracy of shoreline change rate methods and alongshore beach variation on Maui, Hawaii. *Journal of Coastal Research*, 23(1), 87–105.
- Gesch, D.B., 2009. Analysis of lidar elevation data for improved identification and delineation of lands vulnerable to sea-level rise. *Journal of Coastal Research*, SI(53), 49–58.
- Gibbs, A.E. and Richmond, B.M., 2015. National assessment of shoreline change—Historical shoreline change along the north coast of Alaska, U.S.-Canadian border to Icy Cape. *U.S. Geological Survey Open-File Report 2015-1048*, 96p.
- Gibbs, A.E.; Nolan, M., and Richmond, B.M., 2015. Evaluating changes to arctic coastal bluffs using repeat aerial photography and structure-from-motion elevation models. *Proceedings of the Coastal Sediments 2015*, 14p.

- Gould, A.I.; Kinsman, N.E.M., and Hendricks, M.D., 2015. Guide to projected shoreline positions in the Alaska Shoreline Change Tool. *Alaska Division of Geological and Geophysical Surveys: Miscellaneous Publication 158*, 11p.
- Griggs, G.B., 2005. The impacts of coastal armoring. *Shore and Beach*, 73(1), 13–22.
- Hapke, C.J. and Plant, N., 2010. Predicting coastal cliff erosion using a Bayesian probabilistic model. *Marine Geology*, 278(1–4), 140–149.
- Hapke, C.J. and Reid, D., 2007. National assessment of shoreline change, part 4 : historical coastal cliff retreat along the California coast. *U.S. Geological Survey Open-File Report 2007-1133*, 51p.
- Harrington, G.L., 1921. Mineral resources of the Goodnews Bay region. *In: Mineral resources of Alaska*, pp. 207-228.
- Himmelstoss, E.A., 2009. DSAS 4.0 Installation Instructions and User Guide. *In: Thieler, E.R.; Himmelstoss, E.A.; Zichichi, J.L., and Ergul, A. (eds.), 2009 Digital Shoreline Analysis System (DSAS) version 4.0 — An ArcGIS extension for calculating shoreline change.* U.S. Geological Survey Open-File Report 2008-1278, 79p. \*updated for version 4.3.
- Historical Sea Ice Atlas, University of Alaska, 2017. *Historical Sea Ice Atlas: observed estimates of sea ice concentration in Alaska waters.* <http://ckan.snap.uaf.edu/dataset/historical-sea-ice-atlas-observed-estimates-of-sea-ice-concentration-in-alaska-waters>.
- Huntman, D. and Timmons, J., 2014. CIAP WEAR trip report: Platinum (population 63) July 10, 2014. *Alaska Department of Environmental Conservation Solid Waste Program*, 6p.
- Jelesnianski, C.P.; Chen, J., and Shaffer, W.A., 1992. SLOSH: Sea, lake, and overland surges from hurricanes. *NOAA Technical Report, NWS 48, U.S. Department of Commerce*, 71p.
- Jones, B.M.; Arp, C.D.; Jorgenson, M.T.; Hinkel, K.M.; Schmutz, J.A., and Flint, P.L., 2009. Increase in the rate and uniformity of coastline erosion in Arctic Alaska. *Geophysical Research Letters*, 36(3), 1–5.
- Jones, B.M.; Hinkel, K.M.; Arp, C.D., and Eisner, W.R., 2008. Modern erosion rates and loss of coastal features and sites, Beaufort Sea coastline, Alaska. *Arctic Institute of North America*, 61(4), 361–372.
- Jorgenson, M.T.; Yoshikawa, K.; Kanevskiy, M.; Shur, Y.; Romanovsky, V.; Marchenko, S.; Grosse, G.; Brown, J., and Jones, B.M., 2008. Permafrost Characteristics of Alaska. *In Proceedings of the Ninth International Conference on Permafrost*, pp. 121–122.
- Kaufman, D.S.; Young, N.E.; Briner, J.P., and Manley, W.F., 2011. Alaska Palaeo-Glacier Atlas (Version 2). *In: Ehlers, J.; Gibbard, P., and Hughs, P. (eds.), Developments in Quaternary Science*, Vol 15. Amsterdam: Elsevier, pp. 427–445.
- Kinsman, N.E.M. and DeRaps, M.R., 2012. Coastal hazard field investigations in response to the November 2011 Bering Sea storm, Norton Sound, Alaska. *Alaska Division of Geological and Geophysical Surveys: Report of Investigations 2012-2*, 51p.
- Kinsman, N.E.M. and Gould, A.I., 2014. Contemporary shoreline retreat rates at Meshik in Port Heiden, Alaska. *Alaska Division of Geological and Geophysical Surveys: Preliminary Interpretive Report 2014-4*, 21p.

- Leon, J.X.; Heuvelink, G.B.M., and Phinn, S.R., 2014. Incorporating DEM uncertainty in coastal inundation mapping. *PLoS ONE*, 9(9), 1–12.
- Macklin, S.A., 1983. Wind drag coefficient over first-year sea ice in the Bering Sea. *Journal of Geophysical Research*, 88(C5), 2845–2852.
- Maio, C.V.; Gontz, A.M.; Tenenbaum, D.E., and Berkland, E.P., 2012. Coastal hazard vulnerability assessment of sensitive historical sites on Rainsford Island, Boston Harbor, Massachusetts. *Journal of Coastal Research*, 28(1A), 20–33.
- Manley, W.F.; Mason, O.K.; Jordan, J.W.; Lestak, L.R.; Sanzone, D.M., and Parrish, E.G., 2006. Coastal change since 1950 in the southeast Chukchi Sea, Alaska, based on GIS and field measurements. *American Geophysical Union, Fall Meeting 2006, abstract #C44B-04*.
- Mars, J.C. and Houseknecht, D.W., 2007. Quantitative remote sensing study indicates doubling of coastal erosion rate in past 50 yr along a segment of the Arctic coast of Alaska. *Geology*, 35(7), 583–586.
- Mason, O.K.; Jordan, J.W.; Lestak, L.R., and Manley, W.F., 2012. Narratives of shoreline erosion and protection at Shishmaref, Alaska: the anecdotal and the analytical. In: Cooper, J.A.G. and Pilkey, O.H. (eds.), *Pitfalls of Shoreline Stabilization: Selected Case Studies*. Springer, pp. 73–92.
- Mertie, J.B., Jr., 1939. Platinum deposits of the Goodnews Bay District, Alaska. *U.S. Geological Survey Bulletin 910-B*, 115–145.
- Mertie, J.B., Jr., 1940. The Goodnews platinum deposits—Alaska. *U.S. Geological Survey Bulletin 918*, 1–97.
- Moore, L.J., 2000. Shoreline mapping techniques. *Journal of Coastal Research*, 16(1), 111–124.
- National Digital Elevation Program (NDEP), 2004. Guidelines for digital elevation data – Version 1. *National Digital Elevation Program*, 93p.
- Nicholls, R.J. and Cazenave, A., 2010. Sea-level rise and its impact on coastal zones. *Science*, 328, 1517–1520.
- Noh, M.-J. and Howat, I.M., 2015. Automated stereo-photogrammetric DEM generation at high latitudes: surface extraction from TIN-based search minimization (SETSM) validation and demonstration over glaciated regions. *GIScience and Remote Sensing*, 52(2), 198–217.
- Nolan, M.; Larsen, C., and Sturm, M., 2015. Mapping snow depth from manned aircraft on landscape scales at centimeter resolution using structure-from-motion photogrammetry. *The Cryosphere*, 9, 1455–1463.
- Oommen, T.; Prakash, A.; Misra, D.; Naidu, S.; Kelley, J.J., and Bandopadhyay, S., 2008. GIS based marine platinum exploration, Goodnews Bay region, southwest Alaska. *Marine Georesources and Geotechnology*, 26(1), 1–18.
- Parnell, Sean, 2011. December 5, 2011, State of Alaska declaration of disaster emergency. *Juneau, Alaska, Office of the Governor of the State of Alaska*, 4p.
- Pease, C.H.; Salo, S.A., and Overland, J.E., 1983. Drag measurements for first-year sea ice over a shallow sea. *Journal of Geophysical Research*, 88(C5), 2853–2862.

- Perovich, D.K. and Richter-Menge, J.A., 2009. Loss of sea ice in the Arctic. *Annual Review of Marine Science*, 1, 417–441.
- Pilkey, O.H. and Wright, H.L., III, 1989. Seawalls versus beaches. *In: Krauss, N.C. and Pilkey, O.H. (eds.), The Effects of Seawalls on Beaches*. Journal of Coastal Research, Special Issue No. 4, pp. 41–67.
- Romine, B.M.; Fletcher, C.H.; Frazer, L.N.; Genz, A.S.; Barbee, M.M., and Lim, S.-C., 2009. Historical shoreline change, southeast Oahu, Hawaii; applying polynomial models to calculate shoreline change rates. *Journal of Coastal Research*, 25(6), 1236–1253.
- Ruggiero, P.; Komar, P.D.; McDougal, W.G.; Marra, J.J., and Bach, R.A., 2001. Wave runup, extreme water levels and the erosion of properties backing beaches. *Journal of Coastal Research*, 17(2), 407–419.
- Ruggiero, P.; Kratzmann, M.G.; Himmelstoss, E.A.; Reid, D.; Allan, J., and Kaminsky, G., 2013. National assessment of shoreline change: historical shoreline change along the Pacific Northwest coast. *U.S. Geological Survey Open-File Report 2012-1007*, 62p.
- Scenarios Network for Alaska and Arctic Planning (SNAP), University of Alaska, 2017. *Community Charts*.  
[https://www.snap.uaf.edu/sites/all/modules/snap\\_community\\_charts/charts.php](https://www.snap.uaf.edu/sites/all/modules/snap_community_charts/charts.php).
- Schmid, K.; Hadley, B., and Waters, K., 2014. Mapping and portraying inundation uncertainty of bathtub-type models. *Journal of Coastal Research*, 30(3), 548–561.
- Serreze, M.C. and Stroeve, J., 2015. Arctic sea ice trends, variability and implications for seasonal ice forecasting. *Philosophical Transactions of the Royal Society A*, 373(2045), Article 20140159.
- Stockdon, H.F.; Holman, R.A.; Howd, P.A., and Sallenger, A.H., Jr., 2006. Empirical parameterization of setup, swash, and runup. *Coastal Engineering*, 53, 573–588.
- Taylor, A. and Glahn, B., 2008. Probabilistic guidance for hurricane storm surge. *Proceedings of the 88<sup>th</sup> American Meteorological Society Annual Meeting* (New Orleans, Louisiana), pp. 1–8.
- Terenzi, J.; Jorgenson, M.T., and Ely, C.R., 2014. Storm-surge flooding on the Yukon-Kuskokwim Delta, Alaska. *Arctic*, 67(3), 360–374.
- Theuerkauf, E.J. and Rodriguez, A.B., 2012. Impacts of transect location and variations in along-beach morphology on measuring volume change. *Journal of Coastal Research*, 28(3), 707–718.
- Thieler, E.R. and Danforth, W.W., 1994. Historical shoreline mapping (I): Improving techniques and reducing positioning errors. *Journal of Coastal Research*, 10(3), 549–563.
- Thieler, E.R.; Himmelstoss, E.A.; Zichichi, J.L., and Ergul, A., 2009. The Digital Shoreline Analysis System (DSAS) version 4.0 – An ArcGIS© extension for calculating shoreline change. *U.S. Geological Survey Open-File Report 2008-1278*, 79p.
- Tschetter, T.; Kinsman, N.E.M., and Fish, A., 2014. Color-indexed elevation maps for flood-vulnerable coastal communities in western Alaska. *Alaska Division of Geological and Geophysical Surveys Miscellaneous Publication 154*, 17p.



- U.S. Department of Commerce (USDC), 2003. Computational techniques for tidal datums handbook. Silver Spring, Maryland: U.S. Department of Commerce, National Oceanic and Atmospheric Administration, *NOAA Special Publication NOS CO-OPS 2*, 98p.
- U.S. Department of Energy (DOE), 2010. *Environmental impact assessment (EIA) guidance document for coastal and land reclamation activities*. <http://www.doe.gov/my/eia/wp-content/uploads/2010/07/Reclamation.pdf>.
- U.S. General Accounting Office (GAO), 2003. Alaska Native villages—Most are affected by flooding and erosion, but few qualify for federal assistance. *U.S. General Accounting Office Report GAO-04-142*, 82p.
- U.S. Government Accountability Office (GAO), 2009. Alaska Native villages—Limited progress has been made on relocating villages threatened by flooding and erosion. *U.S. Government Accountability Office Report GAO-09-551*, 53p.
- U.S. Army Corps of Engineers (USACE), 2007. Alaska Baseline Erosion Assessment, Erosion Information Paper - Port Heiden, Alaska. *Alaska District U.S. Army Corps of Engineers*, 4p.
- USACE, 2009a. Alaska Barge Landing System Design Statewide Phase 1: Various Locations, Alaska, Final Report. *Alaska District U.S. Army Corps of Engineers*, 158p.
- USACE, 2009b. Alaska Baseline Erosion Assessment: Study Findings and Technical Report. *Alaska District U.S. Army Corps of Engineers*, 68p.
- Vieira da Silva, G.; Muler, M.; Prado, M.F.V.; Short, A.D.; Klein, A.H.F., and Toldo, E.E., Jr., 2016. Shoreline change analysis and insight into the sediment transport path along Santa Catarina Island north shore, Brazil. *Journal of Coastal Research*, 32(4), 863–874.
- Walsh, J.E. and Chapman, W.L., 2015. Variability of sea ice extent over decadal and longer timescales. *Climate Change: Multidecadal and Beyond*, 203-217.
- Wildlife Service, Region 7, 1986. Togiak National Wildlife Refuge: Final Comprehensive Conservation Plan, Wilderness Review, and Environmental Impact Statement. *US Fish and Wildlife Service, Region 7*.
- Wilson, F.H.; Hults, C.P.; Mohadjer, S., and Coonrad, W.L., compilers, 2013. *Reconnaissance geologic map of the Kuskokwim Bay region, southwest Alaska*. U.S. Geological Survey Scientific Investigations Map 3100, scale 1:500,000, 1 sheet.

## APPENDICES

### Appendix I. Photos from 11/16/2003 and 11/11/2011 storms in Goodnews Bay

All photos courtesy of Alice Julius.

Photos taken after 2003 storm surge event:





Photos taken after 2011 storm surge event:



069



071



072



075



079



086



087



090



095



111





## Appendix II. Flood reports from the Alaska District Corps of Engineers Flood Plain Management.

**Goodnews Bay** | City Office: (907) 967-8614 | Revised: October 2011

---

STATUS	2 <sup>nd</sup> class city	LAST FLOOD EVENT	1989
POPULATION	256	FLOOD CAUSE	
BUILDINGS		ELEVATION	
RIVER SYSTEM	none	FLOOD OF RECORD	1979
COASTAL AREA	Kuskokwim Bay	FLOOD CAUSE	wind-driven waves
		ELEVATION	83.5
NFIP STATUS	not participating	WORST FLOOD EVENT	1979
FLOODPLAIN REPORT	yes	FLOOD CAUSE	wind-driven waves
FLOOD INSURANCE STUDY	no	FLOOD GAUGE	no

---

**Comments:** The following survey information is based on a temporary benchmark (TBM) with an assumed elevation of 100.0 ft. The TBM is located on the front door sill of the main entrance of City Hall. This building is the old Bureau of Indian Affairs school, and also contains the clinic.

### SURVEY INFORMATION AS OF SEPTEMBER 1994

Recommended building elevation	85.5
Estimated 1979 flood elevation	83.5
Ground level at Bright's Trading Post	83.1

Flooding in the community is caused by wind-driven waves at high tide. The largest flood event is believed to have occurred in 1979, with wind blowing from the south. One house in the lowest part of town was flooded at that time, but it no longer exists. Water came under the house of Bright's Trading Post in the 1979 storm, but did not flood the first floor. This is now the lowest building in the community. During the 1969 flood the runway was reported to have 6 to 12 inches of water on it. The August 1989 storm also flooded the airstrip.

---

Floodplain Manager | (907) 753-2610

---

ALASKA DISTRICT CORPS OF ENGINEERS  
FLOOD PLAIN MANAGEMENT

HIGH WATER ELEVATION IDENTIFICATION

Community: Goodnews Bay

Date of Visit: 14-15 September 1994

General Observations/Comments:

The village of Goodnews Bay is located approximately 440 miles west of Anchorage and 120 miles southwest of Bethel. It is on the north side of Goodnews Bay near the mouth of the Goodnews River. The bay in front of the village is very shallow, with extensive mud flats at low tide, which has some moderating effect of wave impact on the village.

Historical Record of High Water:

High water and ground flooding of the community is caused by wind driven waves at high tide. The largest flood event is believed to have occurred in 1979, with wind blowing from the south. One house in the lowest part of town was flooded at that time, but it no longer exists. Water came under the house of James Bright in the 1979 storm, but did not flood the first floor. His house is now the lowest building in the village. The August, 1989 storm flooded the airstrip.

People Interviewed:

James Bright

Actions Taken:

No high water elevation signs placed.

Miscellaneous:

The following survey information is based on a temporary bench mark (TBM) with an assumed elevation of 100.00 feet. The TBM is located on the front door sill of the main entrance of city hall. This building is the old Bureau of Indian Affairs school, and also contains the clinic.

Survey information:

TBM, door sill of city hall main entrance	100.00
Rim of manhole cover #1, the first manhole north of city hall	98.16
Rim of manhole cover #2, the second manhole north	91.11

Community: Goodnews Bay

Rim of manhole cover #3, the third manhole north of the city hall, and the first south of the creek	87.36
Rim of manhole cover #4, first manhole north of the creek	83.98
Ground level at James Bright's house	83.11
Tide level of Goodnews bay at 9:45 am, 9/15/94	
Tide estimated to be about mid range	71.35
Estimated 1979 flood elevation	83.50
Recommended minimum building elevation	85.50



Temporary bench mark is the front door sill at the city hall.

Goodnews Bay/30 September 1994

Community: Goodnews Bay



Measured ground elevation at James Bright's house.

Goodnews Bay/30 September 1994

Date: Jan. 11, 92

COMMUNITY INFORMATION FORM

COMMUNITY Name: Goodnews Bay, Alaska Mayor/Chief: Galicia D. Galiga Borough: City of Goodnews Bay  
Status (home rule/2nd class/traditional/IRA, etc.): \_\_\_\_\_ Population: 241 Number Of Homes: 55 to 60  
WATER SUPPLY: How Obtained? Hand carry Is Water Treated? No Electrical Source (owner): A.V.E.C.  
ECONOMIC BASE: (sub. hunting, fishing/mining/comm. fishing/native arts/supply point, etc.): Sub-hunting / Fishing  
COMMUNICATIONS: Owner: United Utilities/Alascom Type Of Communications Available (phone/radio, etc.): phone / radio  
SEWAGE TREATMENT: What Type (cesspools/privies/public health service, etc.): Many Puchel had septic tanks  
TRANSPORTATION: Do You Have an Air Strip? Yes Can We Travel To Your Community From Anchorage By Road/Railroad? No  
GENERAL FLOOD INFORMATION: How Often Is Your Community Flooded? Yearly What Is The Cause Of Most Floods (ice jams/  
stream overflow/storm surge/heavy rains, etc.)? Storm How Many Homes Are Usually Flooded? 0  
What Public Facilities (school, generator, airport, sewage lagoon, etc.) Are Usually Flooded? airport  
What Body of Water Causes Your Floods? comes from Ocean  
LAST FLOOD: When Was The Last Flood (date)? August 17, 1989 What Caused the Last Flood? Storm blowing from the south  
How Deep Did The Water Get (feet)? D/K Where Is a Mark Left By The High Water? Highwater went over the airport  
How Many Homes Flooded? 0 What Public Facilities Flooded? 0  
WORST FLOOD: When Was the Worst Flood (date)? D/K What Caused the Worst Flood? D/K  
How Deep Did The Water Get (feet)? D/K Where Is A Mark Left By The High Water? over airport  
How Many Homes Flooded? 0 What Public Facilities Flooded? None

Prepared By: Galicia D. Galiga Phone Number: 967-8614

PLEASE USE THE REVERSE SIDE OF THIS FORM FOR ANY COMMENTS.

*copy minor*

1173

VILLAGE: Goodnews Bay, Alaska Page 1 of 3  
Present Village Chief (or Mayor): Anecia Nanok  
Village Status (home rule, 2nd class, traditional, IRA, etc): \_\_\_\_\_  
Christen Small for traditional and Evan S. Evan - Kuitsarak Co.  
(President) (President)  
Worst Flood Known (cause and date): 1979  
Depth of Flood (MAXIMUM): 8-9 feet high  
Highwater Marks (Describe & Locate): Front of the village,  
the beach area, and one house distroid,  
two (2) houses unblanced.  
\_\_\_\_\_  
\_\_\_\_\_  
Number of Homes Flooded: 1 house  
Number of Public Facilities and Type Flooded: Part of the  
old airport narrowed down, every time flood  
comes water goes over the old air field.  
Total Damage in \$ 1000.00 est.  
Most frequent cause of flooding (ice jams, stream overflow, wind driven  
waves, etc.): Wind driven waves  
\_\_\_\_\_  
Other Years Flooded: 69, 79, and 82  
Publication: 169 Number of Homes: 69  
Public Facilities: 6  
\_\_\_\_\_

encl 1

VILLAGE: Goodnews Bay

Other Pertinent Information (erosion & other problems): Front  
bank of village, gravel eroding, cause heavy  
rains creek bridge washed away creek  
froze cold spell in month of Feb. - 84  
\_\_\_\_\_  
\_\_\_\_\_  
\_\_\_\_\_

RETURN TO:

District Engineer  
ATTN: NPAEN-PL-FP  
U.S. Army Engineer District, Alaska  
Pouch 898  
Anchorage, Alaska 99506

PREPARED BY:

Jannie Maxwell  
City Clerk  
TITLE



# STATE OF ALASKA

## DEPARTMENT OF MILITARY AFFAIRS

ALASKA DIVISION OF EMERGENCY SERVICES

JAY S. HAMMOND, GOVERNOR

1306 EAST 4TH AVENUE  
ANCHORAGE — 99501

January 15, 1980

Mr. Mason Wade  
Alaska District, Corps of Engineers  
P.O. Box 7002  
Anchorage, Alaska 99510

ATTENTION: NPAEN-PL-FP

Dear Mr. Wade:

This is to update the Corps computerized listing of community flood hazards from field observations by staff of the Alaska Division of Emergency Services. Updating several of the community profiles may be pertinent as a result of a severe coastal storm and subsequent flooding that resulted in varied damages and losses from Sheldon Point to Togiak. Commencing November 8, 1979, at approximately 2300 hours and continuing through November 9, 1979, the storm had severe winds (80mph reports), accompanying wave action and sea surge. These communities had varying degrees of personal and public damages and losses: Togiak, Platinum, Goodnews Bay, Quinhagak, Kongiganak, Kwigillingok, Tuntutuliak, Napakiak, Nightmute, Toksook Bay, Tununak, Chevak, Hooper Bay and Sheldon Point. Based on on-site inspections the following community information may be of value in updating your listings:

✓ Goodnews Bay: Houses in flood hazard area - 3 (one of these houses was destroyed)

Coastal Flood Damage - Erosion along coastline, loss of an estimated 6-10 feet of bank during storm.

Additional Comments - Village residents said 1979 storm-driven waves were worst in 20 years, thus perhaps a "high average" flood hazard may be considered.

- Kwigillingok: Coastal Flood Damage - Village board walks were lifted and floated by the high water. Fuel storage for barreled fuel was flooded.
- Tuntutuliak: ADES staff did not travel to village. However, eight (8) homes were reported flooding according to AVCP and BIA, Bethel. Coastal flooding, wind driven waves at the mouth of the Kuskokwim was the reported flood cause.
- Quinhagak: Additional Comments - Bank erosion approximately 5-10 feet near the old school complex and old mission church.
- Tununak: Coastal flooding 1978 and November 1979, moderate. Beach erosion both years.
- Chevak: Flood damage - Erosion and undercutting of river bank 10-15 feet. Road leading to low portion of village was washed out. Barge receiving area was flooded.
- Hooper Bay: See attached survey form. Village president reported this to be worst flooding since the 1974 storm.

Other communities sustained personal property damage but with no apparent damages to community facilities.

If maps designating the flood hazard are available, we would like to assist you in improving the flood profiles as mapped. Hooper Bay is the only community flood map we had, and several areas not indicated were flooded.

With regard to the Willow Creek flooding our community records indicate flooding of these types in these years: ice jam (glaciation) November 1964, November 1975; log jam flooding August 1971.

The 1979 glaciation flooding has resulted in six (6) houses in the flood hazard area. Based on historic flooding along Willow Creek, the "low average" flood rating may be questionable.

If you have questions, please contact our office at 272-0594.

Sincerely,

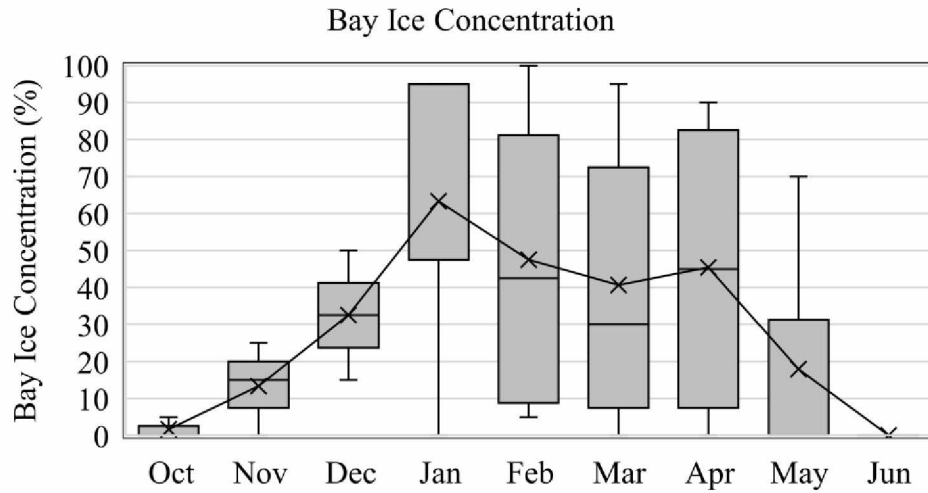
Christy L. Miller  
Sr. Planner

Attachment - 1

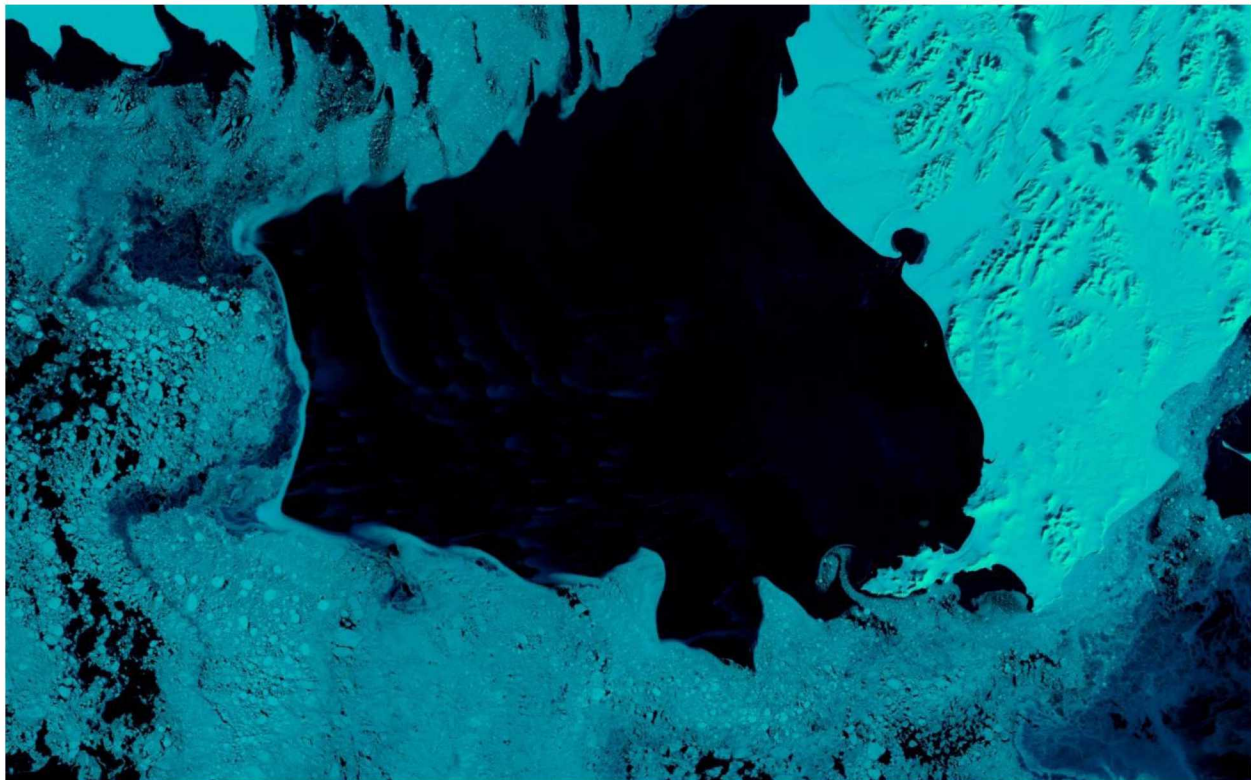


### Appendix III. Qualitative analysis of sea ice formation trends in Goodnews Bay.

Bay ice concentration was determined by viewing all available Landsat imagery (1982-2015) of the bay and estimating the concentration to the nearest 5%.



This landsat color-infrared image shows how offshore ice data may not correlate with bay ice. The bay (16 km across) has frozen to ~80%, but offshore ice is absent for 50-100 km.

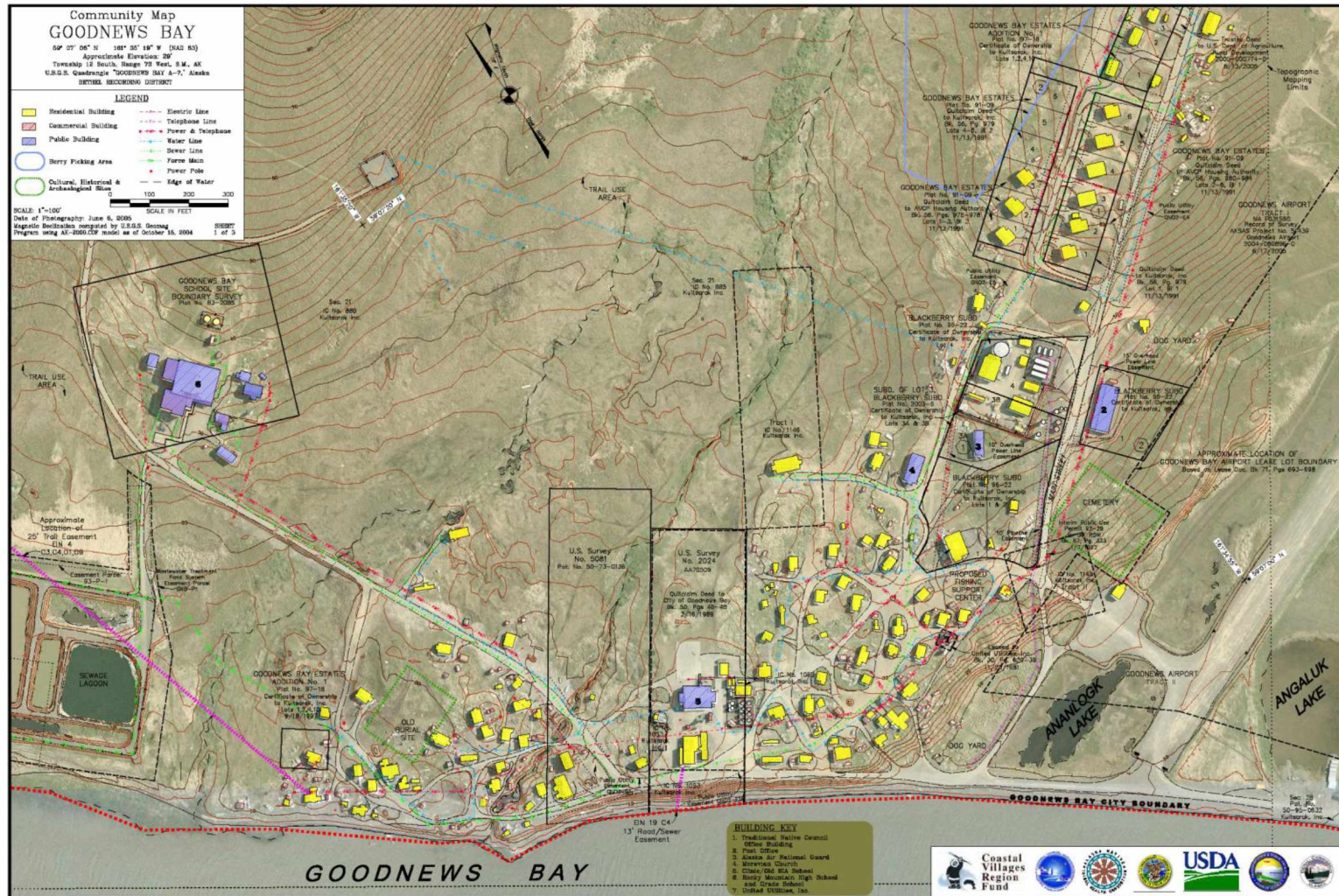


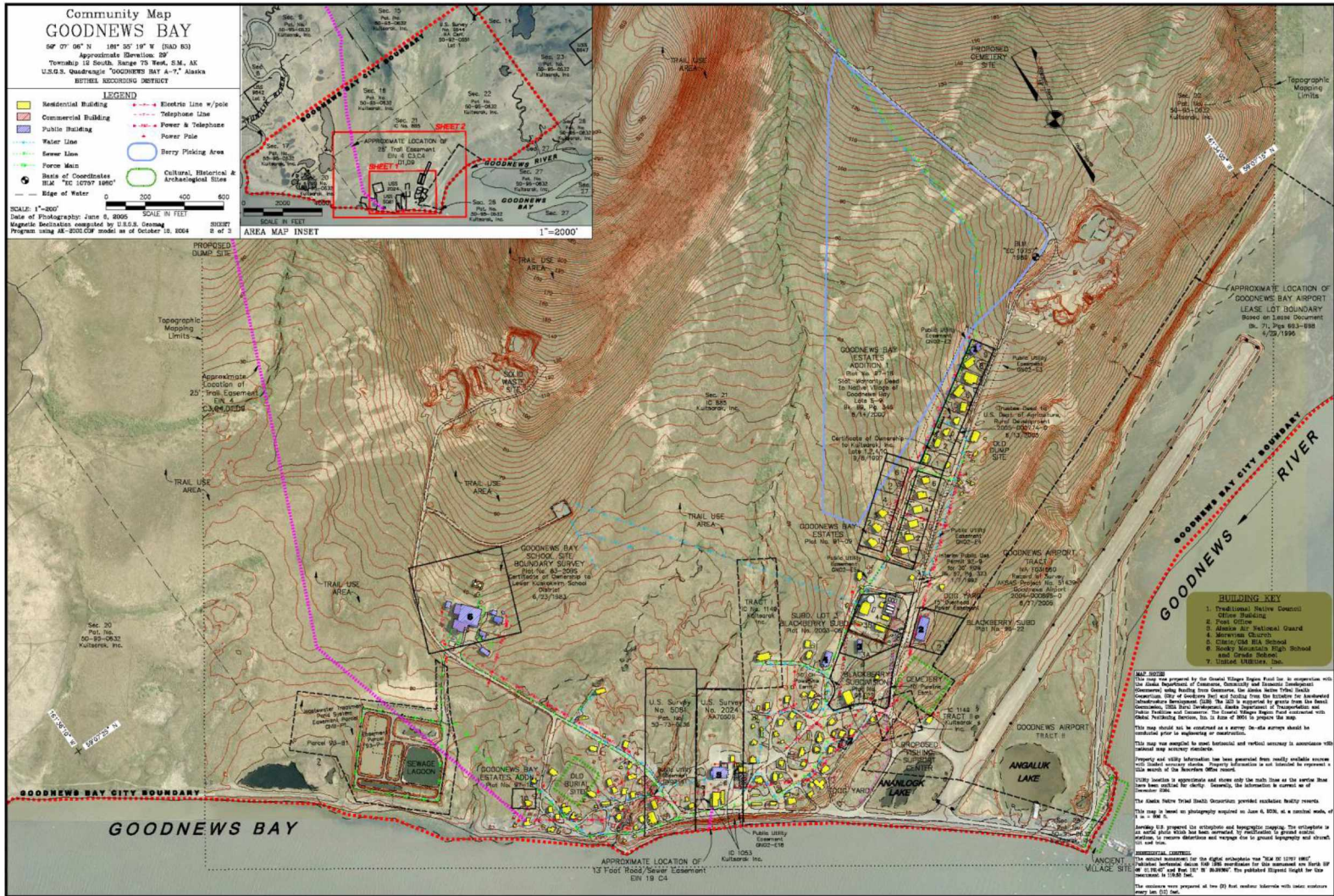
# Appendix IV. Community Profile Maps of Goodnews Bay.

Community profile map .PDFs can be accessed through this online tool:

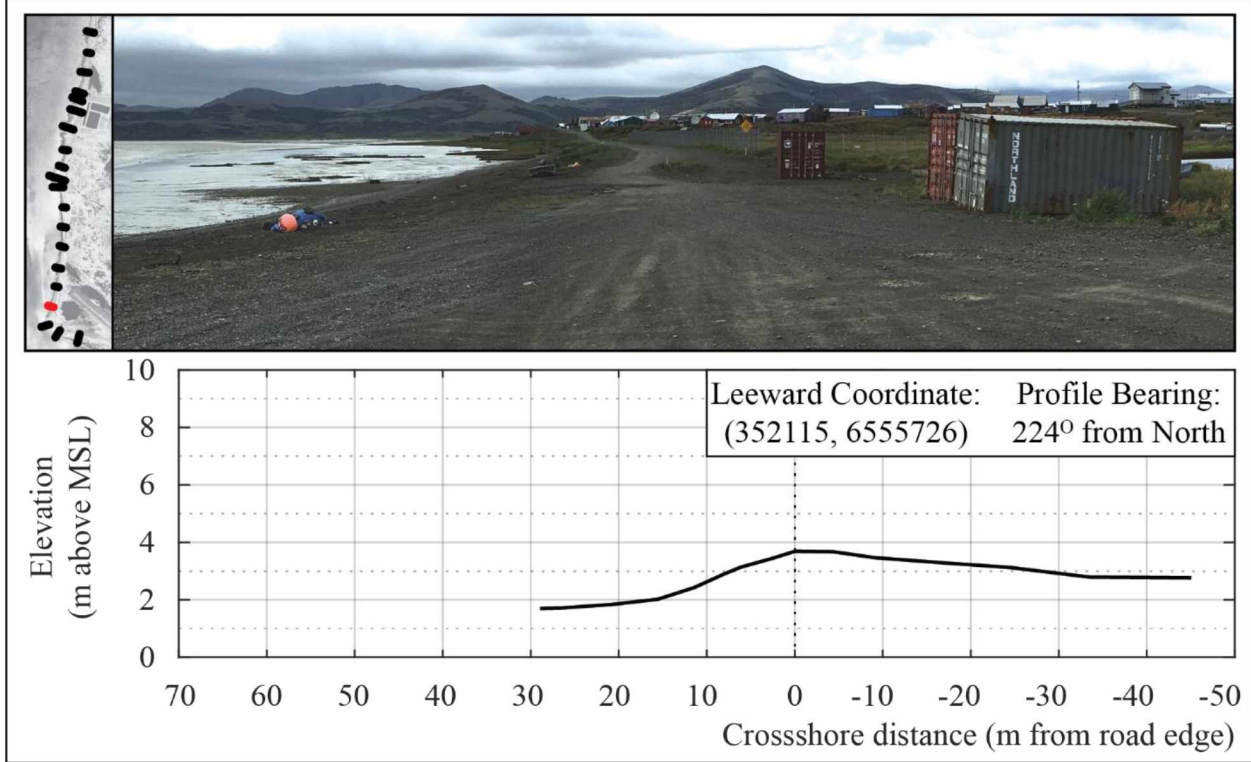
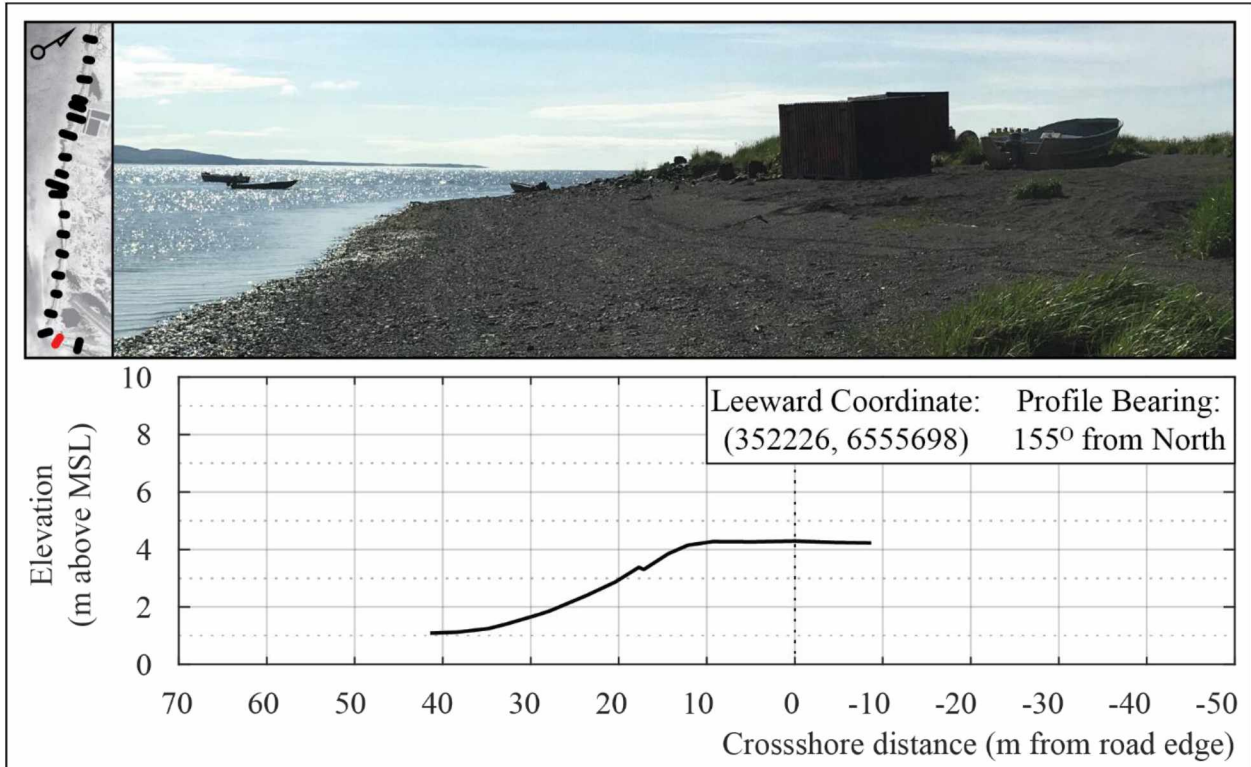
<http://dccc.maps.arcgis.com/apps/Viewer/index.html?appid=8e346292c8df44fa98b7d80740c67b03>

98





Appendix V. Coastal Profile Data for Goodnews Bay.



<b>Profile</b>	<b>Easting</b>	<b>Northing</b>	<b>Elevation</b>	<b>Notes</b>
1	352296.90	6555764.09	3.85	fence post
1	352301.61	6555759.57	3.16	tall grass start
1	352303.56	6555757.85	2.82	tall grass washed by last high
1	352306.71	6555754.58	2.46	muddy grass
1	352311.58	6555748.80	2.28	muddy grass
1	352316.80	6555743.16	2.24	muddy grass
1	352319.28	6555740.54	2.37	edge of mud berm
1	352319.93	6555739.66	2.56	slope rise
1	352321.34	6555738.88	2.47	atv tracks
1	352322.64	6555737.45	2.40	slope seaward edge
1	352324.27	6555735.21	2.14	veg line
1	352326.49	6555733.90	1.87	gravel beach begins under grass
1	352326.85	6555733.46	1.78	mud/gravel
1	352328.04	6555732.45	1.63	mud
1	352328.88	6555731.12	1.54	mud
2	352225.62	6555698.23	4.23	grass edge on road
2	352227.40	6555694.45	4.25	center of road
2	352229.38	6555690.41	4.29	edge of road
2	352231.46	6555686.12	4.27	back beach berm near propane tanks
2	352233.28	6555681.97	4.27	top landward berm
2	352234.48	6555679.38	4.15	seaward edge berm
2	352235.48	6555677.40	3.85	berm slope - large rocks and gravel
2	352236.63	6555674.85	3.30	eroded barrels landward; slope break of smaller berms
2	352236.86	6555674.34	3.38	top smaller berm
2	352237.66	6555671.79	2.87	upper beach - small wrack line
2	352239.17	6555668.91	2.40	wrack line mid beach
2	352241.05	6555665.13	1.86	lower beach with rocks
2	352241.59	6555663.94	1.73	mud-gravel mix; wet dry line
2	352243.47	6555660.87	1.41	mud and gravel
2	352244.31	6555658.96	1.25	end rock; coarse sand/gravel and mud
2	352245.37	6555655.64	1.12	gravel to mud line
2	352247.33	6555653.09	1.09	mud
3	352187.13	6555689.17	3.63	stake landward side road
3	352186.00	6555683.41	4.44	veg line and road
3	352184.24	6555678.46	4.37	center road
3	352180.72	6555670.66	4.33	center road
3	352176.71	6555662.02	4.30	seaward side road before slope
3	352175.73	6555657.08	4.08	slope near boat trailers
3	352175.04	6555654.69	3.76	start beach gravel
3	352173.21	6555648.65	3.11	upper wrack line



<b>Profile</b>	<b>Easting</b>	<b>Northing</b>	<b>Elevation</b>	<b>Notes</b>
3	352172.14	6555644.50	2.83	upper beach; wrack line
3	352170.23	6555638.19	2.27	mid beach; chain top 11th link
3	352168.72	6555633.12	1.73	lower wrack
3	352167.83	6555629.97	1.41	wet dry line
3	352166.46	6555624.82	0.96	mud and gravel
3	352166.00	6555621.35	0.65	water line
4	352149.56	6555754.09	2.76	pond edge
4	352140.34	6555746.91	2.79	grass and water line
4	352133.14	6555741.52	3.12	small gravel fronting pond
4	352127.35	6555736.99	3.28	adjacent conex landward
4	352121.44	6555731.58	3.46	small gravel near road
4	352117.80	6555728.62	3.67	road edge landward
4	352114.59	6555725.65	3.69	road edge seaward
4	352112.48	6555723.98	3.43	slope break; upper beach
4	352109.99	6555721.50	3.13	upper wrack line
4	352108.70	6555720.15	2.89	" " mid beach
4	352106.40	6555717.65	2.42	lower beach and wrack line
4	352103.42	6555714.79	2.02	wet dry line; transition to mud and gravel
4	352099.52	6555711.24	1.83	mud and gravel
4	352095.07	6555707.44	1.71	mud line
4	352093.26	6555706.09	1.70	mud
5	352048.92	6555806.01	4.01	fence
5	352042.48	6555799.39	4.02	road-veg interface, dried mud
5	352040.65	6555797.54	3.87	mud and road gravel turns to sand
5	352039.88	6555796.76	3.72	landward stake
5	352038.75	6555795.34	3.54	gravel and grass wrack line; discontinuous veg line; back to sand
5	352036.37	6555792.71	3.12	gravel berm on sand
5	352035.40	6555791.61	2.91	tiny berm toe
5	352035.27	6555791.46	2.91	tiny berm crest; wrack line; gravel
5	352035.04	6555791.29	2.85	tiny berm end
5	352033.50	6555789.64	2.54	larger rocks mixed in gravel and sand
5	352031.44	6555787.48	2.15	large gravels on mud
5	352030.04	6555786.28	1.96	mud line
5	352028.24	6555784.71	1.92	seaward stake; seaward extent
6	351977.98	6555868.17	4.26	fence
6	351971.54	6555860.61	4.03	gravel road and veg edge
6	351970.37	6555859.49	4.04	grassy gravel berm crest
6	351969.45	6555857.90	3.79	gravel and sand interface
6	351967.34	6555855.86	3.46	gravel and grass wrack line on sand
6	351965.24	6555853.10	2.99	wrack line after atv

<b>Profile</b>	<b>Easting</b>	<b>Northing</b>	<b>Elevation</b>	<b>Notes</b>
6	351964.53	6555852.25	2.82	bottom of gravel atv berm
6	351964.02	6555851.75	2.78	veg edge; mud under veg grass
6	351962.59	6555850.07	2.68	yellow-green grass, downed by water
6	351958.74	6555846.42	2.27	
6	351954.59	6555841.89	2.07	
6	351951.21	6555837.94	1.84	mud line; seaward extent
7	351890.45	6555931.52	4.22	road edge
7	351890.01	6555931.08	4.35	road berm crest
7	351889.83	6555930.55	4.21	berm toe; grass edge
7	351887.69	6555928.30	4.08	grassy bluff top
7	351887.53	6555928.23	3.58	bluff toe, veg line, wwcd, 0.2-4cm gravel on medium sand
7	351885.29	6555925.63	3.11	wrack line; atv tracks; gravel on sand
7	351890.59	6555931.19	4.20	road edge seaward
7	351890.19	6555930.87	4.30	small road berm
7	351889.79	6555930.55	4.16	veg line on road
7	351888.28	6555929.58	4.29	berm crest - high grass
7	351887.35	6555928.57	4.05	berm edge
7	351887.08	6555928.42	3.54	berm toe - sand and gravel
7	351884.83	6555926.52	3.12	upper beach - small wrack line
7	351882.32	6555924.10	2.64	mid beach; chain top 11th link
7	351881.40	6555923.18	2.48	lower beach transition to coarser gravel
7	351879.79	6555921.29	2.19	mud and gravel; wet line
7	351875.75	6555917.58	1.92	mud and gravel
7	351870.15	6555912.95	1.81	top mud
7	351870.13	6555912.95	1.60	mud bottom on top gravel
8	351816.65	6556000.63	7.77	landward road edge
8	351811.76	6555994.74	7.56	road slope break
8	351810.85	6555993.36	7.40	barrier top
8	351816.86	6556000.36	7.75	landward road edge fronting blue house
8	351814.45	6555996.86	7.61	center road
8	351811.41	6555993.06	7.40	riprap edge top
8	351809.03	6555989.44	4.46	riprap toe
8	351806.95	6555987.42	4.06	high grass landward side trail
8	351805.36	6555985.06	3.68	seaward side trail; gravel and sand
8	351803.92	6555983.23	3.32	wrack line in coarse sand
8	351802.75	6555981.88	3.13	veg line landward seaward of trail
8	351800.79	6555979.33	2.73	yellow grass line with mud
8	351797.18	6555975.28	2.29	flat grass and mud
8	351791.52	6555969.48	1.95	veg line seaward; mud line
8	351791.42	6555969.32	1.83	small toe into mud - on top of mud

<b>Profile</b>	<b>Easting</b>	<b>Northing</b>	<b>Elevation</b>	<b>Notes</b>
8	351791.10	6555969.00	1.79	mud depth over gravel
9	351755.26	6556080.48	9.65	telephone pole, ~15cm seaward of
9	351737.17	6556059.05	9.24	middle of crossroads
9	351729.52	6556047.10	8.98	road edge, gravel barrier top
9	351725.57	6556042.55	4.74	barrier bottom
9	351723.45	6556040.17	4.06	slope break
9	351722.28	6556038.87	3.78	grass and beach road edge
9	351721.30	6556038.02	3.46	slope break; wrack line (can't get rtk of road/grass edge)
9	351714.81	6556027.81	2.19	1st grass line, rocks in mud
10	351641.62	6556099.83	6.37	southern edge flat plywood deck
10	351638.96	6556096.58	6.18	landward road edge
10	351632.69	6556087.02	6.02	seaward road edge
10	351631.04	6556084.92	4.44	riprap toe
10	351629.67	6556082.07	4.04	gravel to veg (beach pea) edge
10	351627.28	6556077.63	3.33	landward side atv trail
10	351626.02	6556075.20	3.03	seaward edge trail
10	351620.89	6556067.02	2.85	yellow grass edge with mud
10	351615.24	6556058.78	2.51	flat grass edge
10	351601.15	6556039.85	1.62	veg to mud line
11	351612.83	6556113.10	5.18	landward road edge over culvert
11	351609.78	6556110.16	5.20	seaward road edge over culvert
11	351607.89	6556108.96	3.86	creek front of culvert 85cm offset from edge
11	351603.01	6556103.95	3.44	creek mouth
11	351598.86	6556099.67	3.21	creek edge near wrack line and sand and gravel
11	351594.71	6556096.75	2.94	level point side of creek
11	351591.17	6556094.12	3.08	transition to high grass with moss
11	351587.84	6556091.86	3.01	yellow grass edge
11	351583.56	6556088.68	2.79	flat grass with mud
11	351575.58	6556081.58	2.39	flat grass with mud
11	351565.77	6556074.10	2.06	grass and mud plus gravel edge
11	351559.24	6556068.67	1.91	mud and gravel in stream bed
11	351555.53	6556065.45	1.88	2nd veg edge and mud gravel on grass clump
11	351545.84	6556054.29	1.54	gravel to mud line
12	351564.11	6556153.16	5.32	landward road edge
12	351559.24	6556148.69	5.28	center road
12	351555.42	6556144.66	5.25	seaward road edge
12	351555.12	6556144.21	5.16	riprap edge top
12	351553.20	6556142.46	3.73	riprap toe

<b>Profile</b>	<b>Easting</b>	<b>Northing</b>	<b>Elevation</b>	<b>Notes</b>
12	351551.75	6556141.50	3.36	wrack line - gravel
12	351550.73	6556140.63	3.20	veg and gravel transition to high grass
12	351547.79	6556138.33	2.82	flat grass and mud
12	351543.14	6556134.36	2.46	mud and grass
12	351536.10	6556128.59	2.27	mud and grass
12	351528.13	6556122.73	1.91	veg to mud line
13	351500.53	6556221.04	4.85	tele pole next to JR's house- James Bright
13	351495.53	6556216.49	4.89	tele pole cable with yellow sheath
13	351490.63	6556207.60	4.21	veg edge landward side trail
13	351489.94	6556206.81	4.37	side trail landward
13	351487.87	6556203.75	4.33	seaward edge trail
13	351486.86	6556202.55	3.54	toe of trail
13	351485.56	6556200.79	3.13	high grass line; gravel
13	351484.87	6556199.62	2.97	transition to mud and gravel
13	351483.74	6556198.58	2.82	yellow grass edge
13	351481.88	6556195.78	2.62	edge yellow grass dead grass wrack line
13	351477.72	6556189.59	2.30	bugs; yellow grass
13	351470.42	6556181.08	1.89	grass mud line
14	351421.36	6556284.32	4.29	seaward side trail; veg line and gravel
14	351414.49	6556280.43	3.37	bottom berm
14	351408.45	6556276.38	3.11	wrack line - sticks and flat grass
14	351401.54	6556270.38	3.05	high grass and mud
14	351394.40	6556264.65	2.91	high grass and mud
14	351387.65	6556259.22	2.72	lower wrack - sticks etc; grass with yellow tips
14	351379.34	6556250.61	2.11	lower grass and mud
14	351370.25	6556243.76	1.70	veg-mud edge
15	351372.31	6556368.79	6.09	fence post lagoon center post with cap
15	351370.00	6556366.81	4.67	bottom lagoon rise
15	351369.38	6556366.42	4.39	sewage lagoon trench; mud-some hard mostly
15	351368.38	6556365.12	4.71	lagoon side trail veg edge
15	351365.80	6556362.84	4.77	veg edge seaward side trail
15	351362.71	6556359.95	4.54	stake of com transect top of small bluff
15	351360.04	6556357.45	4.36	berm edge
15	351359.67	6556357.23	4.13	berm toe; high grass
15	351358.01	6556355.90	3.64	trough fronting berm
15	351356.34	6556354.27	3.40	high grass
15	351353.11	6556351.15	3.09	edge high grass and flat grass
15	351346.74	6556345.14	2.83	mud and high grass
15	351342.99	6556342.06	2.63	mud and flat grass
15	351333.23	6556332.94	2.45	mud and flat grass

<b>Profile</b>	<b>Easting</b>	<b>Northing</b>	<b>Elevation</b>	<b>Notes</b>
15	351324.42	6556325.30	2.13	mud and flat grass
15	351317.40	6556321.36	2.01	veg-mud edge
16	351334.73	6556408.87	6.24	4th fence post from NW corner
16	351330.58	6556405.24	4.80	toe of rock barrier
16	351327.86	6556402.67	4.63	end of gravel yard; veg line
16	351323.11	6556399.11	4.49	fireweed field
16	351319.78	6556395.39	4.17	landward road edge
16	351317.53	6556394.05	4.04	seaward road edge; new veg line
16	351315.00	6556392.39	4.07	berm top
16	351314.72	6556391.86	3.81	berm bottom
16	351313.25	6556388.50	3.44	2nd berm top
16	351312.40	6556388.26	3.47	2nd berm bottom
16	351310.87	6556387.22	3.32	thick wrack line, grass downed
16	351307.59	6556384.92	3.14	grass up
16	351302.67	6556381.60	2.94	yellow grass line
16	351299.70	6556379.71	2.94	2nd dry grass wrack line
16	351291.20	6556373.96	2.54	hummocky grassy mud flats
16	351273.60	6556360.96	1.85	muck line
17	351289.62	6556419.23	3.99	road edge
17	351286.96	6556417.56	3.59	vegetated berm bottom
17	351285.77	6556416.10	3.37	grassy muddy slope
17	351284.34	6556414.68	3.38	thick dried grass wrack line; plants growing out, grass flattened
17	351282.20	6556412.20	3.09	grass standing up
17	351280.23	6556410.41	2.96	flat grass in mud; some wrack debris
17	351277.36	6556408.08	2.77	wrack line
17	351264.00	6556396.67	2.26	mud flat with thick grass hummocks
17	351255.75	6556390.38	1.93	mud line; seaward extent
18	351212.44	6556495.59	4.30	seaward trail side; veg line
18	351209.46	6556492.08	4.33	high grass bluff top
18	351208.36	6556490.81	4.17	bluff edge seaward
18	351207.82	6556489.83	3.71	bluff toe; sand and gravel
18	351206.01	6556487.15	3.36	lower trail seaward side; veg line
18	351205.12	6556485.85	3.15	high grass start mud
18	351198.60	6556479.23	2.59	transition area to low marsh grass; muddy bottom
18	351186.00	6556462.79	1.99	veg-mud edge all mud seaward
19	351139.92	6556560.28	5.13	road edge
19	351139.60	6556559.91	5.24	road berm crest
19	351136.54	6556557.73	5.12	bluff edge
19	351136.43	6556557.47	4.72	bluff toe; gravel

<b>Profile</b>	<b>Easting</b>	<b>Northing</b>	<b>Elevation</b>	<b>Notes</b>
19	351135.58	6556556.29	4.59	level spot on lower bluff; small gravel and beach debris
19	351133.39	6556553.89	4.46	level bluff
19	351132.84	6556553.24	4.34	bluff edge seaward
19	351132.15	6556552.58	3.63	bluff toe
19	351130.41	6556551.28	3.39	sand and gravel landward; lower atv trail
19	351129.43	6556550.17	3.21	edge atv trail landward
19	351127.61	6556548.34	2.87	seaward edge atv trail; veg line
19	351125.85	6556545.65	2.70	high grass edge to low marsh grass
19	351121.63	6556541.36	2.09	veg edge to mud
20	351063.46	6556629.20	6.62	stake tope transect; in crowberry s of hill
20	351059.29	6556625.31	6.43	bluff top
20	351057.98	6556624.07	6.37	begin bluff slope
20	351057.66	6556623.66	5.50	bluff slope toe
20	351056.32	6556622.67	5.37	lower slope crest
20	351055.92	6556622.43	5.13	bottom small crest
20	351051.27	6556617.63	4.01	veg-sand line
20	351048.42	6556614.70	3.35	landward side atv trail
20	351046.89	6556613.14	3.13	seaward side atv trail; veg edge
20	351044.00	6556610.89	2.72	high to low sedge grass edge
20	351031.55	6556597.44	1.98	marsh grass edge to mud
21	350985.77	6556689.89	8.39	atv trail landward
21	350982.59	6556685.03	8.54	bluff edge
21	350982.27	6556684.70	7.47	bluff slope
21	350957.53	6556702.03	5.92	observed control point on possible new base spot front of hill
21	350986.81	6556689.16	8.50	S side hill landward side trail
21	350983.15	6556684.91	8.59	bluff edge before slope; where veg breaks
21	350982.65	6556684.33	8.15	bluff bottom
21	350999.26	6556665.84	5.32	bluff toe

